

THE UNIVERSITY OF MICHIGAN  
INDUSTRY PROGRAM OF THE COLLEGE OF ENGINEERING

DESIGN AND ANALYSES OF TALL TAPERED  
REINFORCED CONCRETE CHIMNEYS SUBJECTED TO EARTHQUAKE

Nelson M. Isada

This dissertation was submitted in partial fulfillment of the requirements for the degree of Doctor of Philosophy in the University of Michigan, 1955.

December, 1955

IP-131

#### ACKNOWLEDGEMENT

We would like to express our appreciation to the author for permission to distribute this dissertation under the Industry Program of the College of Engineering.

Copyright By  
Nelson M. Isada  
1955

#### ACKNOWLEDGEMENT

The author would like to thank Professor B. G. Johnston and Professor L. C. Maugh for their close supervision, and through whose research projects the author gained the experience which provided the necessary background for this study; Professor G. E. Hay, for his assistance in the mathematical analysis; Professor H. M. Hansen for his help in the mechanics of vibration; Professor R. H. Sherlock and Professor L. M. Legatski for valuable suggestions; the Department of Aeronautical Engineering for the use of its analogue computer; and Mr. F. L. Bartman and Professor R. M. Howe for their guidance in the use of the analogue computer.



## TABLE OF CONTENTS

	Page
ACKNOWLEDGEMENT	iii
LIST OF TABLES	v
LIST OF FIGURES	v
ABSTRACT	vii
NOMENCLATURE	x
CHAPTER I - INTRODUCTION	1
CHAPTER II - THE DISPLACEMENT EQUATION	5
CHAPTER III-DYNAMIC STRUCTURAL PROPERTIES: FUNDAMENTAL MODE	26
CHAPTER IV - DYNAMIC STRUCTURAL PROPERTIES: SECOND AND HIGHER MODES	44
CHAPTER V - GENERALIZED CO-ORDINATE RESPONSE TO EARTHQUAKE	59
CHAPTER VI - DESIGN SHEARS AND BENDING MOMENTS	66
CHAPTER VII-CONCLUSIONS AND DESIGN RECOMMENDATIONS	72
APPENDIX - Additional Data	83
BIBLIOGRAPHY	90

## LIST OF TABLES

		Page
Table 6.1.	Shear Coefficients	68
Table 6.2.	Bending Moment Coefficients	69

## LIST OF FIGURES

Fig. 2.1.	Single Degree of Freedom System	25
Fig. 2.2.	Two Degree of Freedom System	25
Fig. 3.1.	Newmark's Reaction Formulas	42
Fig. 3.2.	Calculations of First Mode Dynamic Properties	43
Fig. 4.1.	Second Mode Orthogonality Calculations	51
Fig. 4.2.	Calculations of Second Mode Dynamic Properties	52
Fig. 4.3.	Third Mode Orthogonality Calculations	53
Fig. 4.4.	Calculations of Third Mode Dynamic Properties	54
Fig. 4.5.	Calculations of the $\Gamma_j$ Quantities	55
Fig. 4.6.	Deflection Factors. Clifty Creek Stack	56
Fig. 4.7.	Shear Factors. Clifty Creek Stack	57
Fig. 4.8.	Bending Moment Factors. Clifty Creek Stack	58
Fig. 5.1.	Analog Computer Circuit	64
Fig. 5.2.	Generalized Co-ordinate Response	65
Fig. 6.1.	Instantaneous Shear Curves	70
Fig. 6.2.	Instantaneous Bending Moment Curves	71
Fig. 7.1.	Shears and Shear Magnification Factors. Clifty Creek Stack	76
Fig. 7.2.	Bending Moments and Moment Magnification Factors. Clifty Creek Stack	77
Fig. 7.3.	Shear Magnification Factors for Regions of Strong-Motion Earthquakes for 5% and 7.5% of Critical Damping	78

	Page
Fig. 7.4. Bending Moment Magnification Factors for Regions of Strong Motion Earthquakes for 5% and 7.5% of Critical Damping	79
Fig. 7.5. Bending Moment Magnification Factors for Regions of Strong-Motion Earthquakes Compared to ACI Code No. 49-26	80
Fig. 7.6. Shear and Bending Moment Magnification Factors for Regions of Medium-Intensity Earthquakes	81
Fig. 7.7. Shear and Bending Moment Magnification Factors for Regions of Light-Intensity Earthquakes	82
Fig. A.1. Deflection Factors. Modified Selby Stack	84
Fig. A.2. Shear Factors. Modified Selby Stack	85
Fig. A.3. Bending Moment Factors. Modified Selby Stack	86
Fig. A.4. Deflection Factors. Kyger Creek Stack	87
Fig. A.5. Shear Factors. Kyger Creek Stack	88
Fig. A.6. Bending Moment Factors. Kyger Creek Stack	89

## ABSTRACT

### DESIGN AND ANALYSES OF TALL TAPERED REINFORCED CONCRETE CHIMNEYS SUBJECTED TO EARTHQUAKE

by Nelson M. Isada

The object of this study is to formulate rational and orderly rules to be followed in the design and analyses of tall tapered reinforced concrete chimneys on rigid foundations as determined by earthquake stresses.

The study is divided into four major phases, namely:

(1) The accumulation of accelerogram records and a decision to use the records taken at El Centro, California on May 18, 1940 with N-S component, Vernon, California on October 2, 1933 with N08E component, and Los Angeles Subway Terminal on October 2, 1933 with N39E component,

(2) the accumulation of experimental results on the coefficient of damping and a decision to use 5% and 7-1/2% of critical damping for each mode,

(3) the development of the dynamic analyses, divided as follows:

a. Derivation of the instantaneous displacement, shear, and bending moment equations along the height of the chimney by the use of Lagrange's equations. These equations are expressed as the sum of the effects of the various modes of vibration.

b. Determination of the fundamental mode dynamic structural properties of the chimney by the use of the Stodola-Newmark method. These properties are the vibration mode shapes, shear factors, moment factors, natural frequencies, and the generalized co-ordinate factors. The effects of damping in these properties are also discussed.

c. Determination of the second and higher mode dynamic structural properties of the chimney. This part requires the use of the orthogonality relationship of the various modes.

d. Solution of the generalized co-ordinate differential equations for each mode. The Laplace transform and Newmark's step by step methods are summarized. However, in this study the electronic analogue computer is used.

e. Determination of the design shears and bending moments. Here the instantaneous shears and bending moments are computed from the results of the different steps above.

f. Determination of the magnification factors. First, the shears and bending moments are determined by the use of empirical seismic coefficient  $K_e$  for a particular locality. This seismic coefficient is multiplied by the weight of the chimney above the section under consideration to get the forces acting on the chimney. Then the maximum shears and bending moments as obtained from the dynamic analysis in step e are divided by the corresponding shears and bending moments as obtained by the  $W'/g K_e g$  method to get the magnification factors. These magnification factors are the basis for the suggested design rules. They are also compared with the magnification factors suggested by the ACI (49-26) Code. It is concluded that the ACI (49-26) Code requires modification and a new design formula is needed, and

(4) the determination of the suggested design formulas. Envelopes are drawn for the different magnification factor curves. Formulas are then derived from these envelopes which are recommended for use in the preliminary design of tall tapered reinforced concrete chimneys on rigid foundations subjected to earthquakes. The recommended design formulas for the shears and bending moments for regions where earthquakes occur are:

$$V = W'K_e h'' \left[ 1.8 + \left( \frac{x - .5h}{.5h} \right)^2 \right] \quad x \geq .5h,$$

$$= 1.8 W'K_e h'' \quad x \leq .5h,$$

and

$$M = W'K_e h'' \left[ 1 + 8 \left( \frac{x - .2h}{.8h} \right)^2 \right] \quad x \geq .2h,$$

$$= 1.0 W'K_e h'' \quad x \leq .2h,$$

where

$V$  = shear,

$W'$  = weight of chimney above section under consideration, including any portion of lining supported from the chimney shell,

$K_e$  = seismic coefficient; which is equal to 0.20 for localities where the accelerograph records show maximum accelerations of not more than 0.325 of the acceleration due to gravity; 0.06 for localities where the accelerograph records show maximum accelerations of not

## NOMENCLATURE

### Units Used

Kip-foot units where 1 kip = 1,000 lbs.

### Latin Letter Symbols

A, B,	constants
$A_1, A_2, B_2$	mode shape purifying constants
a, b,	constants
a	$EI + m$
E	Young's modulus of elasticity
g	acceleration due to gravity
h	height of stack
h'	distance from section under consideration to the section that is 1/5 of the total height of the chimney above base
h''	distance from section under consideration to center of gravity of chimney mass above the section
$h''_v$	shear magnification factors
$h''_m$	bending moment magnification factors
I	moment of inertia
$K_e$	seismic coefficient
k	spring constant
$M_j$	bending moment factor
$M_j \Gamma_j$	bending moment coefficient
M	bending moment
m	mass per unit length
$m_1, m_2$	concentrated mass
$Q_j$	generalized force corresponding to $q_j$
Q	total resistance of structure
$q_j$	generalized co-ordinates which are functions of time alone

R	vertical reactions
s	symbol used in Laplace transform operation
T	total kinetic energy of entire vibrating system
t	time variable
$t' = \omega t$	new time variable
U	total potential energy of entire vibrating system
$V_j$	shear factor
$V_j \Gamma_j$	shear coefficient
V	shear
W	load per unit length along the beam or stack
W'	weight of chimney above section under consideration, including any portion of lining supported from the chimney shell
w	weight per unit length along the beam or stack
x	distance from base to a general point P on neutral axis
Y	absolute horizontal deflection of mass
y	relative horizontal deflection of the mass with respect to the ground
$y_b$	horizontal motion of the base of the beam or stack
$Z_j$	mode shape or characteristic function

### Greek Letter Symbols

$\alpha_j$	characteristic number
$\beta_j$	ratio of assigned damping to critical damping
$\Delta$	denotes increment
$\Gamma_j$	dynamic structural constant
$\gamma_j$	constant which is equal to $\omega_j^2 + a^2$
$\delta_j$	logarithmic damping decrement
$\theta$	slope of the beam
$\lambda$	length of a segment of a stack

$\Psi_j = 2\beta_j \omega_j$	damping factor
$\tau_j$	natural period in seconds per cycle
$\omega_j$	natural frequency in radians per second
$\omega'_j$	damped frequency in radians per second
$\Phi$	$M + EI$
$\phi_j$	$q_j + \Gamma_j$

### Subscripts and Superscripts

$j$	refers to the mode of vibration
$b$	refers to the base of the stack
$e$	refers to the top of the stack
$f$	denotes final condition
$o$	denotes initial condition
$r$	subscript for the $r$ th mode of vibration
$s$	subscript for the $s$ th mode of vibration
$\dot{q}$	$\partial q / \partial t$
$\ddot{q}$	$\partial^2 q / \partial t^2$
$\dot{y}$	$\partial y / \partial t$
$\ddot{y}$	$\partial^2 y / \partial t^2$
$\ddot{y}_b$	$\partial^2 y / \partial t^2$
$\dot{z}$	$\partial z / \partial x$
$\ddot{z}$	$\partial^2 z / \partial x^2$
$\dddot{z}$	$\partial^3 z / \partial x^3$
$\dots z$	$\partial^4 z / \partial x^4$



DESIGN AND ANALYSES OF TALL TAPERED  
REINFORCED CONCRETE CHIMNEYS SUBJECTED TO EARTHQUAKE

CHAPTER I

INTRODUCTION

The object of this study is to formulate rational and orderly rules to be followed in the design and analyses of tall tapered reinforced concrete chimneys on rigid foundations as determined by earthquake stresses.

During an earthquake, the base of the chimney is subjected to variable ground motion, which causes dynamic stresses along the height of the chimney. These dynamic stresses are the cause of the failures of chimneys during an earthquake.

The dissertation program is divided into four major phases. The first involves the accumulation of accelerogram records and a decision as to which earthquakes to use. From the work of Alford, J. L., et al. (1)\* it is decided to use three accelerogram records. The first accelerogram chosen is the record taken at El Centro, California on May 18, 1940 with N-S component. This accelerogram takes care of the localities where the maximum acceleration recorded is 0.09g or more. The decision for choosing this accelerogram for localities subjected to strong-motion earthquakes is based on the "spectrum analyses" of Alford, J. L., et al. (1). Their "spectrum analyses" show this earthquake to cause maximum response. The second accelerogram chosen is the record taken at Vernon, California on October 2, 1933 with NO8E component. This

\*This and subsequent numbers in parenthesis refer to the bibliography on page 90.

covers localities whose recorded accelerograms show maximum accelerations of from 0.05g to 0.09g. The third accelerogram chosen is the record taken at the Los Angeles Subway Terminal on October 2, 1933 with N39E component. This accelerogram covers localities whose accelerogram records show maximum accelerations of less than 0.05g.

The second phase of the program is the accumulation of experimental results on the coefficient of damping. Hisada, T. (2), Merritt, G. (3), White, M. P. (4), and others have studied and performed experiments to determine the values of the coefficient of damping. From their studies it has been concluded that 5% and 7-1/2% of critical damping for each mode should be used in this study.

The third and most important phase is the series of analytical studies, divided as follows:

1. Derivation of the instantaneous displacement, shear, and bending moment equations along the height of the chimney. These equations are expressed as the sum of the effects of the various modes of vibration. This derivation is discussed in detail in Chapter II.

2. Determination of the fundamental mode dynamic structural properties of the chimney. These properties are the vibration mode shapes, shear factors, moment factors, natural frequencies, and the generalized co-ordinate factors. The effects of damping in these properties are also discussed. Chapter III covers this part of the study.

3. Determination of the second and higher mode dynamic structural properties of the chimney. This part requires the use of the orthogonality relationship of the various modes. The various steps are discussed in Chapter IV.

4. Solution of the generalized co-ordinate differential equations for each mode. The Laplace Transform and Newmark's step by step methods are summarized. However, in this study the electronic analogue computer is used. Chapter V covers this step.

5. Determination of the design shears and bending moments. First, the instantaneous shears and bending moments along the height of the stack are computed from the results of the different steps above. This step is done in Chapter VI.

6. Determination of the magnification factors. First, the shears and bending moments are determined by the use of the empirical seismic coefficient  $K_e$  for a particular locality. This seismic coefficient is multiplied by the weight of the chimney above the section under consideration to get the forces acting on the chimney. The maximum shears and bending moments from the results of Chapter VI are also plotted. Then the maximum shears and bending moments as obtained from the dynamic analysis are divided by the corresponding shears and bending moments as obtained by the  $W/g K_e g$  method to get the magnification factors. These magnification factors are the basis for the suggested design rules. They are also compared with the magnification factors suggested by the ACI (49-26) Code. It is concluded that the ACI (49-26) Code requires modification and a new design formula is needed.

Determination of the suggested design formulas. Envelopes are drawn for the different magnification factor curves. Formulas are then derived from these envelopes which are recommended for use in the preliminary design of tall tapered reinforced concrete chimneys on rigid foundations subjected to earthquakes. The recommended design formulas for the shears and bending moments for regions where earthquakes occur are:

$$V = W'K_e h'' \left[ 1.8 + \left( \frac{x - .5h}{.5h} \right)^2 \right], \quad x \geq .5h, \quad (1.1)$$

$$= 1.8W'K_e h'' \quad x \leq .5h, \quad (1.1a)$$

and

$$M = W'K_e h'' \left[ 1 + 8 \left( \frac{x - .2h}{.8h} \right)^2 \right], \quad x \geq .2h, \quad (1.2)$$

$$= 1.0W'K_e h'' \quad x \leq .2h, \quad (1.2a)$$

where

V = shear,

W' = weight of chimney above section under consideration, including any portion of lining supported from the chimney shell,

$K_e$  = seismic coefficient; which is equal to 0.20 for localities where the accelerograph records show maximum accelerations of not more than 0.325 of the acceleration due to gravity; 0.06 for localities where the accelerograph records show maximum accelerations of not more than 0.0875 of the acceleration due to gravity; and 0.03 for localities where the accelerograph records show maximum accelerations of not more than 0.050 of the acceleration due to gravity,

$h''$  = distance from section under consideration to center of gravity of chimney mass above the section,

x = distance of section under consideration above the base of the chimney,

h = height of chimney,

M = bending moment,

and for reinforced concrete chimneys whose fundamental periods are from 2.4 to 3.0 seconds per cycle.

CHAPTER II  
THE DISPLACEMENT EQUATION

If a sudden load is applied to an elastic system such as a mass-spring system, a building, or a beam, the system is no longer in equilibrium because the unbalanced forces cause it to be in vibratory motion. Systems like beams are capable of vibrating in different modes (5).

Take a simple case wherein a system can vibrate in one mode only. This system is called a single degree of freedom system. An example is given below.

In Fig. 2.1, let  $k$  be the spring constant and  $m_1$  the mass. Then if the mass  $m_1$  is given a displacement  $y$ , then by Newton's principle the differential equation for free vibration of the system is

$$m_1 \frac{d^2y}{dt^2} + ky = 0, \quad (2.1)$$

or

$$\frac{d^2y}{dt^2} + \omega^2 y = 0, \quad (2.1a)$$

where

$$\omega^2 = \frac{k}{m_1}. \quad (2.1b)$$

The solution of eq. (2.1a) is

$$y = A \cos \omega t + B \sin \omega t, \quad (2.2)$$

where A and B are constants which are determined from the boundary conditions. The term  $\omega$  is known as the natural frequency. Eq. (2.2) shows that the mass is vibrating in such a way that the motion is repeated after an interval of time  $\tau$  which is known as the period of vibration. The value of  $\tau$  is

$$\tau = \frac{2\pi}{\omega} . \quad (2.3)$$

The maximum value that y may have is called the amplitude.

Now take as an example a two-degree of freedom system as shown in Fig. 2.2. The combined stiffness of the columns for each story corresponds to the spring constant for that story. The sum of the mass of the floor, walls and columns for each story corresponds to the mass for that story. The building is idealized as shown in Fig. 2.2(b). Again by Newton's principle the differential equations for free vibration for the configuration shown in Fig. 2.2(c) are

$$m_1 \frac{d^2 y_1}{dt^2} + k_1 y_1 - k_2 (y_1 - y_2) = 0 , \quad (2.4)$$

and

$$m_2 \frac{d^2 y_2}{dt^2} + k_2 (y_2 - y_1) = 0 .$$

Eqs. (2.4) may be solved by means of the Laplace Transform or by some other method. Since the object is to arrive at the differential equations in this stage of this study, the solutions of eqs. (2.4) are not discussed at this point.

A three-degree of freedom system may be exemplified by a three-story building. The building may also be idealized in the same manner as in the example in Fig. 2.2.

Eq. (2.1) and eqs. (2.4) can also be derived by means of Lagrange's equation. This equation is

$$\frac{d}{dt} \left( \frac{\partial T}{\partial \dot{q}_j} \right) - \frac{\partial T}{\partial q_j} + \frac{\partial U}{\partial q_j} = Q_j, \quad (2.5)$$

where

$T$  = total kinetic energy of the whole system,

$q_j$  =  $j^{\text{th}}$  generalized co-ordinate,

$U$  = total potential energy of the whole system, which is a function of the configuration of the system only,

$\dot{q}_j$  =  $dq_j/dt$ ,

$Q_j$  =  $j^{\text{th}}$  generalized force, which is a function of time only.

In the example shown in Fig. 2.1, we may regard  $y$  as the generalized co-ordinate  $q$ . The expression for the kinetic energy  $T$  is

$$T = \frac{1}{2} m_1 \dot{y}^2,$$

where

$$\dot{y} = \frac{dy}{dt},$$

and

$$\frac{\partial T}{\partial \dot{q}_j} = \frac{\partial T}{\partial \dot{y}} = m_1 \dot{y},$$

$$\frac{d}{dt} \left( \frac{\partial T}{\partial \dot{q}_j} \right) = \frac{d}{dt} \left( \frac{\partial T}{\partial \dot{y}} \right) = m_1 \ddot{y}, \quad (2.6)$$

where

$$\ddot{y} = \frac{d^2 y}{dt^2}.$$

Also,

$$\frac{\partial T}{\partial q_j} = \frac{\partial T}{\partial y} = 0, \quad (2.7)$$

since  $T$  does not contain  $y$  explicitly. The expression for the potential energy  $U$  is

$$U = \frac{1}{2} ky^2,$$

and so

$$\frac{\partial U}{\partial q_j} = \frac{\partial U}{\partial y} = ky. \quad (2.8)$$

The values of  $Q_j$  as explained before depend only on forces which are functions of time only. Since there are no damping and applied forces in this example, the generalized force is zero, that is,

$$Q_j = 0 . \quad (2.9)$$

Substitution of eqs. (2.6), (2.7), (2.8), and (2.9) into eq. (2.5) yields

$$m_1 \frac{d^2y}{dt^2} + ky = 0 , \quad (2.10)$$

which is the same as eq. (2.2).

In the example shown in Fig. 2.2,

$$T = \frac{1}{2} m_1 \dot{y}_1^2 + \frac{1}{2} m_2 \dot{y}_2^2 , \quad (2.11)$$

and

$$U = \frac{1}{2} k_1 y_1^2 + \frac{1}{2} k_2 (y_2 - y_1)^2 . \quad (2.12)$$

Differentiation of  $T$  with respect to  $\dot{q}_1$  or  $\dot{y}_1$  gives

$$\frac{\partial T}{\partial \dot{q}_1} = \frac{\partial T}{\partial \dot{y}_1} = m_1 \dot{y}_1 .$$

Thus,

$$\frac{d}{dt} \left( \frac{\partial T}{\partial \dot{q}_1} \right) = \frac{d}{dt} \left( \frac{\partial T}{\partial \dot{y}_1} \right) = m_1 \ddot{y}_1 , \quad (2.13)$$

and

$$\frac{\partial T}{\partial q_1} = \frac{\partial T}{\partial y_1} = 0 . \quad (2.13a)$$

Differentiation of  $U$  with respect to  $q_1$  yields

$$\frac{\partial U}{\partial q_1} = \frac{\partial U}{\partial y_1} = k_1 y_1 - k_2 (y_1 - y_2) . \quad (2.14)$$

Furthermore,

$$Q_1 = 0 . \quad (2.14a)$$

Therefore, eq. (2.5) becomes,

$$m_1 \ddot{y}_1 + k_1 y_1 - k_2 (y_1 - y_2) = 0 , \quad (2.15)$$



which is the same as the first equation of eqs. (2.4). Similarly,

$$\frac{\partial T}{\partial \dot{q}_2} = \frac{\partial T}{\partial \dot{y}_2} = m_2 \dot{y}_2 ,$$

$$\frac{d}{dt} \left( \frac{\partial T}{\partial \dot{q}_2} \right) = \frac{d}{dt} \left( \frac{\partial T}{\partial \dot{y}_2} \right) = m_2 \ddot{y}_2 ,$$

$$\frac{\partial T}{\partial q_2} = \frac{\partial T}{\partial y_2} = 0 ,$$

$$\frac{\partial U}{\partial q_2} = \frac{\partial U}{\partial y_2} = k_2 (y_2 - y_1) ,$$

$$Q_2 = 0 .$$

Therefore, eq. (2.5) becomes

$$m_2 \ddot{y}_2 + k_2 (y_2 - y_1) = 0 , \quad (2.16)$$

which is the same as the second equation of eqs. (2.4).

In the examples given above, in the derivation for the expressions for the kinetic and potential energies the vertical component of the motion of the system is neglected. This assumption can be applied to all systems with horizontal oscillations which are large compared to the vertical oscillations.

The differential equations of motion may also be checked by Lagrange's set of equations for any system. Treatments of more complicated systems may be found in books on advanced vibrations or dynamics. The advantages of Lagrange's equation are not apparent in the examples given above. Advantages will appear if one deals with "normal co-ordinates" which are defined and exemplified by an example below.

The lateral vibration of a beam is analyzed (6) with the following assumptions:

(1) The cross section of the beam is small compared to its length so that the effect of shear and rotary inertia on the configuration of the beam may be neglected.

(2) The beam is elastic.

The beam equations below are found in books on mechanics of vibration (5):

$$EI \frac{\partial^2 y}{\partial x^2} = -M, \quad (2.17)$$

$$\frac{d}{dx} \left( EI \frac{\partial^2 y}{\partial x^2} \right) = -\frac{dM}{dx} = -V, \quad (2.18)$$

$$\frac{d^2}{dx^2} \left( EI \frac{\partial^2 y}{\partial x^2} \right) = -\frac{dV}{dx} = W, \quad (2.19)$$

where

E = Young's modulus of elasticity,

I = moment of inertia,

x = distance from base to a general point P on neutral axis of bending,

y = lateral displacement of neutral axis of bending,

M = bending moment,

V = shear,

W = load per unit length.

If the beam is vibrating, the load per unit length W of eq. (2.19) is the inertia force per unit length. By Newton's principle the load per unit length is

$$W = -\frac{w}{g} \frac{\partial^2 y}{\partial t^2} = -m \frac{\partial^2 y}{\partial t^2}, \quad (2.20)$$

where

w = weight per unit length,

t = time variable,

m = mass per unit length along the beam.

The negative sign in eq. (2.20) is from the fact that the direction of the inertia force is opposite the direction of the acceleration. Substitution of eq. (2.20) into eq. (2.19) yields

$$\frac{\partial^2}{\partial x^2} \left( EI \frac{\partial^2 y}{\partial x^2} \right) = -m \frac{\partial^2 y}{\partial t^2}, \quad (2.21)$$

which is the general equation for the free lateral vibration of beams without damping.

If the flexural rigidity  $EI$  and the cross sectional area of the beam are constant eq. (2.21) becomes

$$EI \frac{\partial^4 y}{\partial x^4} = -m \frac{\partial^2 y}{\partial t^2},$$

or

$$a^2 \frac{\partial^4 y}{\partial x^4} + \frac{\partial^2 y}{\partial t^2} = 0, \quad (2.22)$$

where

$$a^2 = \frac{EI}{m}. \quad (2.23)$$

Particular solutions of eq. (2.22) are of the type (7)

$$y = Z(x) q(t), \quad (2.24)$$

where  $Z(x)$  is a function of  $x$  alone and  $q(t)$  is a function of  $t$  alone.

From eq. (2.24) one obtains

$$\frac{\partial y}{\partial x} = \dot{Z}q, \quad \frac{\partial^4 y}{\partial x^4} = \dots Zq, \quad (2.25)$$

$$\frac{\partial y}{\partial t} = Z\dot{q} \quad \frac{\partial^2 y}{\partial t^2} = Z\ddot{q}.$$

Substitution of eqs. (2.25) into eq. (2.22) gives

$$a^2 \ddot{Z}q = -Z\ddot{q}. \quad (2.26)$$

By separation of variables, eq. (2.26) becomes

$$\frac{\ddot{Z}}{Z} = -\frac{1}{a^2} \frac{\ddot{q}}{q}. \quad (2.27)$$

Since the left-hand side of eq. (2.27) can not vary with  $t$  and the right-hand side can not vary with  $x$ , both sides of eq. (2.27) must be equal to a constant. Call this constant  $\gamma$ , so that

$$\ddot{Z} - \gamma Z = 0, \quad (2.28)$$

and

$$\ddot{q} + \gamma a^2 q = 0. \quad (2.29)$$

By means of the theory of ordinary differential equations the solution of eq. (2.29) is

$$q = A \cos \omega t + B \sin \omega t, \quad (2.30)$$

where

$$\omega = \sqrt{\gamma a^2}. \quad (2.31)$$

The constant  $\omega$  is called the natural frequency and the constants  $A$  and  $B$  are determined by the boundary conditions. The solution of eq. (2.28) is

$$Z = C \sin \alpha x + D \cos \alpha x + E \sinh \alpha x + F \cosh \alpha x, \quad (2.32)$$

where

$$\alpha^4 = \frac{\omega^2}{a^2}. \quad (2.33)$$

For a cantilever beam whose clamped end is at  $x = 0$ , the boundary conditions are:

$$\left. \begin{aligned} (1) \quad (Z)_{x=0} &= 0, \text{ since the deflection at the clamped end is zero.} \\ (2) \quad (dZ/dx)_{x=0} &= 0, \text{ since the slope at the clamped end is zero.} \\ (3) \quad (d^2Z/dx^2)_{x=h} &= 0, \text{ since the bending moment at the free end is zero.} \\ (4) \quad (d^3Z/dx^3)_{x=h} &= 0, \text{ since the shear at the free end is zero.} \end{aligned} \right\} (2.34)$$

Substitution of the four boundary conditions above into the general solution in eq. (2.32) gives the frequency equation

$$\cos \alpha h \cosh \alpha h = -1. \quad (2.35)$$

The roots of eq. (2.35) can be determined by series expansion of  $\cos \alpha h$  and  $\cosh \alpha h$ . As soon as the different values of  $\alpha_j$  are known, the corresponding characteristic function or mode shape  $Z_j$  can be obtained from eq. (2.32). The corresponding natural frequency  $\omega_j$  can be obtained from eq. (2.33). Thus, the constants in eq. (2.32) become  $C_j$ ,  $D_j$ ,  $E_j$ , and  $F_j$  are also determined by the boundary conditions of the beam. It has been shown (7) that the characteristic functions  $Z_j$  form an orthogonal set with respect to the weight function  $m$  over the interval from 0 to  $h$ , that is,

$$\int_0^h m Z_r Z_s dx = 0, \quad \text{when } r \neq s. \quad (2.36)$$

By superimposing all possible solutions of the type

$$y_j = Z_j(x) q_j(t),$$

the general equation for the free lateral vibration of a uniform cantilever beam without damping becomes

$$y = \sum_{j=1}^{\infty} Z_j (A_j \cos \omega_j t + B_j \sin \omega_j t). \quad (2.37)$$

Therefore, the equation for the  $j^{\text{th}}$  mode of vibration from eq. (2.37) is

$$y_j = Z_j (A_j \cos \omega_j t + B_j \sin \omega_j t). \quad (2.37a)$$

Differentiation of eq. (2.37a) twice with respect to time gives

$$\frac{\partial^2 y_j}{\partial t^2} = -\omega_j^2 Z_j (A_j \cos \omega_j t + B_j \sin \omega_j t),$$

or

$$\frac{\partial^2 y_j}{\partial t^2} = -\omega_j^2 y_j. \quad (2.38)$$

But from eq. (2.37a)

$$Z_j = \text{maximum value of } |y_j|, \quad (2.38a)$$

if  $\sqrt{A_j^2 + B_j^2} = 1$  or if the maximum value of  $|q_j| = 1$ ,

so that the differential equation for the  $j^{\text{th}}$  mode of vibration becomes

$$\frac{\partial^2}{\partial x^2} \left( EI \frac{\partial^2 Z_j}{\partial x^2} \right) = -m\omega_j^2 Z_j . \quad (2.38b)$$

Equation (2.38b) may be solved by the Stodola-Newmark method.

The first step is to assume  $Z_j$ . Then multiply the assumed deflection curve  $Z_j$  by  $-m\omega_j^2$  and integrate the product twice with respect to  $x$ . The result of the double integration is equal to  $EI (\partial^2 Z_j / \partial x^2)$ . Divide the result of the double integration by  $EI$  and then integrate twice. The final result is the derived deflection curve. If the derived deflection curve for  $Z_j$  is the same as the assumed deflection curve, then the assumed  $Z_j$  is the  $j^{\text{th}}$  mode shape. The Stodola-Newmark integration method is used in this study, and the method is explained in detail in Chapters IV and V.

If a maximum value of, say, unity is assigned to  $Z_j$  at the top or free end of the beam, the deflection factors along the beam in terms of unity at the top are obtained. Corresponding to the unit deflection factor at the top of the beam for a particular mode are the shear and bending moment factors. These deflection, bending moment, and shear factors are also discussed in detail in Chapters IV and V.

Now consider the case where there is ground motion during an earthquake. Let

$y_b(t)$  = motion of the base,

$Y_x(t)$  = horizontal absolute motion of the  $x^{\text{th}}$  point along the neutral axis of the bending of the beam,

$y_x(t)$  = motion of the  $x^{\text{th}}$  point relative to the base.

Thus,

$$Y_x(t) = y_b(t) + y_x(t) .$$

Since the inertia force in eq. (2.21) is based on absolute acceleration, eq. (2.21) becomes

$$\frac{\partial^2}{\partial x^2} \left( EI \frac{\partial^2 y}{\partial x^2} \right) = -m \left( \frac{\partial^2 y}{\partial t^2} + \frac{\partial^2 y_b}{\partial t^2} \right) \quad (2.39)$$

Based upon the experience derived from the separation of variables in the case of free vibration, let a solution of eq. (2.39) with the boundary conditions in eq. (2.34) also be of the form

$$y = Z(x) q(t), \quad (2.40)$$

where, as before,  $Z_j(x)$  is a function of  $x$  alone and  $q_j(t)$  is a function of  $t$  alone. Hence,

$$\begin{aligned} \frac{\partial y}{\partial t} &= Z \frac{\partial q}{\partial t} = Z \dot{q}, & \frac{\partial^2 y}{\partial t^2} &= Z \frac{\partial^2 q}{\partial t^2} = Z \ddot{q}, \\ \frac{\partial y}{\partial x} &= \frac{\partial Z}{\partial x} q = \dot{Z} q, & \frac{\partial^2 y}{\partial x^2} &= \frac{\partial^2 Z}{\partial x^2} q = \ddot{Z} q. \end{aligned} \quad (2.41)$$

Substitution of eq. (2.41) into eq. (2.39) gives

$$\frac{1}{m} \frac{\partial^2}{\partial x^2} (EI \ddot{Z} q) = - (\ddot{Z} q + \ddot{y}_b). \quad (2.42)$$

Direct separation of variables can not be used in eq. (2.42). Therefore we resort to Lagrange's equations.

In eq. (2.40), Timoshenko (6) has shown that  $Z_j$  and  $\dot{Z}_j$  are orthogonal functions with respect to the weight function  $m$ , i.e.,

$$\int_0^h m Z_r(x) Z_s(x) dx = 0, \quad \text{when } r \neq s, \quad (2.43)$$

and

$$\int_0^h m \dot{Z}_r(x) \dot{Z}_s(x) dx = 0, \quad \text{when } r \neq s. \quad (2.43a)$$

Now, let

$$y_j = Z_j(x) q_j(t)$$

be a solution of eq. (2.39). Superimposition of all the possible solutions gives the general solution

$$y = \sum_{j=1}^{\infty} Z_j q_j . \quad (2.44)$$

For free vibration  $\dot{Q}_j = 0$ , so that Lagrange's equation becomes

$$\frac{d}{dt} \left( \frac{\partial T}{\partial \dot{q}_j} \right) - \frac{\partial T}{\partial q_j} + \frac{\partial U}{\partial q_j} = 0 . \quad (2.45)$$

From elementary strength of materials, the expression for the potential energy of a bent beam is

$$U = \int_0^h \frac{1}{2} M \frac{d\theta}{dx} dx , \quad (2.46)$$

where

$M$  = bending moment,

$\theta$  = slope.

But,

$$M = -EI \frac{\partial^2 y}{\partial x^2} ,$$

and

$$d\theta = -\frac{1}{EI} M dx = + \frac{\partial^2 y}{\partial x^2} dx .$$

Therefore, eq. (2.46) becomes

$$U = \frac{1}{2} \int_0^h EI \left( \frac{\partial^2 y}{\partial x^2} \right)^2 dx , \quad (2.47)$$

or,

$$U = \frac{1}{2} \int_0^h EI \left( \sum_{j=1}^{\infty} \dot{Z}_j q_j \right)^2 dx , \quad (2.47a)$$

or,

$$U = \frac{1}{2} \int_0^h EI \left( \ddot{Z}_1 q_1 + \ddot{Z}_2 q_2 + \ddot{Z}_3 q_3 + \dots + \ddot{Z}_{\infty} q_{\infty} \right)^2 dx . \quad (2.47b)$$

Since  $EI$  can be expressed in terms of a constant times  $m$ , the terms containing the products  $\dot{Z}_r \dot{Z}_s$  when  $r$  is not equal to  $s$  vanish according to eq. (2.43a). Therefore, the expression for the potential energy becomes



$$U = \frac{1}{2} \int_0^h EI \sum_{j=1}^{\infty} \dot{Z}_j^2 q_j^2 dx . \quad (2.48)$$

Since  $\dot{Z}_j$  are functions of  $x$  alone and  $q_j$  are functions of  $t$  alone, eq. (2.48) becomes

$$U = \frac{1}{2} \sum_{j=1}^{\infty} q_j^2 \int_0^h EI (\dot{Z}_j)^2 dx , \quad (2.48a)$$

and for a uniform beam,  $EI$  is constant, thus eq. (2.48a) becomes

$$U = \frac{EI}{2} \sum_{j=1}^{\infty} q_j^2 \int_0^h (\dot{Z}_j)^2 dx . \quad (2.48b)$$

Hence, for a uniform beam,

$$\frac{\partial U}{\partial q_j} = EI q_j \int_0^h \dot{Z}_j^2 dx . \quad (2.49)$$

The kinetic energy  $T$  of a beam during free vibration is

$$T = \frac{1}{2} \int_0^h m \left( \frac{\partial y}{\partial t} \right)^2 dx , \quad (2.50)$$

or,

$$T = \frac{1}{2} \int_0^h m \left( \sum_{j=1}^{\infty} Z_j \dot{q}_j \right)^2 dx , \quad (2.50a)$$

or,

$$T = \frac{1}{2} \int_0^h m (Z_1 \dot{q}_1 + Z_2 \dot{q}_2 + Z_3 \dot{q}_3 + \dots + Z_{\infty} \dot{q}_{\infty})^2 dx . \quad (2.50b)$$

Again, From eq. (2.43) the terms containing  $Z_r Z_s$  vanish when  $r \neq s$ .

Therefore, the expression for the kinetic energy  $T$  is

$$T = \frac{1}{2} \int_0^h m \sum_{j=1}^{\infty} Z_j^2 \dot{q}_j^2 dx . \quad (2.51)$$

Since  $Z_j$  are functions of  $x$  alone and  $\dot{q}_j^2$  are functions of  $t$  alone, eq. (2.51) becomes

$$T = \frac{1}{2} \sum_{j=1}^{\infty} \dot{q}_j^2 \int_0^h m Z_j^2 dx . \quad (2.51a)$$

For a uniform beam  $m$  is constant, and

$$T = \frac{1}{2} m \sum_{j=1}^{\infty} \dot{q}_j^2 \int_0^h Z_j^2 dx, \quad (2.51b)$$

also

$$\frac{\partial T}{\partial \dot{q}_j} = m \dot{q}_j \int_0^h Z_j^2 dx. \quad (2.52)$$

Also

$$\frac{d}{dt} \left( \frac{\partial T}{\partial \dot{q}_j} \right) = m \ddot{q}_j \int_0^h Z_j^2 dx, \quad (2.53)$$

and

$$\frac{\partial T}{\partial q_j} = 0. \quad (2.54)$$

Therefore, Lagrange's equation for the  $j$ th mode free vibration of a uniform beam without damping becomes

$$\dot{q}_j m \int_0^h Z_j^2 dx - q_j EI \int_0^h Z_j^{\cdot\cdot}{}^2 dx = 0, \quad (2.55)$$

or,

$$\ddot{q}_j + a^2 \gamma_j q_j = 0, \quad (2.55a)$$

where

$$a^2 = \frac{EI}{m},$$

$$\gamma_j = - \frac{\int_0^h Z_j^{\cdot\cdot}{}^2 dx}{\int_0^h Z_j^2 dx}.$$

It is interesting to note that eq. (2.55a) is the same as eq. (2.29).

This shows clearly the advantage of using Lagrange's equations together with the orthogonal conditions of the mode shapes which is the reduction of the problem to solve one differential equation for  $q_j$  at a time, provided the mode shapes and the natural frequencies are known.

In eq. (2.55a) let the natural frequency

$$\omega_j = \sqrt{a^2 \gamma_j} , \quad (2.56)$$

thus (2.55a) becomes

$$\ddot{q}_j + \omega_j^2 q_j = 0 , \quad (2.57)$$

whose solution by the theory of ordinary differential equation is

$$q_j = A_j \cos \omega_j t + B_j \sin \omega_j t . \quad (2.58)$$

The constants  $A_j$  and  $B_j$  are determined by the boundary conditions.

Therefore, the equation for free vibration of a uniform beam without damping is the sum of all possible solutions, i.e.,

$$y = \sum_{j=1}^{\infty} Z_j (A_j \cos \omega_j t + B_j \sin \omega_j t) , \quad (2.59)$$

which is again the same as the solution given by eq. (2.37) which is obtained by direct separation of variables.

Now, consider the case during an earthquake. The expression for the potential energy will remain the same. The kinetic energy  $T$  will be different because the kinetic energy is based on absolute velocity. The kinetic energy becomes

$$T = \frac{1}{2} \int_0^h m (\dot{Y})^2 dx , \quad (2.60)$$

or,

$$T = \frac{1}{2} \int_0^h m [\dot{y}_b + \sum_{j=1}^{\infty} Z_j \dot{q}_j]^2 dx , \quad (2.60a)$$

or,

$$T = \frac{1}{2} \int_0^h m [\dot{y}_b + Z_1 \dot{q}_1 + Z_2 \dot{q}_2 + Z_3 \dot{q}_3 + \dots + Z_{\infty} \dot{q}_{\infty}]^2 dx \quad (2.60b)$$

Again, from eq. (2.43) the terms containing  $Z_r Z_s$  vanish when  $r \neq s$ .

Therefore, the expression for the kinetic energy during an earthquake is

$$T = \frac{1}{2} \int_0^h m (\dot{y}_b + \sum_{j=1}^{\infty} Z_j \dot{q}_j)^2 dx, \quad (2.61)$$

or,

$$T = \frac{1}{2} \int_0^h m \sum_{j=1}^{\infty} (\dot{y}_b^2 + 2\dot{y}_b Z_j \dot{q}_j + Z_j^2 \dot{q}_j^2) dx, \quad (2.61a)$$

or,

$$T = \frac{1}{2} \int_0^h m \dot{y}_b^2 dx + \int_0^h m \sum_{j=1}^{\infty} \dot{y}_b Z_j \dot{q}_j dx + \frac{1}{2} \int_0^h m \sum_{j=1}^{\infty} Z_j^2 \dot{q}_j^2 dx, \quad (2.61b)$$

or,

$$T = \frac{1}{2} \dot{y}_b^2 \int_0^h m dx + \dot{y}_b \sum_{j=1}^{\infty} \dot{q}_j \int_0^h m Z_j dx + \frac{1}{2} \sum_{j=1}^{\infty} \dot{q}_j^2 \int_0^h m Z_j^2 dx. \quad (2.62)$$

The kinetic energy for a uniform beam during an earthquake is

$$T = \frac{1}{2} m \dot{y}_b^2 \int_0^h dx + m \dot{y}_b \sum_{j=1}^{\infty} \dot{q}_j \int_0^h Z_j dx + \frac{1}{2} m \sum_{j=1}^{\infty} \dot{q}_j^2 \int_0^h Z_j^2 dx. \quad (2.63)$$

Also, for a uniform beam,

$$\frac{\partial T}{\partial \dot{q}_j} = m \dot{y}_b \int_0^h Z_j dx + m \dot{q}_j \int_0^h Z_j^2 dx, \quad (2.64)$$

$$\frac{d}{dt} \left( \frac{\partial T}{\partial \dot{q}_j} \right) = m \ddot{y}_b \int_0^h Z_j dx + m \ddot{q}_j \int_0^h Z_j^2 dx, \quad (2.65)$$

and

$$\frac{\partial T}{\partial q_j} = 0. \quad (2.66)$$

Therefore, Lagrange's equation for the  $j$ th mode during an earthquake without damping becomes

$$m \ddot{y}_b \int_0^h Z_j dx + m \ddot{q}_j \int_0^h Z_j^2 dx - q_j EI \int_0^h \ddot{Z}_j^2 dx = 0, \quad (2.67)$$

or,

$$\ddot{q}_j - \frac{EI \int_0^h \ddot{Z}_j^2 dx}{m \int_0^h Z_j^2 dx} q_j = - \frac{m \int_0^h Z_j dx}{m \int_0^h Z_j^2 dx} \ddot{y}_b, \quad (2.67a)$$

or,

$$\ddot{q}_j + \omega_j^2 q_j = -\Gamma_j \ddot{y}_b, \quad (2.67b)$$

where

$$\Gamma_j = \frac{m \int_0^h Z_j dx}{m \int_0^h Z_j^2 dx}. \quad (2.68)$$

Now take the case of a tall tapered chimney. A tall tapered chimney may be considered as a slender cantilever beam provided the foundation is rigid. Therefore, the steps in the analysis will be the same as the steps for the uniform beam. The modification required is to use the general expressions for U and T. The potential energy

U becomes

$$U = \frac{1}{2} \sum_{j=1}^{\infty} q_j^2 \int_0^h EI \dot{Z}_j^2 dx, \quad (2.48a)$$

and

$$\frac{\partial U}{\partial q_j} = q_j \int_0^h EI \dot{Z}_j^2 dx. \quad (2.69)$$

The kinetic energy T becomes

$$T = \frac{1}{2} \dot{y}_b^2 \int_0^h m dx + \dot{y}_b \sum_{j=1}^{\infty} \dot{q}_j \int_0^h m Z_j dx + \frac{1}{2} \sum_{j=1}^{\infty} \dot{q}_j^2 \int_0^h m Z_j^2 dx, \quad (2.62)$$

and

$$\frac{\partial T}{\partial \dot{q}_j} = \dot{y}_b \int_0^h m Z_j dx + \dot{q}_j \int_0^h m Z_j^2 dx \quad (2.70)$$

Thus,

$$\frac{d}{dt} \left( \frac{\partial T}{\partial \dot{q}_j} \right) = \ddot{y}_b \int_0^h m Z_j dx + \ddot{q}_j \int_0^h m Z_j^2 dx, \quad (2.71)$$

and

$$\frac{\partial T}{\partial q_j} = 0. \quad (2.72)$$

Hence, Lagrange's equation for the jth mode of a tall tapered chimney during an earthquake without damping is

$$\ddot{y}_b \int_0^h mZ_j dx + \dot{q}_j \int_0^h mZ_j^2 dx - q_j \int_0^h EI\ddot{Z}_j^2 dx = 0, \quad (2.73)$$

or,

$$\ddot{q}_j + \omega_j^2 q_j = -\Gamma_j \dot{y}_b, \quad (2.73a)$$

where

$$\omega_j^2 = -\frac{\int_0^h EI \dot{Z}_j^2 dx}{\int_0^h mZ_j^2 dx}, \quad (2.74)$$

$$\Gamma_j = \frac{\int_0^h mZ_j dx}{\int_0^h mZ_j^2 dx}. \quad (2.75)$$

The practice in taking damping into account is to introduce damping assumed effectively to be viscous, for each mode. This is done by introducing a fraction of critical damping for the particular mode. The term is  $2\beta_j \omega_j \dot{q}_j$ , where  $\beta_j$  is the fraction of critical damping. This damping term is discussed in detail in Chapter III.

With the viscous damping term, eq. (2.73a) becomes

$$\ddot{q}_j + 2\beta_j \omega_j \dot{q}_j + \omega_j^2 q_j = -\Gamma_j \ddot{y}_b. \quad (2.76)$$

Let

$$\phi_j = \frac{q_j}{\Gamma_j}.$$

Thus, eq. (2.76) becomes

$$\ddot{\phi}_j + 2\beta_j \omega_j \dot{\phi}_j + \omega_j^2 \phi_j = -\ddot{y}_b. \quad (2.76a)$$

Eq. (2.76a) may be solved either by the Laplace Transform method, Newmark's step by step method, or by the use of the electronic analogue computer. Since the function on the right hand side of eq. (2.76a) does not follow a simple algebraic or trigonometric function and since there are infinite values of  $\omega_j$ , the electronic analogue computer is used. However, for the sake of completeness, the procedures for the first two methods are explained in Chapter V.

Therefore, the general solution of the tall tapered chimney with damping during an earthquake is

$$y = \sum_{j=1}^{\infty} Z_j \Gamma_j \phi_j . \quad (2.77)$$

The procedures in getting the values of  $Z_j$  and  $\Gamma_j$  are explained in detail in Chapters III and IV. In getting the values of  $Z_j$ , the corresponding Shear  $V_j$  and Bending Moment  $M_j$  factors for a unit  $Z_j$  at the top of the stack are also derived. Hence, if the shear  $V_j$  and moment  $M_j$  factors for each mode are known, then the total shear  $V$  and moment  $M$  may be obtained by adding the effect of each mode, i.e.,

$$V = \sum_{j=1}^{\infty} V_j y e_j = \sum_{j=1}^{\infty} V_j \Gamma_j \phi_j , \quad (2.78)$$

and

$$M = \sum_{j=1}^{\infty} M_j \Gamma_j \phi_j . \quad (2.79)$$

The advantage of this approach is the fact that the deflection, shear, and moment factors for each mode are based on the structural properties only. Hence, these factors can be studied separately. The generalized co-ordinates  $\phi_j$  depend on the frequencies, damping and accelerographs only. Therefore,  $\phi_j$  may be studied directly by changing the values of damping and natural frequencies for a particular accelerograph. The values of damping to be used in this study are 5% and 7-1/2% of critical damping. With the above values of critical damping, the values of  $\phi_j$  for different periods of the chimney, say from 0.3 to 3.0 seconds per cycle, are obtained.

If the response curves for  $\phi_j$  are available then the shear and bending moment curves along the chimney at different time instances may be obtained. The next step is to draw envelopes of these shear and

bending moment curves and these values compared with the shear and bending moment curves as obtained by using the ACI specifications. These steps are explained in detail in Chapter VI.



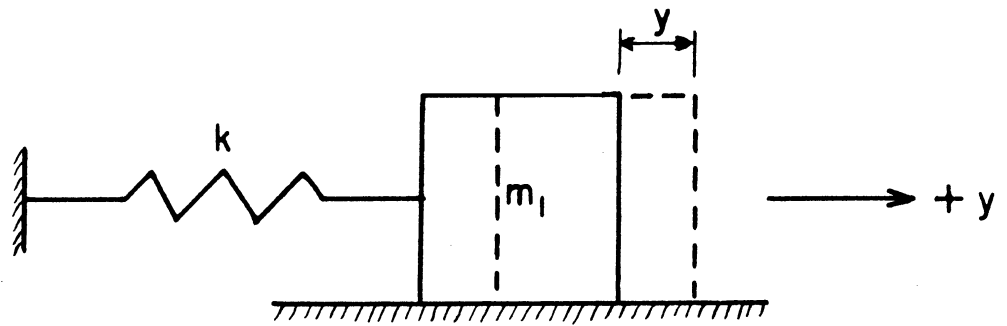


FIG. 2.1. SINGLE DEGREE OF FREEDOM SYSTEM.

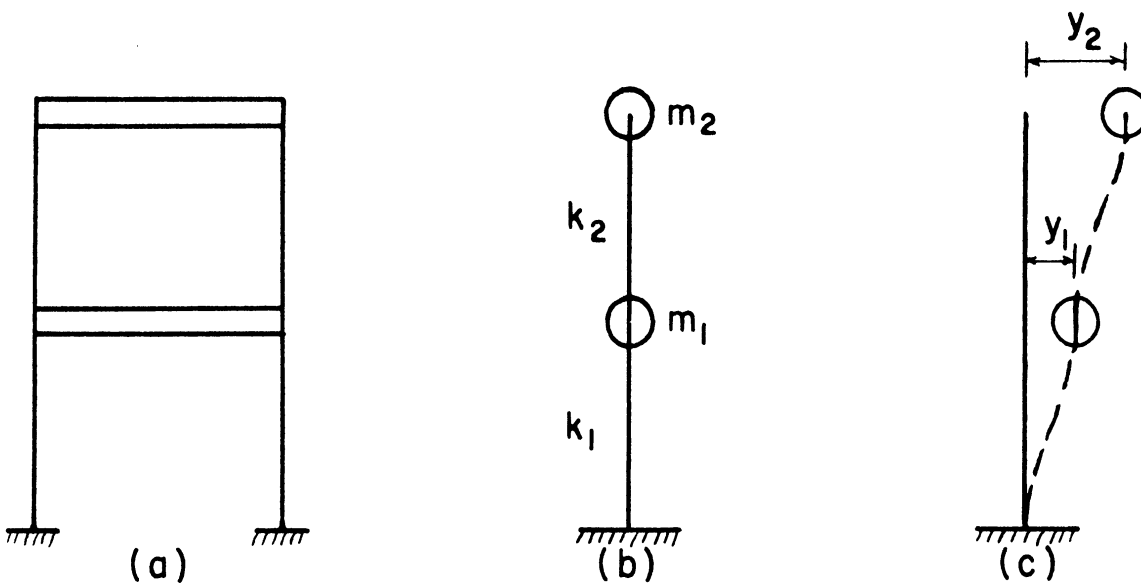


FIG. 2.2. TWO DEGREE OF FREEDOM SYSTEM.

## CHAPTER III

### DYNAMIC STRUCTURAL PROPERTIES: FUNDAMENTAL MODE

Any elastic curve  $y(x)$  which may be induced in the stack can be split up into a series of "orthogonal" curves (8).

As stated in Chapter II, the first step in the solution of eq. (2.21) is to find the orthogonal elastic curves.

To find these elastic curves ( $Z_j$ ) which are oftentimes called mode shapes, Stodola's method is essentially used. A modification based upon Newmark's assumption of regional parabolic shape of elastic and inertia load curves are used in the integration processes to find the derived elastic curve.

This modified Stodola's method for the first mode is briefly divided into different steps below:

1. Divide the stack into equal segments and then record the mass intensities, moment of inertias, and length of each segment;
2. Assume a reasonable deflection curve  $Z_1(x)$ ;
3. Multiply the assumed deflections by the product of the mass and the square of the unknown frequency. The result of this operation is the assumed inertia load per unit length  $m_{0j}^2 Z_1$ . Equivalent concentrated inertia loads are computed and the results are added to the additional concentrated inertia loads due to the concentrated masses. Newmark's method of integration is used to get the equivalent concentrated inertia loads from the inertia load per unit length;
4. With the concentrated inertia loads, the deflection curve  $Z_1$  is obtained by means of the Newmark's method. Newmark's method of obtaining the deflection curve is explained in later paragraphs;

5. Repetition of steps (2), (3), and (4) until the derived deflection curve obtained from the assumed inertia load coincides with the assumed deflection curve. It is shown later that this procedure converges rapidly;

6. To obtain the natural frequency from the derived deflection curve.

The procedures for the second and higher modes of vibration are discussed in the next chapter.

The different steps in the Stodola-Newmark's method for the fundamental mode of vibration are now discussed in detail:

1. The first step simply requires straightforward computations, that is, by dividing the stack, say, into ten equal segments. Then compute the mass per unit length and the moment of inertias for each segment. Concentrated masses are recorded separately. In this chapter an example is given. The data and results are given in Fig. 3.2 at the end of this chapter. Note that in Fig. 3.2 there is a column at the extreme right marked "Multiplier". This multiplier is used simply to avoid large figures.

2. The second step is to assume a reasonable deflection curve  $Z_1$ . This assumed deflection curve must be based upon previous studies made in this field. Since there is hardly any data available regarding the natural mode shapes of tapered chimneys, it is hoped that this study will be of some use, at least as a guide for this purpose as well as in analysis and design.

3. The third step is the computation of the inertia load. The inertia load, if damping is neglected, is equal to the right side of eq. (2.38b). Equation (2.38b) is

$$\frac{\partial^2}{\partial x^2} \left( EI \frac{\partial^2 Z_j}{\partial x^2} \right) = -m\omega_j^2 Z_j . \quad (2.38b)$$

However, for purposes of comparison, damping which is assumed to be effectively "viscous" is now taken into account. The  $j$ th mode equation for free vibration with damping from eq. (2.40) is

$$y_j = Z_j q_j . \quad (2.40)$$

The differential equation for  $q_j$  is

$$\ddot{q}_j + 2\beta_j \omega_j \dot{q}_j + \omega_j^2 q_j = 0 . \quad (3.1)$$

Let

$$\psi_j = 2\beta_j \omega_j . \quad (3.2)$$

Thus, eq. (3.1) becomes

$$\ddot{q}_j + \psi_j \dot{q}_j + \omega_j^2 q_j = 0 . \quad (3.3)$$

The Laplace transform method is used to solve eq. (3.3). The symbols used by Churchill (9) are also used. Thus, eq. (3.3) takes the form

$$s^2 q_j(s) - s q_j(0) - \dot{q}_j(0) + \psi_j s q_j(s) - \psi_j q_j(0) + \omega_j^2 q_j(s) = 0 . \quad (3.4)$$

Let

$$\begin{aligned} c_1 &= q_j(0) , \\ c_2 &= \dot{q}_j(0) . \end{aligned} \quad (3.5)$$

Then eq. (3.4) becomes

$$q_j(s) = \frac{c_2}{(s^2 + \frac{\psi_j}{2})^2 + (\omega_j^2 - \frac{1}{4} \psi_j^2)} + \frac{c_1 s}{(s^2 + \frac{\psi_j}{2})^2 + (\omega_j^2 - \frac{1}{4} \psi_j^2)} . \quad (3.5a)$$

Let

$$\omega_j' = \sqrt{\omega_j^2 - (1/4) \psi_j^2} . \quad (3.5b)$$

Thus eq. (3.5a) becomes

$$q_j(s) = \frac{1}{\omega_j'} \frac{c_2}{(s^2 + \frac{1}{2} \psi_j)^2 + (\omega_j')^2} + \frac{c_1 (s + \frac{1}{2} \psi_j) - \frac{1}{2} c_1 \psi_j}{(s^2 + \frac{1}{2} \psi_j)^2 + (\omega_j')^2} \quad (3.5c)$$

or,

$$\begin{aligned}
 \ddot{d}_j = & \left[ \frac{c_2}{\omega'_j} e^{-\beta_j \omega_j t} \sin \omega'_j t \right] [-(\omega'_j)^2 + \beta_j^2 \omega_j^2] + \\
 & + \left[ \frac{c_2}{\omega'_j} e^{-\beta_j \omega_j t} \cos \omega'_j t \right] [-2\beta_j \omega'_j \omega_j] \\
 & + \left[ -\frac{\beta_j c_1}{\omega'_j} e^{-\beta_j \omega_j t} \sin \omega'_j t \right] [-(\omega'_j)^2 + \beta_j^2 \omega_j^2] \\
 & + \left[ -\frac{\beta_j c_1}{\omega'_j} e^{-\beta_j \omega_j t} \cos \omega'_j t \right] [-2\beta_j \omega'_j \omega_j] \\
 & + [c_1 e^{-\beta_j t} \cos \omega_j t] [-(\omega'_j)^2 + \beta_j^2 \omega_j^2] \\
 & + [c_1 e^{-\beta_j \omega_j t} \sin \omega'_j t] [-2\beta_j \omega'_j \omega_j] .
 \end{aligned} \tag{3.8}$$

The value of  $(\omega'_j)^2$  is large compared to  $\beta_j^2 \omega_j^2$ . For example, if  $\beta = 0.1$ , then the error is approximately 1% if it is assumed that  $\omega'_j$  is approximately equal to  $\omega_j$ . Thus eq. (3.8) reduces to

$$\begin{aligned}
 \ddot{d}_j \approx & \left[ \frac{c_2}{\omega'_j} e^{-\beta_j \omega_j t} \sin \omega'_j t \right] [-(\omega'_j)^2] \\
 & + \left[ \frac{c_2}{\omega'_j} e^{-\beta_j \omega_j t} \cos \omega'_j t \right] [-2\beta_j \omega'_j \omega_j] \\
 & + \left[ -\frac{\beta_j c_1}{\omega'_j} e^{-\beta_j \omega_j t} \sin \omega'_j t \right] [-(\omega'_j)^2] \\
 & + \left[ -\frac{\beta_j c_1}{\omega'_j} e^{-\beta_j \omega_j t} \cos \omega'_j t \right] [-2\beta_j \omega'_j \omega_j] \\
 & + [c_1 e^{-\beta_j \omega_j t} \cos \omega'_j t] [-(\omega'_j)^2] \\
 & + [c_1 e^{-\beta_j \omega_j t} \sin \omega'_j t] [-2\beta_j \omega'_j \omega_j] .
 \end{aligned} \tag{3.9}$$

The terms containing  $-2\beta_j \omega_j'$  are small compared to the terms containing  $(\omega_j')^2$  because  $(\omega_j')^2$  is larger than  $-2\beta_j \omega_j'$  plus the fact that the sine and cosine functions are  $90^\circ$  out of phase. Several authors on vibration have shown that the terms containing  $-2\beta_j \omega_j'$  are negligible. In fact, almost all text books on vibrations neglect these terms. Thus eq. (3.9) becomes

$$\ddot{q}_j \approx \left[ \frac{c_2}{\omega_j} e^{-\beta_j \omega_j' t} \sin \omega_j' t - \frac{\beta_j \omega_j' c_1}{\omega_j} e^{-\beta_j \omega_j' t} \sin \omega_j' t + c_1 e^{-\beta_j \omega_j' t} \cos \omega_j' t \right] [-(\omega_j')^2] . \quad (3.10)$$

or

$$\ddot{q}_j \approx -(\omega_j')^2 q_j . \quad (3.11)$$

Therefore, the inertia load per unit length becomes

$$m \frac{\partial^2 y_j}{\partial t^2} = -m Z_j \ddot{q}_j = -m \omega_j'^2 Z_j q_j = -m \omega_j'^2 y_j . \quad (3.12)$$

If  $y_j$  is maximum, then the equation corresponding to the  $j$ th mode is

$$\frac{\partial^2}{\partial x^2} \left( EI \frac{\partial^2 Z_j}{\partial x^2} \right) = -m \omega_j'^2 Z_j \quad (3.13)$$

What remains now is to show that the damped frequency  $\omega_j'$  can be regarded as the undamped natural frequency  $\omega_j$ . Equation (3.5b) gives

$$\omega_j' = \sqrt{\omega_j^2 - (1/4)\psi_j^2} , \quad (3.5b)$$

where

$\omega_j$  = undamped natural frequency,

$\omega_j'$  = damped natural frequency,

$\psi_j$  =  $2\beta_j \omega_j$  = damping factor.

Experimental studies express values of  $\psi_j$  in terms of critical damping.

The expression for the critical damping given by Myklestad (10) is

$$c_{cj} = 2m\omega_j . \quad (3.14)$$

But experimental data usually give the viscous constant  $c_j$  as a fraction of the critical damping  $c_{cj}$ . The damping constant  $c_j$  expressed mathematically is

$$c_j = \beta_j c_{cj} = 2\beta_j m\omega_j, \quad (3.14a)$$

where  $\beta_j$  is the fraction of critical damping. But

$$\psi_j = \frac{c_j}{m}, \quad (3.14b)$$

Thus,

$$\psi_j = 2\beta_j \omega_j. \quad (3.14c)$$

Now, consider the effect of damping on the undamped natural frequency  $\omega_j$ . Let  $\beta_j$  be equal to 10%, then

$$\psi_j = 2(0.1)\omega_j = 0.2\omega_j. \quad (3.14d)$$

Thus,

$$\omega'_j = \sqrt{\omega_j^2 - (1/4)(.04\omega_j^2)} = 0.995\omega_j \quad (3.14e)$$

Hence, it is seen that the effect of damping on the undamped frequency is only around 0.5%. Therefore, the conclusion that the undamped natural frequency is approximately equal to the damped natural frequency is justified.

One may ask about the physical significance of the damping factor  $\psi_j$  or the damping coefficient  $\beta_j$ . The physical significance is seen readily in the last term

$$c_1 e^{-(1/2)\psi_j t} \cos \omega_j t,$$

of eq. (3.5d). In this term, the amplitudes diminish in the ratio

$$e^{-(1/2)\psi_j t} : 1,$$

between time  $t$  and  $(t + \tau_j)$ , where  $\tau_j$  is the period in seconds per cycle.

Timashenko (11) expresses the term  $(1/2)\psi_j \tau_j$  as the difference between the logarithms of the two consecutive amplitudes at the instants  $t$  and  $(t + \tau_j)$ .

The symbol usually given to the logarithmic damping decrement is  $\delta_j$ , so that

$$\delta_j = \frac{1}{2} \psi_j \tau_j = \frac{1}{2} 2\beta_j \omega_j \frac{2\pi}{\omega_j}, \quad (3.14f)$$

or,

$$\delta_j = 2\pi\beta_j. \quad (3.14g)$$

Therefore,

$$c_j = \frac{m\omega_j \delta_j}{\pi}, \quad (3.14h)$$

in the equation

$$m\ddot{q}_j + c_j \dot{q}_j + m\omega_j^2 q_j = 0. \quad (3.14i)$$

Therefore, if damping is neglected, eq. (3.13) becomes

$$\frac{\partial^2}{\partial x^2} \left( EI \frac{\partial^2 Z_j}{\partial x^2} \right) = -m\omega_j^2 Z_j. \quad (3.13a)$$

Equation (3.13a) is similar to eq. (3.13). The difference lies only in the assumption that  $\omega_j = \omega_j'$ , whose error has been shown to be only 0.5%. Therefore, the above result leads to the conclusion that the undamped mode shapes are practically equal to the damped mode shapes.

4. Having found the inertia loads, the deflected curve can then be constructed by means of the conjugate beam, graphical statics, or Newmark's method. Actually, the three methods are based on the same basic steps of integration of the inertia load  $-m\omega_j^2 Z_j$  twice and division of the result by EI and then integrate two times more. The inertia load  $W_j$  is integrated twice to arrive at the bending moment  $M_j$ . The first integration performed on the inertia load  $W_j$  gives the shear  $V_j$ , the second the bending moment  $M_j$ . Integration of the  $M_j/EI$ -diagram twice gives the deflected curve  $Z_j$ , which is derived from the relationship,  $M_j/EI = d^2 Z_j(x)/dx^2$ . The Newmark method (12) affords an orderly arrangement and a very rapid means of making these integration procedures, which gives as its final result the deflected curve  $Z_j$ . The



difference from the conjugate beam method is the fact that the inertia load is assumed to be regionally parabolic instead of a straight line and that the figures used in the computations are tabulated. As an example, a stack is shown in Fig. 3.1. Figure 3.1a divides the stack into ten segments, Fig. 3.1b shows the inertia load per unit length, Fig. 3.1c shows one segment cut from the stack, and Fig. 3.1d shows two segments cut from the stack. The equation of the parabola is  $y = c_1x^2 + c_2x + c_3$ . By taking moments about point a one finds that the infinitesimal reaction is

$$dR_{ba} = \frac{xydx}{\lambda}, \quad (3.15)$$

and integration of eq. (3.15) yields

$$\begin{aligned} R_{ba} &= \int_0^\lambda \frac{xydx}{\lambda} = \int_0^\lambda \frac{c_1x^3 + c_2x^2 + c_3x}{\lambda} dx, \\ &= \frac{1}{\lambda} \left[ \frac{c_1x^4}{4} + \frac{c_2x^3}{3} + \frac{c_3x^2}{2} \right]_0^\lambda, \end{aligned} \quad (3.16)$$

Thus,

$$R_{ba} = \frac{\lambda}{12} [3c_1\lambda^2 + 4c_2\lambda + 6c_3]. \quad (3.16a)$$

But the equation of the parabola is  $y = c_1x^2 + c_2x + c_3$ , and the boundary conditions are:

$$\left. \begin{aligned} \text{when } x &= 0, & y &= a, \\ \text{when } x &= \lambda, & y &= b, \\ \text{when } x &= 2\lambda, & y &= c, \end{aligned} \right\} \quad (3.17)$$

thus,

$$c = a, \quad (3.17a)$$

$$b = c_1\lambda^2 + c_2\lambda + a, \quad (3.17b)$$

$$c = c_14\lambda^2 + c_22\lambda + a. \quad (3.17c)$$

Substitution of eqs. (3.17a), (3.17b), and (3.17c) gives

$$c_1 = \frac{1}{2\lambda^2} (a - 2b + c), \quad (3.18a)$$

$$c_2 = \frac{1}{2\lambda} (-3a + 4b - c), \quad (3.18b)$$

$$c_3 = a. \quad (3.18c)$$

Substitution of eqs. (3.18a, b, c,) into eq. (3.16a) gives

$$R_{ba} = \frac{\lambda}{12} (1.5a + 5b - 0.5c). \quad (3.19)$$

Similarly, if moments are taken about b,

$$R_{ab} = \frac{\lambda}{12} (3.5a + 3b - 0.5c). \quad (3.20)$$

Also, if the same procedure is used for the segment bc,

$$R_{bc} = \frac{\lambda}{12} (-0.5a + 5b + 1.5c), \quad (3.21)$$

and

$$R_{cb} = \frac{\lambda}{12} (3.5c + 3b - 0.5a). \quad (3.21a)$$

Addition of the effects of the two segments gives the reaction at b,

which is,

$$R_b = R_{ba} + R_{bc} = \frac{\lambda}{12} (a + 10b + c). \quad (3.22)$$

For the sake of completeness, the formulas for the reactions if a straight line connected the points a, b, and c are given below. They are:

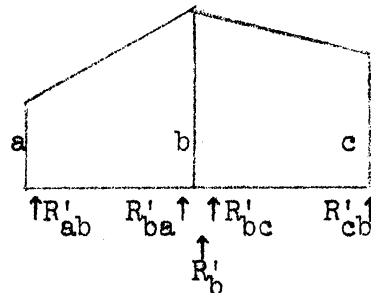
$$R'_{ab} = \frac{\lambda}{12} (4a + 2b),$$

$$R'_{ba} = \frac{\lambda}{12} (2a + 4b),$$

$$R'_{bc} = \frac{\lambda}{12} (4b + 2c),$$

and

$$R'_b = \frac{\lambda}{12} (2a + 8b + 2c).$$



$$(3.19)$$

It can be seen that the formulas for the reactions are quite different for the parabolic and straight line assumptions.

Newmark (13) and others have shown that the reactions based upon the parabolic assumption do not differ much from the trigonometric, 3rd order, and 4th order algebraic equations. However, a considerable deviation has been found from the straight line assumption. In addition, the parabolic assumption gives excellent results of the first mode shape if a uniform stack is divided into ten segments or more and gives satisfactory results if divided into as low as six segments. The three reaction formulas based on Newmark's parabolic assumption which are used in this study are summarized in Fig. 3.1.

The three reaction formulas, eqs. (3.20), (3.21a), and (3.22) are used to compute the concentrated inertia loads due to the distributed inertia loads. To these concentrated inertia loads which are computed from the distributed inertia loads, are added the concentrated inertia loads caused by the concentrated masses like floors, corbels, and water tank. Then the two computed concentrated inertia loads are added together to get the total concentrated inertia loads at the various stations along the stack. Since the shear at the top of the stack (the free end) is zero, the total concentrated inertia loads are summed from top to bottom to get the average shears at the midpoints of the various adjacent stations along the stack. Actually, this paragraph is equivalent to the first integration of the relationship  $W_j = d^2M_j/dx^2$ .

After the shear is found, one can easily compute the bending moments at any station along the stack by recalling that the area under the shear diagram is the bending moment. Since the segments are of equal length which is denoted by  $\lambda$ , the bending moment contributed by each segment is the average shear multiplied by  $\lambda$  which is the area of the shear diagram for that segment. For convenience the factor  $\lambda$  is

taken out and combined with the previous multiplier. Therefore, to get the bending moment, the average shears are summed from top to bottom since again the bending moment at the top of the stack is also zero (free end). The factor  $\lambda$  is also taken out and is incorporated with the previous multiplier. This process is the second integration of the relationship  $W_j = d^2M_j/dx^2$ .

The next step is to divide the bending moment diagram by EI to get the  $M_j/EI$ -diagram. After the division is performed, the concentrated  $M_j/EI$ -values are computed by using the same procedure that is used in computing the concentrated inertia loads. Here, the same reaction formulas are used. Similarly, these concentrated  $M_j/EI$ -values are summed, only this time the order of summation is from the bottom to the top of the stack since the bottom of the stack has zero slope (fixed end) to arrive at the average slopes. The physical significance of this procedure is the fact that the  $M_j/EI$ -values is the rate of change of slope, so that the rate of change of slope contributed by each segment is being added. This process is the first integration of the relationship  $M_j/EI = d^2Z_j(x)/dx^2$ .

Similarly, the area under this slope-diagram is the deflection. For the same reason that the average shear is multiplied by  $\lambda$ , the average slope is also multiplied by  $\lambda$  which is the area of the slope-diagram for that segment which is really the deflection contributed by that segment. Since the bottom of the stack is fixed, the deflection at the bottom of the stack is zero and therefore to get the total deflection at any station along the stack, the order of summation is from the bottom to the top of the stack. Again, for convenience the factor  $\lambda$  is taken out and is combined with the previous multiplier. The process in this paragraph is the second integration of the relationship  $M_j/EI = d^2Z_j(x)/dx^2$ .

It must be noted, however, that when the deflection is computed, the effect of the bending moment only is taken into account. In other words shear and rotary inertia are neglected. Timoshenko (14) has shown that the effect of rotary inertia is very small and can be neglected for practical purposes. However, the effect of shear becomes increasingly large when the beam gets chubby, i.e., when the length of the beam is not large compared to its cross-sectional dimensions. Jacobsen (15) made a comprehensive study of the effect of shear on the natural periods of uniform cantilever beams. He found that for a square box cross-section, the error in neglecting the shear effect on the lower mode natural periods is small as long as the ratio of the length to the width of the beam is greater than seven. For a cylindrical cross-section with a length-width ratio of seven, the width here being the diameter, the effect is even less. In the Clifty-Creek Plant stack (16), the height is 707' and the average diameter is 42' so that the length-diameter ratio is 17. Since this study is confined to tall reinforced-concrete chimneys whose length-diameter ratios are large, the effect of shear and rotary inertia on the lower mode shapes is neglected.

5. If the derived deflection curve  $Z_1(x)$  coincides with the originally assumed deflection curve  $Z(x)$ , then  $Z_1(x)$  is exactly the normal elastic curve. If, however, the derived  $Z_1(x)$  does not coincide with the assumed  $Z(x)$ , then steps (2), (3), and (4) are repeated, only this time the derived  $Z_1(x)$  from the previous trial is used as the assumed deflection curve. It is fortunate that for the fundamental mode, which is the most significant mode, the procedure is a very rapidly converging process. The proof of the convergence of Stodola's method may be found in den Hartog's (17) book.

Figure 3.2 shows the tabulated computations for the fundamental mode.

6. The natural frequency is obtained from the fundamental mode shape arrived at by using steps (1) to (5). For example, at the top of the stack the way to obtain the natural frequency is by using the relationship

$$1.0Z_{e1} = c \frac{w\lambda^4\omega_1^2}{gEI} Z_{e1} \quad (3.24)$$

where

$\lambda$  = length of segment

$c$  = figure arrived at the top of the stack by steps (1) to (5)

$w$  = weight per unit length

$g$  = acceleration of gravity

$E$  = modulus of elasticity

$I$  = moment of inertia.

In the example shown in Fig. 3.2, the natural frequencies based on different stations along the stack are computed and the average of the values taken. If the natural frequencies agree closely, then the mode shape is relatively accurate. It is to be noted again that the average natural frequency is really the undamped natural frequency but as discussed previously, the error being around 0.5%, it is used as the damped natural frequency for the first mode.

Figure 3.2 shows how the different steps and data are tabulated to obtain the fundamental mode shape and natural frequency of the tapered chimney.

For comparison, Muktabhant's uniform chimney (18) has been analyzed also. The results of this method show close agreement with his data, both for the fundamental mode shape and the natural frequency.

Note that in the computation of the mode shape and the natural frequency, the shear and bending moment factors are automatically computed. Hence, it can be concluded that the Newmark-Stodola method of finding the natural frequencies, deflection, shear, and bending moment factors is orderly and efficient. These factors are plotted at the end of Chapter IV.

In this Stodola-Newmark's method, the effect of shear along the height of the stack and the rocking or rotation of the base may also be considered. One extra line is needed after the EI line. This line is for the shear spring constant which is the shear required to produce a unit deflection for the segment. Three more lines are needed after the deflection line due to the bending moment. The first line is for the increment of deflection, contributed by each segment, due to shear. The second line is for the deflection due to shear which is obtained by summation of the increment of deflection due to shear from right to left. The third line is for the total derived deflection curve which is obtained by adding the deflection due to shear and the deflection due to the bending moment.

In the case of the rocking or rotation at the base, it is necessary to compute the stiffness of the foundation in terms of the bending moment at the base due to the  $j$ th mode. Then the concentrated  $\phi$  at the base due to rocking is added to the conc.  $\phi$  at the base in line 12 of Fig. 3.2 to get the total conc.  $\phi$  at the base. Since the effect of shear and rocking is not considered in this study, the details of the computations are not discussed.

As a numerical example, consider the computations shown in Fig. 3.2. Line 1 is the station designation. Line 2 is the distributed

weight per unit length. Line 3 is the EI value. Line 4 is the assumed deflection curve. Multiply the figures in line 4 by the corresponding figures in line 5 to get line 6, and at the same time multiply the multiplier by  $1/g\omega_1^2$ . For example for station e, line 6 becomes

$$(1.000 \times 7.5)[(\omega_1^2 Z_{e1} + 12g) \times \lambda/12] .$$

Line 7 is obtained from line 6 by Newmark's method of integration discussed previously. For example for station e, line 7 becomes

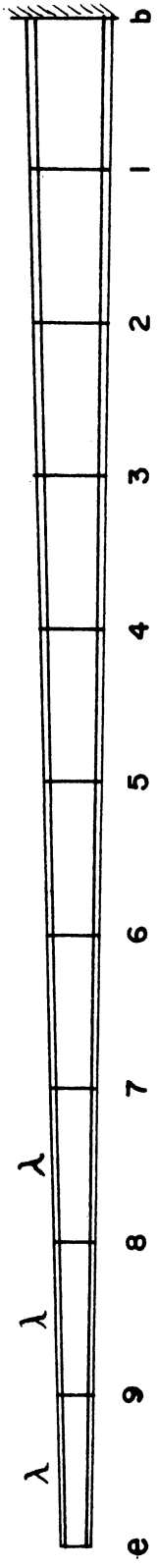
$$(3.5 \times 7.500 + 3.0 \times 7.591 - 0.5 \times 6.954)[\lambda\omega_1^2 Z_{e1} + 12g] .$$

Line 8 is obtained by multiplication of line 5 by line 3 with the product multiplied by  $12/\lambda$  to balance the factor  $\lambda/12$  in line 7. For example for station e, line 8 becomes

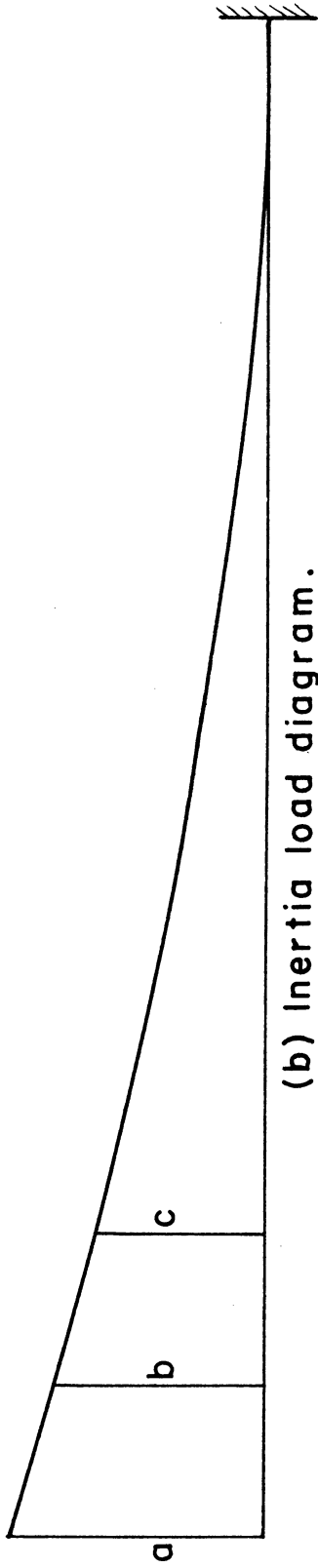
$$(1.000 \times 87.03 \times 12/70.7)[(\omega_{12} Z_{e1} + g) \times \lambda/12] .$$

Line 9 is obtained by addition of line 7 and line 8. At station e, line 9 is  $(45.55 + 14.77)$ . The other lines follow the same procedures. Before leaving this discussion, note that the inertia load per unit length has a discontinuity in station 2. In this station, eqs. (3.20) and (3.21a) are used.

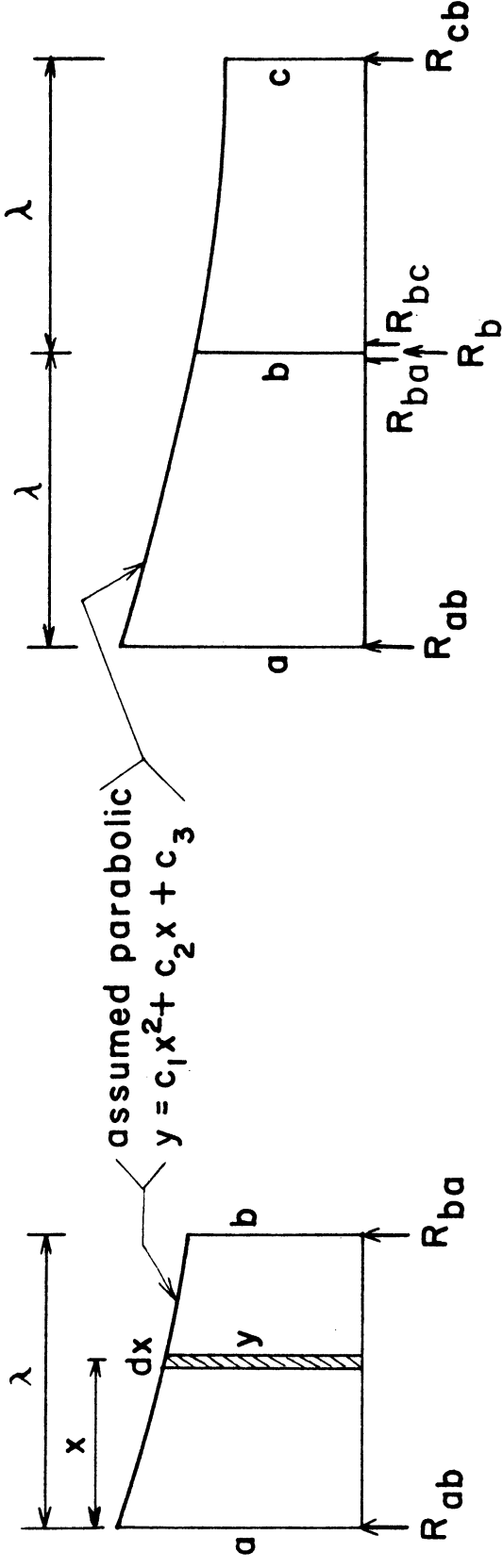




(a) Stack divided into ten equal segments.



(b) Inertia load diagram.



(c) One segment of stack.

(d) Two segments of stack.

BASIC FORMULAS:

$$R_{ab} = \frac{\lambda}{12} (3.5a + 3b - 0.5c) \dots \dots \dots (3.20)$$

FIG. 3.1. NEWMARK'S

$$R_b = \frac{\lambda}{12} (a + 10b + c) \dots \dots \dots (3.22)$$

REACTION FORMULAS.

$$R_{cb} = \frac{\lambda}{12} (3.5c + 3b - 0.5a) \dots \dots \dots (3.21a)$$



**First Mode**

MULTIPLIER  
Ft.-kip units

	e	9	8	7	6	5	4	3	2	1	b	
1) Station												
2) Weight (w)	7.5	9.5	11.4	15.1	20.3	23.1	29.1	42.1	70.0 42.1	52.0	76.5	Kips per ft.
3) " Conc.	87.03	191.08	72.03	71.90	77.34	86.69	95.30	149.00	427.48	2355.87		Added Wt. (Kips)
4) EI	1.00	1.55	2.70	5.20	9.25	12.95	20.70	35.80	51.85	69.25	115.90	EIe
5) Assumed Zi	1.000	.799	.610	.445	.309	.199	.119	.063	.026	.006	0	Zei
6) Inertia Load Int.	7.500	7.591	6.954	6.720	6.273	4.597	3.463	2.652	1.820 1.095	0.312	0	$\omega_1^2 Z_{ei} \div g$
7) Conc. In. Load	45.55	90.36	83.85	80.43	74.05	55.71	41.88	31.80	17.36	4.22		$\lambda \omega_1^2 Z_{ei} \div 12g$
8) " "	14.77	25.91	7.46	5.43	4.06	2.93	1.92	1.59	1.89	2.40		Do
9) Avg. Shear (V)	60.32	176.59	267.90	353.76	431.87	490.51	534.31	567.70	586.95	593.57		Do
10) Moment (M)	0	60.3	236.9	504.8	858.6	1290.4	1781.0	2315.3	2883.0	3470.0	4063.5	$\lambda^2 \omega_1^2 Z_{ei} \div 12g$
11) $M \div EI (\phi)$	0	38.90	87.74	97.08	92.82	99.64	86.04	64.67	55.60	50.11	35.06	$\lambda^2 \omega_1^2 Z_{ei} \div 12EI_e g$
12) Conc. $\phi$		476.7	1013.4	1151.4	1124.9	1175.3	1024.7	788.3	670.8	591.8	245.2	$\lambda^3 \omega_1^2 Z_{ei} \div 144EI_e g$
13) Avg. Slope $\sum$	8263	7786	6772	5621	4496	3321	2296	1508	837	245		Do
14) Deflection $\sum$	41145	32882	25096	18324	12703	8207	4886	2590	1082	245	0	$\lambda^4 \omega_1^2 Z_{ei} \div 144EI_e g$
15) Relative Zi	1.000	.799	.610	.445	.309	.199	.119	.063	.026	.006	0	Zei
16) Relative Vi	.102	.298	.451	.596	.728	.826	.900	.956	.989	1.000		Vbi
17) Relative Mi	0	.015	.058	.124	.211	.318	.438	.570	.709	.854	1.00	Mbi
18) $\omega_1^2$	4.54	4.54	4.54	4.54	4.54	4.54	4.54	4.54	4.54	4.54	4.54	(radians per sec.) <sup>2</sup>

Deflection Multiplier =  $(\lambda^4 \omega_1^2 Z_{ei}) \div (144EI_e g) = (70.4^4 \omega_1^2 Z_{ei}) \div (144 \cdot 3.5 \cdot 144 \cdot 1000 \cdot 2000 \cdot 32.2) = 5.35 \cdot 10^{-6} \omega_1^2 Z_{ei}$

Average First Mode Frequency  $\omega_1 = 2.13$  radians per second

" " " Period  $T_1 = 2.95$  seconds per cycle

**FIG. 3.2. CALCULATIONS OF FIRST MODE DYNAMIC PROPERTIES.**

## CHAPTER IV

### DYNAMIC STRUCTURAL PROPERTIES: SECOND AND HIGHER MODES

For the second and higher modes, the procedure outlined in Chapter III is not a convergent process. This is because in processing any assumed mode shape, any impurity of the lower modes is magnified more than that of the higher mode. After a large number of repetitions it is found that the higher modes disappear altogether and that only the fundamental mode remains (19). However, the process can be modified a little by utilizing the suggestion made by N. Newmark that the modification requires purification of the lower harmonic impurities.

To give a clearer insight into the nature of "normal modes of motion", a brief discussion of the theory of "normal functions" and their applications is necessary.

It is known that for a string and the beam on two hinged supports, the various normal elastic curves are sine functions, that is,

$$u_j = A_j \sin \frac{j\pi x}{h} . \quad (4.1)$$

From the theory of Fourier series, it is a well-known fact that eq. (4.1) form an "orthogonal" system (20) in the interval  $0 < x < h$ ; that is, the integral over that interval of the product of any two distinct functions of the system is zero. The statement above is expressed mathematically by the equation

$$\int_0^h \sin \frac{r\pi x}{h} \sin \frac{s\pi x}{h} dx = 0 , \quad \text{if } r \neq s , \quad (4.1a)$$

$$= 1/2h , \quad \text{if } r = s . \quad (4.1b)$$

The orthogonal or orthonormal relationship derived above means that any elastic curve  $Z(x)$  which may be given to the simply supported uniform beam can be split up into a series of "normal" components. This is true not only for the uniform beam on two hinged supports with its sine functions as the "normal functions", but it is also true for any elastic system. However, for the case of a uniform cantilever beam or of a stack with variable cross-section, the normal elastic curves are not simple sine or cosine functions but are complicated curves.

If the normal elastic curves of a system of length  $h$  are  $Z_1(x), Z_2(x), \dots, Z_j(x)$ , then any arbitrary deflection curve of that system can be developed into a series

$$Z(x) = \phi_1 Z_1(x) + \phi_2 Z_2(x) + \dots + \phi_j Z_j(x) . \quad (4.2)$$

Moreover, the relation

$$\int_0^h m(x) Z_r(x) Z_s(x) dx = 0 , \quad \text{if } r \neq s , \quad (4.3)$$

holds, so that any coefficient  $\phi_j$  in eq. (4.2) can be found to be

$$\phi_j = \frac{\int_0^h m(x) Z(x) Z_j(x) dx}{\int_0^h m(x) Z_j^2(x) dx} . \quad (4.4)$$

Equations (4.2), (4.3), and (4.4) give a generalization of the theory of Fourier series.

A rigorous proof of eq. (4.3) is found in den Hartog's (21) book. The proof is not necessary here because in the computations of the higher mode shapes, the orthogonality condition of eq. (4.3) has to be satisfied first.

With eq. (4.3) as a tool, one can proceed with the computations for the second and higher modes of vibration. As stated previously, for the second mode, the first step is to purify the assumed deflection curve of the first mode impurity. Let  $Z(x)$  be the assumed second mode which

of course contains some first harmonic impurity, call it  $A_1 Z_1(x)$ . Then the purified second mode shape is

$$Z_2(x) = Z(x) - A_1 Z_1(x), \quad (4.5)$$

which is free from first harmonic impurity. To solve for  $A_1$ , substitute eq. (4.5) into the orthogonal relationship of eq. (4.3) to get

$$\int_0^h m(x)[Z(x) - A_1 Z_1(x)] Z_1(x) dx = 0 \quad (4.6)$$

or

$$A_1 = \frac{\int_0^h m(x) Z(x) Z_1(x) dx}{\int_0^h m(x) Z_1^2(x) dx} \quad (4.6a)$$

Again, Newmark's method of integration, with the regionally parabolic assumption of the curves  $m(x)Z(x)Z_1(x)$  and  $m(x)Z_1(x)$ , is a fast and orderly way of integrating the numerator and the denominator of eq. (4.6a) and also in finding the value of  $A_1$ . To provide a check, Muktabhant's (18) uniform stack has also been analyzed and the results are consistent. The operations are shown in Figs. 4.1 and 4.2 at the end of this chapter for the tapered chimney.

In Fig. 4.1, the denominator of eq. (4.6a) is computed first. The stack is also divided into ten segments as in Chapter III. The steps are self-explanatory. After getting the value of

$$\int_0^h m(x) Z_1^2(x) dx,$$

then the value of

$$\int_0^h m(x) Z(x) Z_1(x) dx$$

is computed. To get the value of  $A_1$  the latter integral is divided by the former. The results of the processes are tabulated in Fig. 4.1.

After finding the value of  $A_1$ , then the assumed deflection curve is purified. Each value of  $Z_1$  is multiplied by  $A_1$  as shown in

Fig. 4.2 and then the corresponding  $Z_1A_1$  is subtracted from the assumed  $Z$ . The relative purified deflections are then computed. The same procedures used in Chapter III are used to obtain the derived second mode deflections from the assumed relative purified deflections. If the derived deflection curve  $Z_2$  agrees with assumed  $Z$ , then the result is exactly the second mode deflection curve, but if not then the process is repeated only this time the derived  $Z_2$  is the assumed deflection curve which has to be purified. It is shown in Fig. 4.2 that the derived deflection curve  $Z_2$  agrees closely with the assumed  $Z$  making further trials unnecessary. The second mode shape of Muktabhant's uniform stack has also been analyzed and the results are also consistent with his results.

The computation of the natural frequency for the second mode is the same as that of the first mode. The natural frequencies based upon the various stations are computed and then the average is taken.

The procedure is similar for the third mode. However, this time the assumed deflection curve has to be purified from both the first and second modes by the same orthogonality relationship of eq. (4.3). For the third mode, let the assumed deflection curve be  $Z(x)$ , so that the purified deflection  $Z_3(x)$  becomes

$$Z_3(x) = Z(x) - A_2Z_1(x) - B_2Z_2(x), \quad (4.7)$$

where

$Z(x)$  = assumed third mode deflection curve,

$Z_3(x)$  = purified assumed third mode deflection curve,

$Z_1(x)$  = from previous computations of first mode shape,

$Z_2(x)$  = from previous computations of second mode shape,

$A_2$  and  $B_2$  are constants of purification.

Substitution of eq. (4.7) into eq. (4.3) gives

$$\int_0^h m(x) [Z(x) - A_2 Z_1(x) - B_2 Z_2(x)] Z_2(x) dx = 0, \quad (4.8)$$

or

$$B_2 = \frac{\int_0^h m(x) Z(x) Z_2(x) dx - A_2 \int_0^h m(x) Z_1(x) Z_2(x) dx}{\int_0^h m(x) Z_2^2(x) dx}. \quad (4.8a)$$

But the integral

$$\int_0^h m(x) Z_1(x) Z_2(x) dx$$

is zero if  $Z_1(x)$  and  $Z_2(x)$  are pure first and second mode shapes, so that eq. (4.8a) reduces to

$$B_2 = \frac{\int_0^h m(x) Z(x) Z_2(x) dx}{\int_0^h m(x) Z_2^2(x) dx}. \quad (4.8b)$$

Similarly, substitution of eq. (4.7) into eq. (4.3) gives

$$\int_0^h m(x) [Z_3(x) - A_2 Z_1(x) - B_2 Z_2(x) Z_1(x)] dx = 0, \quad (4.9)$$

or

$$A_2 = \frac{\int_0^h m(x) Z(x) Z_1(x) dx - B_2 \int_0^h m(x) Z_1(x) Z_2(x) dx}{\int_0^h m(x) Z_1^2(x) dx}. \quad (4.9a)$$

Also,

$$\int_0^h m(x) Z_1(x) Z_2(x) dx = 0$$

if  $Z_1(x)$  and  $Z_2(x)$  are pure first and second mode harmonics, so that eq. (4.9a) is reduced to

$$A_2 = \frac{\int_0^h m(x) Z(x) Z_1(x) dx}{\int_0^h m(x) Z_1^2(x) dx}. \quad (4.14b)$$

Newmark's method of integration, with the parabolic assumption of the curves  $m(x) Z(x) Z_2(x)$ ,  $m(x) Z_2^2(x)$ ,  $m(x) Z(x) Z_1(x)$ , and  $m(x) Z_1^2(x)$

within three adjacent stations, is used to get the values of  $A_2$  and  $B_2$ .

It is noted here that the value of

$$\int_0^h m(x)Z_1^2(x) dx$$

had been evaluated already in finding the second mode shape.

The computations of  $A_2$  and  $B_2$  are shown in Fig. 4.3. The procedure here is the same as in evaluating  $A_1$  for the second mode. The computations of the derived third mode shape are shown in Fig. 4.4. The procedure is also similar to finding the deflection curves for the first and second modes, only this time the assumed third mode shape is corrected for both the first and second harmonics by  $-A_2Z_1(x)$  and by  $-B_2Z_2(x)$  respectively, giving the purified assumed curve  $Z_3(x)$  shown in Fig. 4.4. If the derived third mode shape is not the same as the assumed third harmonic, then the procedure is repeated and further trials are needed until they become close.

The results of the procedure for the third mode shape for the uniform stack also agree with Muktabhant's computations.

The natural frequency computation is the same as for the first and second modes. Figure 4.4 shows the natural frequencies based on the various stations with the average also computed.

The procedure for the fourth and higher modes of vibration is the same as for the first, second, and third modes. The only difference is that the assumed higher mode has to be purified from the lower modes. Therefore, the Stodola-Newmark method requires the computations of the lower modes before proceeding with the higher modes. It is fortunate that the effect of the higher modes is small so that in this study only the first, second, and third modes are considered.



Now, the constants  $\Gamma_j$  can be evaluated. The formula for  $\Gamma_j$  from eq. (2.75) is

$$\Gamma_j = \frac{\int_0^h m(x) Z_j(x) dx}{\int_0^h m(x) Z_j^2(x) dx} \quad (4.10)$$

Again it is fortunate that some of the previous computations can be used. Wherever more computations are needed Newmark's method of integration is used, with the assumption that the curves  $m(x) Z_j(x)$  and  $m(x) Z_j^2(x)$  are regionally parabolic within three adjacent stations. The computations and results are shown in Fig. 4.5. The steps are self-explanatory. Already, the data for the first two terms of the equations

$$y = \sum_{j=1}^n Z_j \Gamma_j \phi_j, \quad (2.77)$$

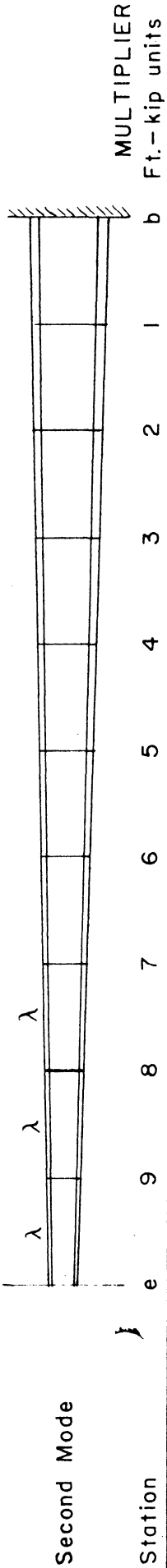
$$v = \sum_{j=1}^n V_j \Gamma_j \phi_j, \quad (2.78)$$

$$M = \sum_{j=1}^n M_j \Gamma_j \phi_j \quad (2.79)$$

are available.

The values of  $Z_j$ ,  $V_j$  and  $M_j$  for the 707' Clifty Creek stack are plotted at the end of this chapter. The curves for the 605' Modified Selby (22) and the 562' Kyger Creek (23) stacks are in the appendix.

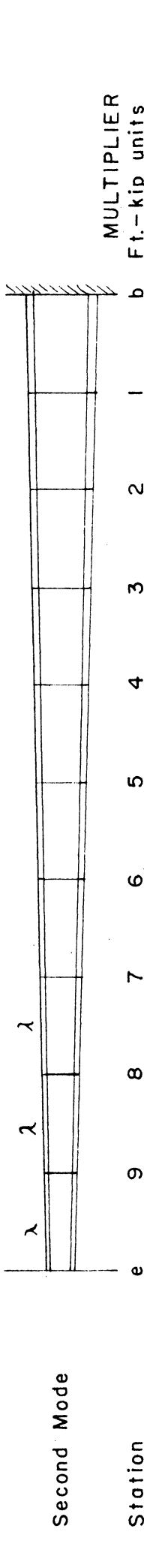
The next step is to find the values of  $\phi_j$ . This step is discussed in the next chapter.



Station	e	9	8	7	6	5	4	3	2	1	b	MULTIPLIER Ft.-kip units
Weight (w)	7.5	9.5	11.4	15.1	20.3	23.1	29.1	42.1	70.0 42.1	52.0	76.5	Kips per ft.
" Conc.	87.03	191.08	72.03	71.90	77.34	86.69	95.30	149.00	427.48	2355.87		Added Wt. (kips)
Z <sub>1</sub>	1.000	.799	.610	.445	.309	.199	.119	.063	.026	.006	0	Z <sub>e1</sub>
Z <sub>1</sub> <sup>2</sup>	1.000	.638	.372	.198	.095	.040	.014	.004	.001	0	0	Z <sub>e1</sub> <sup>2</sup>
mZ <sub>1</sub> <sup>2</sup>	7.500	6.061	4.241	2.990	1.929	.924	.407	.168	.070 .042	0	0	Z <sub>e1</sub> <sup>2</sup> ÷ g
Conc. mZ <sub>1</sub> <sup>2</sup>	42.31	72.35	51.46	36.07	23.20	11.58	5.16	2.16	0.81	0.04	0	λ Z <sub>e1</sub> <sup>2</sup> ÷ 12g
" "	14.77	20.69	4.55	2.42	1.25	0.59	0.23	0.10	0.07	0	0	D <sub>0</sub>
Σ (Conc. mZ <sub>1</sub> <sup>2</sup> )	57.08	150.12	206.13	244.62	269.07	281.24	286.63	288.89	289.77	289.81		D <sub>0</sub>
$\int_0^h mZ_1^2 dx = 289.81(D_0)$												
Assumed Z <sub>2</sub>	1.000	.433	-.026	-.297	-.397	-.381	-.293	-.183	-.086	-.021	0	Z <sub>e2</sub>
Z <sub>1</sub> Z <sub>2</sub>	1.000	.346	-.016	-.132	-.123	-.076	-.035	-.012	-.002	-.00013	0	Z <sub>e1</sub> Z <sub>e2</sub>
mZ <sub>1</sub> Z <sub>2</sub>	7.500	3.287	-.182	-1.993	-2.497	-1.756	-1.019	-.505	-.140 -.084	-.007	0	Z <sub>e1</sub> Z <sub>e2</sub> ÷ g
Conc. mZ <sub>1</sub> Z <sub>2</sub>	36.202	40.188	-0.526	-22.609	-28.719	-21.076	12.451	-6.209	-1.810	-0.154		λ Z <sub>e1</sub> Z <sub>e2</sub> ÷ 12g
" "	14.772	11.222	-0.196	-1.611	-1.615	-1.118	-0.566	-0.303	-0.145	-0.050		D <sub>0</sub>
Σ (Conc. mZ <sub>1</sub> Z <sub>2</sub> )	50.974	102.384	101.662	77.442	47.108	24.914	11.897	5.385	3.430	3.226		D <sub>0</sub>
$\int_0^h mZ_1Z_2 dx = 3.226(D_0)$												

Since  $Z_{e1} = Z_{e2} = \text{unity}$ , then  $A_1 = \frac{\int_0^h mZ_1Z_2 dx}{\int_0^h mZ_1^2 dx} = \frac{3.226}{289.81} = +0.01113$

FIG. 4.1. SECOND MODE ORTHOGONALITY CALCULATIONS.



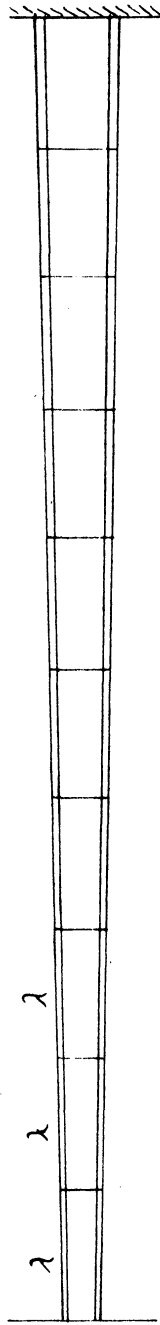
Station	e	9	8	7	6	5	4	3	2	1	b	MULTIPLIER Ft.-kip units
Weight (w)	7.5	9.5	11.4	15.1	20.3	23.1	29.1	42.1	70.0 42.1	52.0	76.5	76.5 kips per ft.
" Conc.	87.03	191.08	72.03	71.90	77.34	86.69	95.30	149.00	427.48	235.587		Added Wt. (kips)
EI	1.00	1.55	2.70	5.20	9.25	12.95	20.70	35.80	51.85	69.25	115.90	90E <sub>1</sub> e
Assumed Z <sub>2</sub>	1.000	.433	-.026	-.297	-.397	-.381	-.293	-.183	-.086	-.021	0	Z <sub>e2</sub>
A <sub>1</sub> Z <sub>1</sub>	.011	.009	.007	.005	.003	.002	.001	.001	0	0	0	Z <sub>e1</sub>
Purified Z <sub>2</sub>	.989	.424	-.033	-.302	-.401	-.383	-.294	-.184	-.086	-.021	0	Z <sub>e2</sub>
Relative Purified Z <sub>2</sub>	1.000	.429	-.033	-.305	-.405	-.387	-.297	-.186	-.087	-.021	0	Z <sub>e2</sub>
Inertia Ld. Int.	7.500	4.076	-.376	-.4606	-.8.222	-.8.940	-.8.643	-.7.831	-.6.090 -3.663	-.1.092	0	ω <sub>2</sub> <sup>2</sup> Z <sub>e2</sub> ÷ g
Conc. In. Load	38.666	47.884	-.4.290	-.54.658	-.95.766	-.106.265	-.103.201	-.93.043	-.56.583	-.14.583		λ ω <sub>2</sub> <sup>2</sup> Z <sub>e2</sub> ÷ 12g
" "	14.772	13.913	-.403	-.3.722	-.5.316	-.5.694	-.4.804	-.4.704	-.6.312	-.8.397	0	D <sub>0</sub>
Avg. Shear (V)	53.438	115.235	110.542	52.162	-.48.920	-.160.879	-.268.884	-.366.631	-.429.526	-.452.506		D <sub>0</sub>
Moment (M)	0	53.438	168.673	279.215	331.377	282.457	121.578	-.147.306	-.513.937	-.943.46	-.1395.97	λ <sup>2</sup> ω <sub>2</sub> <sup>2</sup> Z <sub>e2</sub> ÷ 12g
M ÷ EI (φ)	0	34.476	62.471	53.695	35.825	21.811	5.873	-.4.115	-.9.912	-.13.624	-.12.045	λ <sup>2</sup> ω <sub>2</sub> <sup>2</sup> Z <sub>e2</sub> ÷ 12E <sub>1</sub> e <sub>g</sub>
Conc. φ		407.231	712.881	635.246	433.756	259.808	76.426	-.45.189	-.116.859	-.158.197	-.780.74	λ <sup>3</sup> ω <sub>2</sub> <sup>2</sup> Z <sub>e2</sub> ÷ 144E <sub>1</sub> e <sub>g</sub>
Avg. Slope Σ	2127.029	1719.798	1006.917	371.671	-.62.085	-.321.893	-.398.319	-.353.130	-.236.271	-.78.074		D <sub>0</sub>
Deflection Σ	3775.64	1648.61	-.71.18	-.1078.10	-.1449.77	-.1387.69	-.1065.79	-.667.48	-.314.35	-.78.07	0	λ <sup>4</sup> ω <sub>2</sub> <sup>2</sup> Z <sub>e2</sub> ÷ 144E <sub>1</sub> e <sub>g</sub>
Relative Z <sub>2</sub>	1.000	.437	-.019	-.286	-.384	-.368	-.282	-.177	-.083	-.021	0	Z <sub>e2</sub>
Relative V <sub>2</sub>	.118	.255	.244	.115	-.108	-.356	-.594	-.810	-.949	-.1.000		V <sub>b2</sub>
Relative M <sub>2</sub>	0	.038	.121	.200	.237	.202	.087	-.106	-.368	-.676	-.1.00	M <sub>b2</sub>
ω <sub>2</sub> <sup>2</sup>	49.6	49.6	49.6	49.6	49.6	49.6	49.5	49.6	49.5	49.6		(radians per second) <sup>2</sup>

Deflection Multiplier =  $5.35 \cdot 10^{-6} \omega_2^2 Z_{e2}$ , from Fig. 3.2.  
 Average Second Mode Frequency  $\omega_2 = 7.05$  radians per second  
 " " " Period  $\tau_2 = 0.88$  second per cycle

FIG. 4.2. CALCULATIONS OF SECOND MODE DYNAMIC PROPERTIES.

Third Mode		MULTIPLIER											
		e	9	8	7	6	5	4	3	2	1	b	Ft. - kip units
Weight(w)		7.5	9.5	11.4	15.1	20.3	23.1	29.1	42.1	70.0	52.0	76.5	Kips per ft.
"	Conc.	87.03	191.08	72.03	71.90	77.34	86.69	95.30	149.00	427.48	235.587	5.87	Added Wt. (kips)
$Z_2$		1.000	.429	-.033	-.305	-.405	-.387	-.297	-.186	.087	-.021	0	$Z_{e2}$
$Z_2^2$		1.000	.184	.001	.093	.164	.150	.088	.035	.008	.00044	0	$Z_{e2}^2$
$mZ_2^2$		7.500	1.748	.011	1.404	3.329	3.465	2.561	1.474	.560	.023	0	$Z_{e2}^2 \div g$
Conc. $mZ_2^2$		31.49	24.99	3.26	17.38	38.16	40.54	30.55	17.86	6.35	0.57	0	$\lambda Z_{e2}^2 \div 12g$
"		14.77	5.97	0.01	1.14	2.15	2.21	1.42	0.89	0.58	0.18	0	Do
$\sum$ (Conc. $mZ_2^2$ )												240.47	Do
$\int_0^h mZ_2^2 dx = 240.47 (Do)$													
Assumed $Z_3$		1.000	-.053	-.604	-.536	-.178	.162	.319	.292	.171	.049	0	$Z_{e3}$
$Z_2 Z_3$		1.000	-.023	.020	.163	.072	-.063	-.095	-.054	-.015	-.001	0	$Z_{e2} Z_{e3}$
$mZ_2 Z_3$		7.500	-.219	.228	2.461	1.462	-1.455	-2.765	-2.273	-1.050	-.052	0	$Z_{e2} Z_{e3} \div g$
Conc. $mZ_2 Z_3$		25.48	5.54	4.52	26.30	15.63	-15.85	-31.38	-26.55	-11.48	-1.15	0	$\lambda Z_{e2} Z_{e3} \div 12g$
"		14.77	-.75	.24	1.99	.95	-.93	-1.54	-1.37	-1.09	-.40	0	Do
$\sum$ (Conc. $mZ_2 Z_3$ )												2.93	Do
Since $Z_{e2} = Z_{e3} = \text{unity}$ , then $B_2 = (2.93) \div (240.47) = +0.012184$													
$Z_1$		1.000	.799	.610	.445	.309	.199	.119	.063	.026	.006	0	$Z_{e1}$
$Z_1 Z_3$		1.000	-.042	-.368	-.239	-.055	.032	.038	.018	.004	.0003	0	$Z_{e1} Z_{e3}$
$mZ_1 Z_3$		7.500	-.399	-4.195	-3.609	-1.117	.739	1.106	.758	.280	.016	0	$Z_{e1} Z_{e3} \div g$
Conc. $mZ_1 Z_3$		27.15	-.69	-45.96	-41.40	-14.04	7.38	12.56	8.97	3.34	.33	0	$Z_{e1} Z_{e3} \div 12g$
"		14.77	-1.36	-4.50	-2.92	-.72	.47	.61	.45	.29	.12	0	Do
$\sum$ (Conc. $mZ_1 Z_3$ )												-35.15	Do
Since $Z_{e1} = Z_{e3} = \text{unity}$ , then $A_2 = (-35.15) \div (289.81) = -0.12129$													

FIG. 4.3. THIRD MODE ORTHOGONALITY CALCULATIONS.



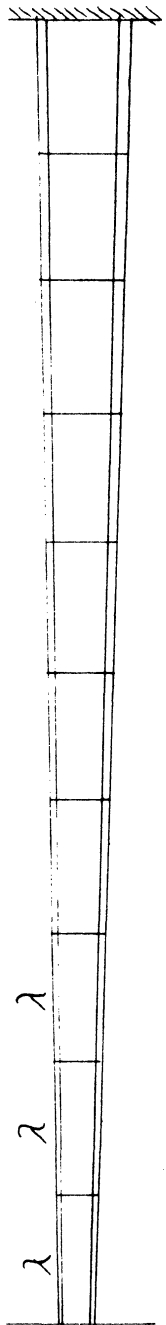
MULTIPLIER  
Ft.-kip units

Third Mode	e	9	8	7	6	5	4	3	2	1	b
Weight (w)	7.5	9.5	11.4	15.1	20.3	23.1	29.1	42.1	70.0	52.0	76.5
" Conc.	87.03	191.08	72.03	71.90	77.34	86.69	95.30	149.00	427.48	2355.87	Added Wt. (kips)
EI	1.00	1.55	2.70	5.20	9.25	12.95	20.70	35.80	51.85	69.25	115.90E1e
Assumed Z <sub>3</sub>	1.000	-.053	-.604	-.536	-.178	.162	.319	.292	.171	.049	0 Z <sub>e3</sub>
A <sub>2</sub> Z <sub>1</sub>	-.121	-.097	-.074	-.054	-.037	-.024	-.014	-.008	-.003	-.001	0 Z <sub>e1</sub>
B <sub>2</sub> Z <sub>2</sub>	.012	.005	0	-.004	-.005	-.005	-.004	-.002	-.001	0	0 Z <sub>e2</sub>
Purified Z <sub>3</sub>	1.109	.039	-.530	-.478	-.136	.191	.337	.302	.175	.050	0 Z <sub>e3</sub>
Relative Purified Z <sub>3</sub>	1.000	.035	-.478	-.431	-.123	.172	.304	.272	.158	.045	0 Z <sub>e3</sub>
Inertia Load Int.	7.500	.333	-5.449	-6.508	-2.497	3.973	8.846	11.451	11.060	2.340	0 ω <sub>3</sub> <sup>2</sup> Z <sub>e3</sub> ÷ g
Conc. Inertia Load	29.974	5.381	-60.665	-73.026	-27.505	46.079	103.884	134.416	98.942	30.052	λ ω <sub>3</sub> <sup>2</sup> Z <sub>e3</sub> ÷ 12g
" "	14.772	1.135	-5.844	-5.260	-1.615	2.531	4.917	6.883	11.464	17.994	Do
Avg. Shear (V)	44.746	51.562	-15.247	-93.533	-122.653	-74.043	34.758	176.057	286.463	334.509	Do
Moment (M)	0	44.746	96.008	80.761	-12.772	-135.425	-209.468	-174.710	1.347	287.810	622.319 λ <sup>2</sup> ω <sub>3</sub> <sup>2</sup> Z <sub>e3</sub> ÷ 12g
M ÷ EI (φ)	0	28.868	35.559	15.531	-1.381	-10.458	-10.119	-4.880	.026	4.156	5.369 λ <sup>2</sup> ω <sub>3</sub> <sup>2</sup> Z <sub>e3</sub> ÷ 12Eleg
Concentrate φ		324.239	399.989	189.488	-8.737	-116.080	-116.528	-58.983	-.464	46.955	31.247 λ <sup>3</sup> ω <sub>3</sub> <sup>2</sup> Z <sub>e3</sub> ÷ 144Eleg
Avg. Slope φ	691.126	366.887	-33.102	-222.590	-213.853	-97.773	18.755	77.738	78.202	31.247	Do
Deflection φ	696.637	5.511	-361.376	-328.274	-105.684	108.169	205.942	187.187	109.449	31.247	0 λ <sup>4</sup> ω <sub>3</sub> <sup>2</sup> Z <sub>e3</sub> ÷ 144Eleg
Relative Z <sub>3</sub>	1.000	.008	-.519	-.471	-.152	.155	.296	.269	.157	.045	0 Z <sub>e3</sub>
Relative V <sub>3</sub>	.134	.153	-.046	-.280	-.367	-.221	.104	.526	.856	1.000	V <sub>b3</sub>
Relative M <sub>3</sub>	0	.072	.154	.130	-.021	-.218	-.337	-.281	.002	.462	1.00 M <sub>b3</sub>
ω <sub>3</sub> <sup>2</sup>	269	269	269	269	269	269	269	269	268	269	(radians per second) <sup>2</sup>

Average Third Mode Frequency ω<sub>3</sub> = 16.4 radians per second

" " " Period τ<sub>3</sub> = 0.38 second per cycle

FIG. 4.4. CALCULATIONS OF THIRD MODE DYNAMIC PROPERTIES.



Station	e	9	8	7	6	5	4	3	2	1	b	MULTIPLIER
Weight (w)	7.5	9.5	11.4	15.1	20.3	23.1	29.1	42.1	70.0	52.0	76.5	Ft.- kip units
" Conc.	87.03	191.08	72.03	71.90	77.34	86.69	95.30	149.00	427.48	2355.87		Kips per ft.
Z <sub>3</sub>	1.000	.035	-.478	-.431	-.123	.172	.304	.272	.158	.045	0	Z <sub>e3</sub>
Z <sub>3</sub> <sup>2</sup>	1.000	.001	.228	.186	.015	.030	.092	.074	.025	.002	0	Z <sub>e3</sub> <sup>2</sup>
mZ <sub>3</sub> <sup>2</sup>	7.500	.010	2.599	2.809	.305	.693	2.677	3.115	1.750	.104	0	Z <sub>e3</sub> <sup>2</sup> ÷ g
Conc. mZ <sub>3</sub> <sup>2</sup>	24.98	10.20	28.81	30.99	6.55	9.91	30.58	35.58	18.13	2.09		λ Z <sub>e3</sub> <sup>2</sup> ÷ 12g
" "	14.77	.03	2.79	2.27	.20	.44	1.49	1.87	1.81	.80		D <sub>0</sub>
Σ (Conc. mZ <sub>3</sub> <sup>2</sup> )												224.29
												D <sub>0</sub>

From FIG. 4.4,  $\int_0^h mZ_3 dx = 334.51(D_0)$ , from FIG. 4.5,  $\int_0^h mZ_3^2 dx = 224.29(D_0)$ ,  
 from FIG. 4.2,  $\int_0^h mZ_2 dx = -452.51(D_0)$ , from FIG. 4.3,  $\int_0^h mZ_2^2 dx = 240.47(D_0)$ ,  
 from FIG. 3.2,  $\int_0^h mZ_1 dx = 593.57(D_0)$ , from FIG. 4.1,  $\int_0^h mZ_1^2 dx = 289.81(D_0)$ ,

and  $Z_{e3} = Z_{e1} = \text{unity}$ , therefore

$$\Gamma_1 = \int_0^h mZ_1 dx \div \int_0^h mZ_1^2 dx = 593.57 \div 289.81 = +2.048$$

$$\Gamma_2 = \int_0^h mZ_2 dx \div \int_0^h mZ_2^2 dx = -452.51 \div 240.47 = -1.882$$

$$\Gamma_3 = \int_0^h mZ_3 dx \div \int_0^h mZ_3^2 dx = 334.51 \div 224.29 = +1.491$$

FIG. 4.5. CALCULATIONS OF THE  $\Gamma_j$  QUANTITIES.

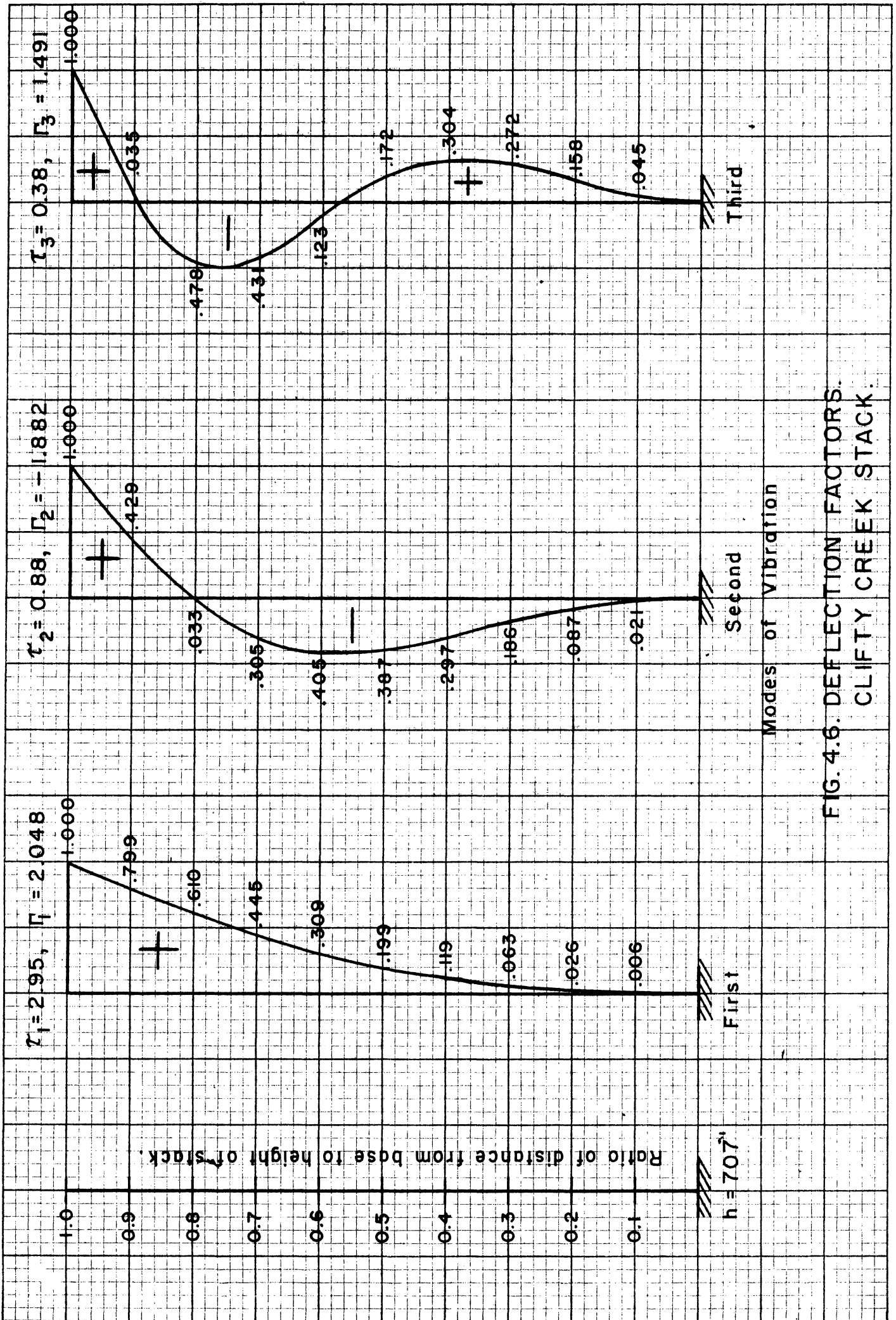


FIG. 4.6. DEFLECTION FACTORS.  
CLIFTY CREEK STACK.

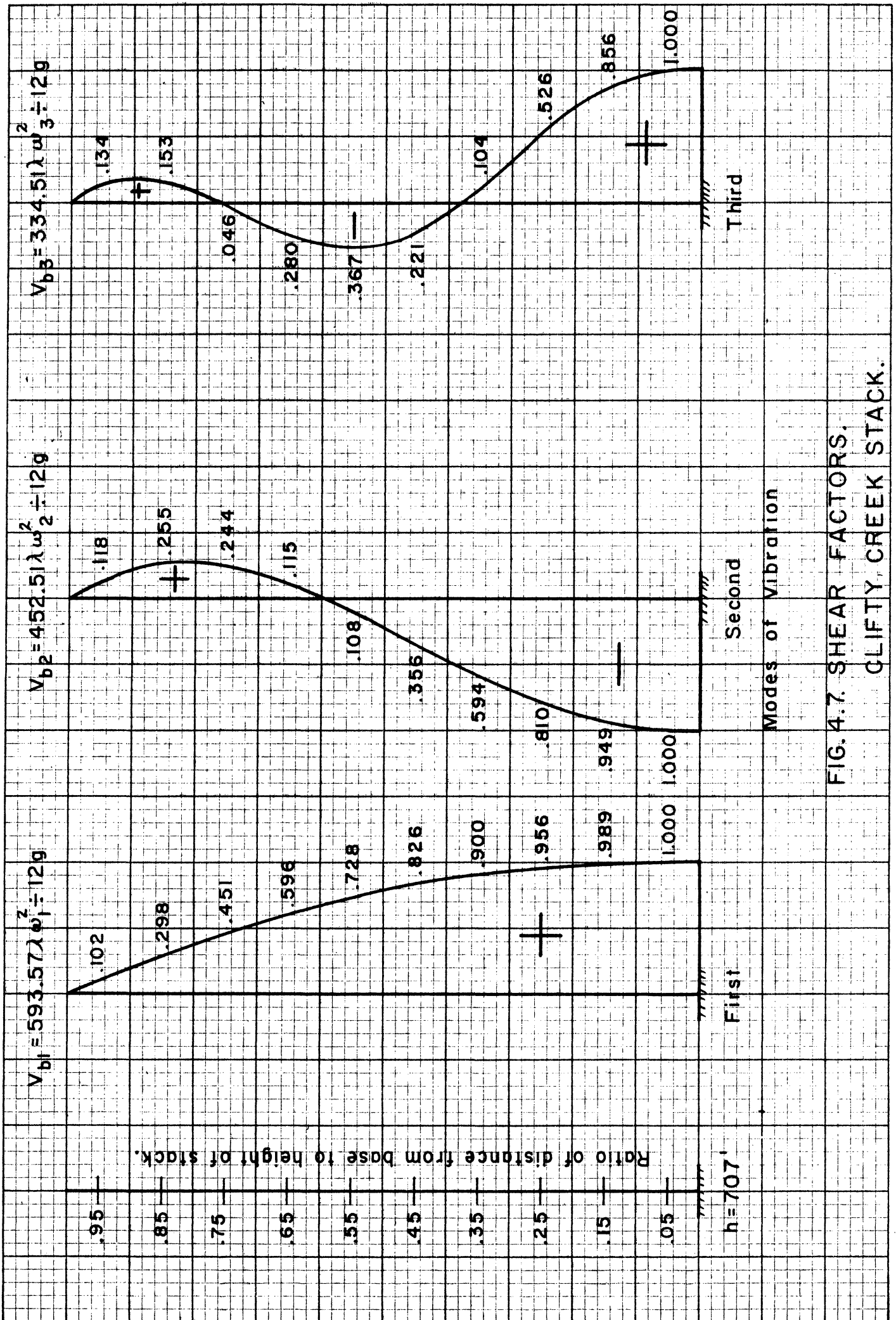


FIG. 4.7. SHEAR FACTORS.  
CLIFTY CREEK STACK.



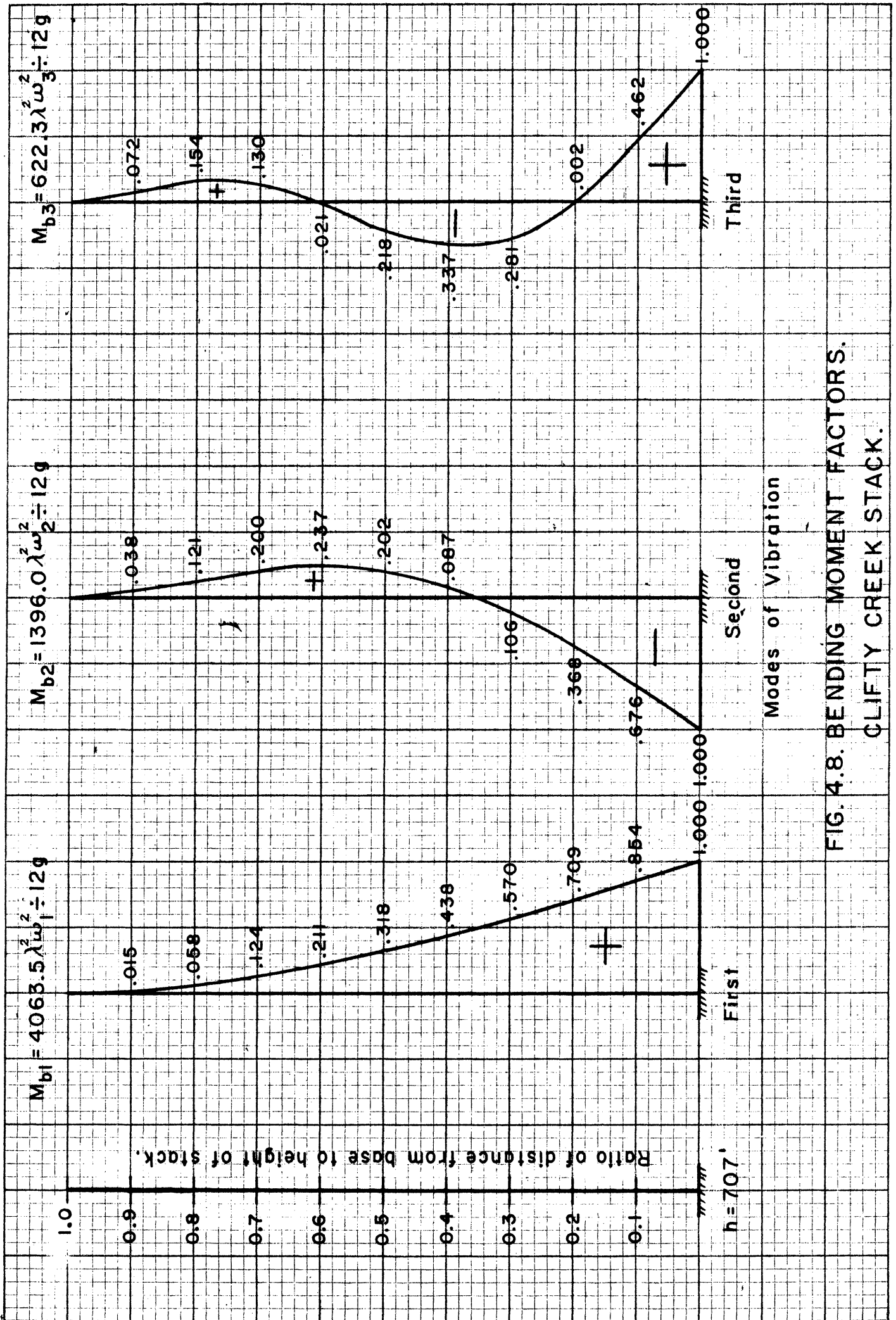


FIG. 4.8. BENDING MOMENT FACTORS.  
CLIFTY CREEK STACK.

## CHAPTER V

### GENERALIZED CO-ORDINATE RESPONSE TO EARTHQUAKE

The general equation for the generalized co-ordinate  $\phi_j$  with the effect of ground motion as derived in Chapter III is

$$\ddot{\phi}_j + 2\beta\omega_j\dot{\phi}_j + \omega_j^2\phi_j = -\ddot{y}_b \quad (2.76a)$$

Equation (2.76a) can be solved either by the Laplace Transform method, Newmark's step by step method, or by the use of the analogue computer. Since the function  $\ddot{y}_b$  does not follow a simple algebraic or trigonometric function, the analogue computer is used in this study.

In the case of the earthquake, the initial conditions for eq. (2.76a) are:

$$\begin{aligned} \phi(0) &= 0, \\ \dot{\phi}(0) &= 0, \end{aligned} \quad (5.1)$$

since the stack is assumed to be in its neutral position.

By the use of Churchill's (9) Laplace Transform symbols for solving the differential equation, eq. (2.76a) becomes

$$s^2\phi(s) - s\phi(0) - \dot{\phi}(0) + 2\beta\omega s\phi(s) - 2\beta\omega\phi(0) + \omega^2\phi(s) = -f(s) \quad (5.2)$$

Substitution of the boundary conditions in eq. (5.1) into eq. (5.2) gives

$$(s^2 + 2\beta\omega s + \omega^2)\phi(s) = -f(s) \quad (5.2a)$$

or

$$\phi(s) = -\frac{f(s)}{s^2 + 2\beta\omega s + \omega^2} = -\frac{f(s)}{s^2 + 2\beta\omega s + \frac{(2\beta\omega)^2}{4} + \left[\omega^2 - \frac{(2\beta\omega)^2}{4}\right]}$$

or

$$\phi(s) = -\frac{f(s)}{\left(s^2 + \frac{2\beta\omega}{2}\right)^2 + \frac{4\omega^2 - (2\beta\omega)^2}{4}} = -\frac{f(s)}{(s^2 + \beta\omega)^2 + (\omega\sqrt{1-\beta^2})^2} \quad (5.3)$$

Let

$$\omega' = \omega\sqrt{1-\beta^2} \quad (5.3a)$$

Thus, eq. (5.3) becomes

$$\phi(s) = \frac{1}{\omega'} \frac{f(s) \cdot \omega'}{(s^2 + \beta\omega)^2 + (\omega')^2} \quad (5.3b)$$

Therefore,

$$\phi(t) = -\frac{1}{\omega'} \ddot{y}_b(t) * e^{-\beta\omega t} \sin \omega' t, \quad (5.4)$$

or

$$\phi(t) = \frac{1}{\omega'} \int_0^t e^{-\beta\omega(t-\tau)} \ddot{y}_b \sin \omega' (t - \tau) d\tau. \quad (5.5)$$

Since we have shown that  $\omega'$  is approximately equal to  $\omega$ , eq.

(5.5) can be written in the form

$$\phi_j(t) = \frac{1}{\omega_j} \int_0^t e^{-\beta_j\omega_j(t-\tau)} \ddot{y}_b \sin \omega_j(t - \tau) d\tau, \quad (5.5a)$$

for the  $j$ th mode of vibration.

Equation (5.5a) can be used if small time intervals are taken because of the random nature of the accelerograph  $\ddot{y}_b$ . To complete the analysis of one accelerograph plus the fact that there are many values of  $\omega_j$  is time-consuming and hence this method is not used in this study. The analysis is presented only for the sake of completeness and for the use of those who might not have the analogue computer at their disposal.

The response  $\phi_j(t)$  is actually the response due to a single degree of freedom system which is best exemplified by a spring-mass system. The maximum value of  $\phi_j(t)$  is often called the "displacement spectrum" (1).

For the benefit of those who are not familiar with the Laplace Transform method, the Newmark's step by step method is discussed briefly. In eq. (2.76a), the mass is assumed to be unity, and therefore the Resistance Curve has a slope equal to  $\omega_j^2$ . The velocity  $\dot{\phi}_j$  is expressed in terms of the acceleration ( $\ddot{\phi}_j$ ) and the increment of time ( $\Delta t$ ). The

displacement  $\phi_j$  can be expressed in terms of velocities and increment of time. These relationships are:

$$\dot{\phi}_f = \dot{\phi}_o + \frac{\Delta t}{2} (\ddot{\phi}_o + \ddot{\phi}_f) , \quad (5.6)$$

$$\phi_f = \phi_o + \Delta t \dot{\phi}_o + \frac{\Delta t}{2} \ddot{\phi}_o + \frac{\Delta t}{6} \ddot{\phi}_f , \quad (5.7)$$

where the subscripts f and o denote final and initial conditions respectively. These relationships for increment of time, acceleration, velocity, and displacement are the basic tools of Newmark's Method. First assume a trial total resistance Q. Then subtract Q from the applied force P (in this case  $-\ddot{y}_b$ ). The quantity (P - Q) is really the net force in Newton's second law of motion. Divide the net force (P - Q) by the mass m which is unity in this case to get the trial acceleration. The trial velocity and displacement are then derived by the use of the relationships discussed above. Then the damping force  $2\beta\omega_j\dot{\phi}_j$  is obtained from the velocity, and the resistance force  $\omega_j^2\phi_j$  is derived from the displacement. The derived total resistance force is obtained by adding the damping force to the resistance force. Details of the theory and computations can be found in Newmark's (24) paper. As in the Laplace Transform method the process is laborious.

Since the electronic analogue computer is available for this study, it is used.

The theory, design, and operation of the analogue computer can be found in the report of C. E. Howe and R. E. Howe (25). According to the above report, the basic computing element is the operational amplifier which consists of a high-gain d.c. amplifier plus an input impedance and a feedback impedance. The operational amplifier can do three basic operations, namely; addition, sign inversion, and integration. The first

amplifier is called the "summer", the second, "sign inverter", and the third "integrator". In all the operations, voltages proportional to the physical quantities are used as the inputs and the outputs are also voltages. For example if a voltage equivalent to  $\phi$  is fed into an integrator, then the output voltage is equivalent to  $-\dot{\phi}$ . Note that the sign is changed besides the integration process.

Potentiometers are also available to control the voltages simulating the physical quantities.

Besides the computing element and potentiometers, a separate unit known as the function generator is also required to simulate the forcing function which in this case is the accelerograph.

In this study the Reeves Electronic Analogue Computer (REAC Model No. C101 ) with the Reeves Servo is used. The Reeves Function Generator (Model No. IC-101) is also used. The Brush Recorder is used to record the physical elements. Detailed descriptions of the above units can be found in the manuals issued by the Reeves Company and the Brush Company.

Before leaving the units, it might be well to say that the Servo has been used in this study to put voltages with more accuracy in the potentiometers and the integrators (for initial conditions). In the Function Generator, there is a drum around which is wrapped a stiff paper. In this stiff paper a wire following the outline of the forcing function is glued. The maximum value of the ordinates is +100 volts and the minimum is -100 volts. One sweep of the drum is 190 volts.

In this part of this study Mr. F. L. Bartman and Professor R. E. Howe have given indispensable assistance.

Since the range of the periods of chimneys is from 0.3 to 3.0 seconds, it is advisable to express eq. (2.76a) in terms of a new variable  $t'$ . Let,

$$t' = \omega t . \quad (5.8)$$

Then,

$$\frac{d\phi}{dt} = \frac{d\phi}{dt'} \cdot \frac{dt'}{dt} = \omega \frac{d\phi}{dt'} , \quad (5.9)$$

and

$$\frac{d^2\phi}{dt^2} = \frac{d}{dt} \left( \frac{d\phi}{dt} \right) = \frac{d}{dt} \left( \omega \frac{d\phi}{dt'} \right) = \frac{d}{dt'} \left( \omega \frac{d\phi}{dt'} \right) \frac{dt'}{dt} = \omega^2 \frac{d^2\phi}{dt'^2} . \quad (5.10)$$

Similarly,

$$\frac{d^2y_b}{dt^2} = \omega^2 \frac{d^2y_b}{dt'^2} . \quad (5.11)$$

Therefore eq. (2.76a) becomes

$$\omega^2 \frac{d^2\phi}{dt'^2} + 2\beta\omega^2 \frac{d\phi}{dt'} + \omega^2\phi = -\omega^2 \frac{d^2y_b}{dt'^2} \quad (5.12)$$

or,

$$\frac{d^2\phi}{dt'^2} + 2\beta \frac{d\phi}{dt'} + \phi = -\frac{d^2y_b}{dt'^2} = -\frac{1}{\omega^2} \frac{d^2y_b}{t'^2} . \quad (5.12a)$$

The computer circuit for eq. (5.12a) is shown in Fig. 5.1.

As an illustration, the response curves  $\phi_j$  for the El Centro, California earthquake of May 18, 1940 with N-S component are shown in Fig. 5.2. These curves are for the Clifty Creek Stack ( $h = 707'$ ) whose first three periods are  $\tau_1 = 3.0$  seconds/cycle,  $\tau_2 = 0.88$ , and  $\tau_3 = 0.38$ , and for a damping coefficient  $\beta_j = 0.050$  for each mode.

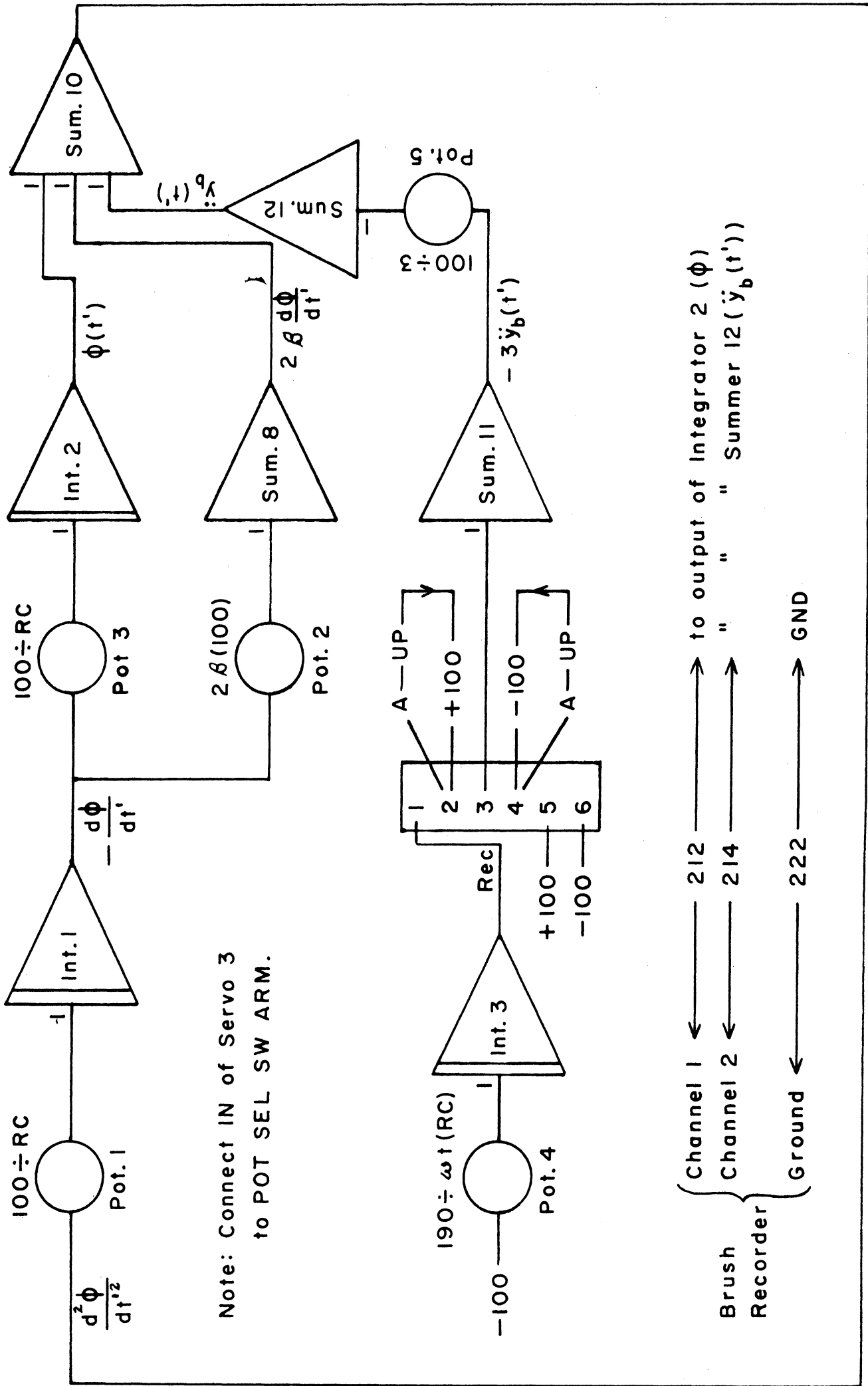


FIG. 5.1. ANALOG COMPUTER CIRCUIT.

Earthquake of El Centro, Cal., May 18, 1940 N-S.  $\beta = 0.050$

$\tau_1 = 2.95$ . One Vertical Division =  $0.04875g \div 5\omega_1^2$

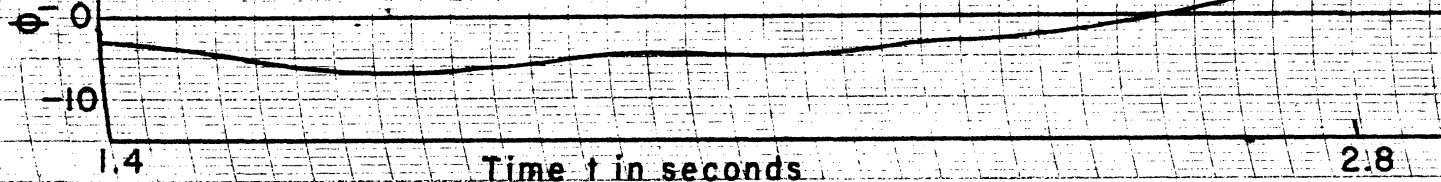
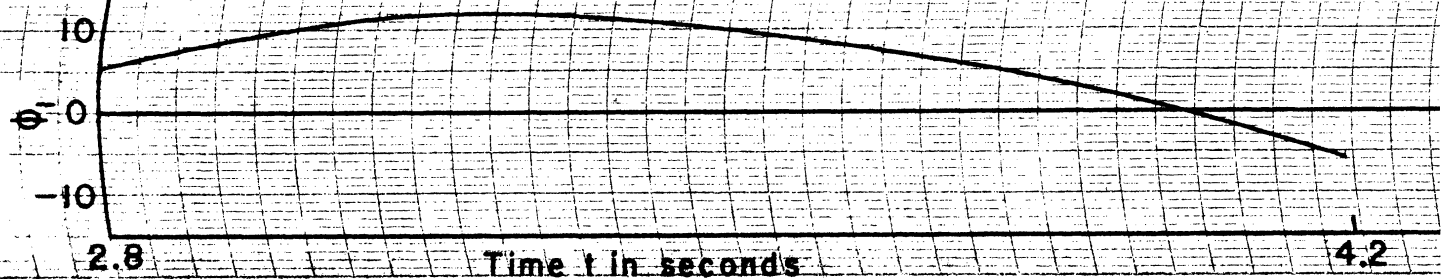


CHART NO. BL 909

BRUSH ELECTRONICS

$\tau_1 = 2.95$



$\tau_2 = 0.88$ . One Vert. Div. =  $.04875g \div \omega_2^2$

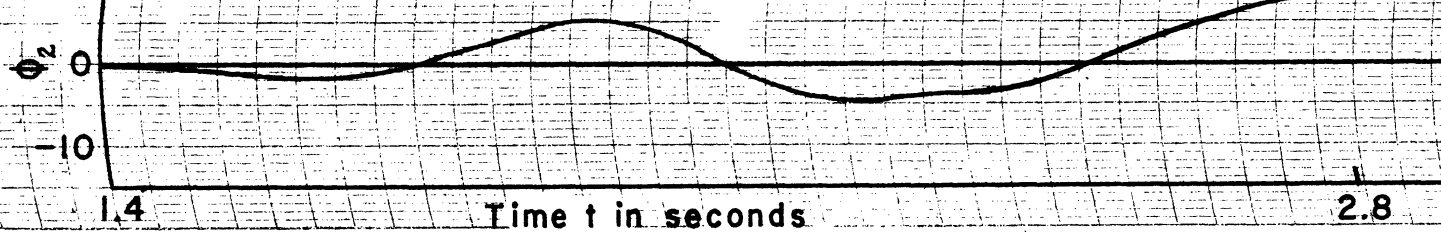
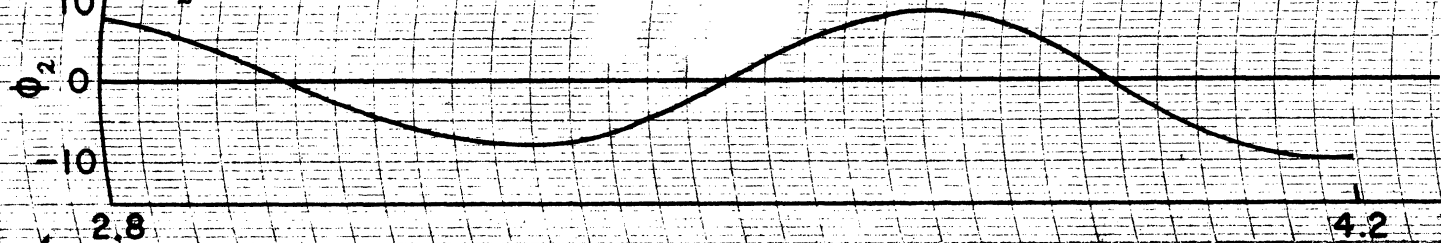


CHART NO. BL 909

BRUSH ELECTRONICS

$\tau_2 = 0.88$



$\tau_3 = 0.38$ . One Vert. Div. =  $.04875g \div \omega_3^2$

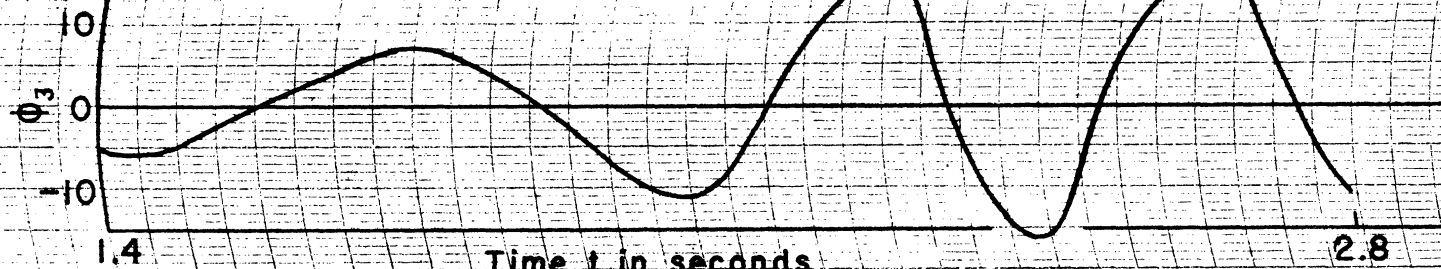


CHART NO. BL 909

BRUSH ELECTRONICS

$\tau_3 = 0.38$  sec. per cycle

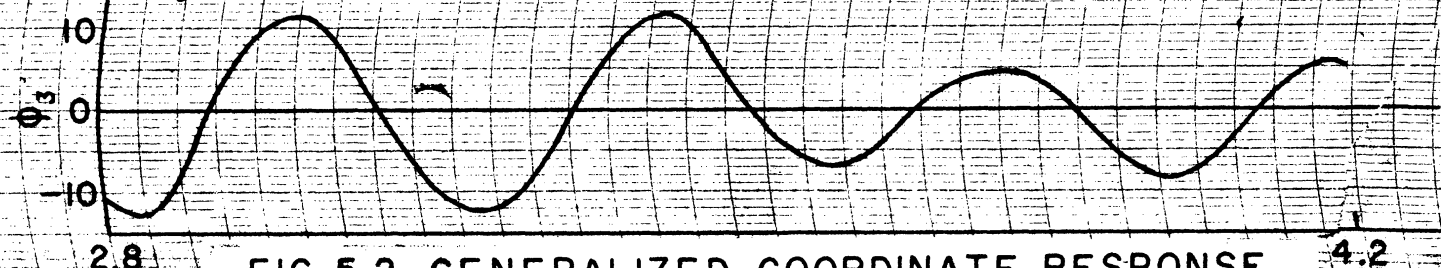


FIG. 5.2. GENERALIZED COORDINATE RESPONSE.



## CHAPTER VI

### DESIGN SHEARS AND BENDING MOMENTS

From the results of Chapters IV and V the instantaneous shears and bending moments can be computed by the use of eq. (2.78) and eq. (2.79) which are:

$$V = \sum_{j=1}^{\infty} V_j \Gamma_j \phi_j \quad , \quad (2.78)$$

$$M = \sum_{j=1}^{\infty} M_j \Gamma_j \phi_j \quad . \quad (2.79)$$

The procedure is as follows:

1. Multiply the first two dynamic structural properties to get  $V_j \Gamma_j$  and  $M_j \Gamma_j$  and express the results in terms of the maximum value which occurs at the base of the stack of the first mode. Call these quantities shear coefficients ( $V_j \Gamma_j$ ) and bending moment coefficients ( $M_j \Gamma_j$ ).
2. Multiply the results of step (1) by the response  $\phi_j(t)$  at different instants as given in Chapter V.
3. Plot the results of step (2) and obtain the maximum shears and bending moments at various points along the stack.

The Clifty Creek Stack ( $h = 707'$ ) is used as a numerical example, taking the base of the stack first. For the shear at the base,

$$V_{b1} \Gamma_1 = (593.6 \lambda \omega_1^2 + 12g)(2.048) = 1215.7 \lambda \omega_1^2 + 12g \quad , \quad (6.1)$$

$$V_{b2} \Gamma_2 = (-452.5 \lambda \omega_2^2 + 12g)(-1.882) = 851.6 \lambda \omega_2^2 + 12g \quad , \quad (6.2)$$

$$V_{b3} \Gamma_3 = (334.5 \lambda \omega_3^2 + 12g)(1.491) = 498.7 \lambda \omega_3^2 + 12g \quad , \quad (6.3)$$

Table 6.1  
Shear Coefficients

Stack → x ÷ h	Clifty Creek h = 707'			Modified Selby h = 605'			Kyger Creek h = 562'		
	V <sub>1</sub>   V <sub>2</sub>   V <sub>3</sub>	V <sub>1</sub>   V <sub>2</sub>   V <sub>3</sub>	V <sub>1</sub>   V <sub>2</sub>   V <sub>3</sub>	V <sub>1</sub>   V <sub>2</sub>   V <sub>3</sub>	V <sub>1</sub>   V <sub>2</sub>   V <sub>3</sub>	V <sub>1</sub>   V <sub>2</sub>   V <sub>3</sub>	V <sub>1</sub>   V <sub>2</sub>   V <sub>3</sub>	V <sub>1</sub>   V <sub>2</sub>   V <sub>3</sub>	V <sub>1</sub>   V <sub>2</sub>   V <sub>3</sub>
1.00									
.95	.102	-.080	.055	.089	-.075	.048	.093	-.079	.057
.85	.298	-.179	.063	.267	-.173	.070	.306	-.190	.084
.75	.451	-.171	-.019	.431	-.177	-.007	.487	-.181	-.011
.65	.596	-.081	-.115	.580	-.091	-.113	.624	-.084	-.120
.55	.728	.076	-.150	.706	.060	-.156	.731	.070	-.169
.45	.826	.250	-.091	.805	.240	-.105	.816	.255	-.125
.35	.900	.416	.043	.885	.427	.031	.888	.461	.015
.25	.956	.568	.216	.950	.604	.217	.950	.674	.239
.15	.989	.665	.351	.984	.711	.352	.989	.825	.439
.05	1.000	.701	.410	1.000	.762	.425	1.000	.872	.512
0	Fac <sub>tor</sub> = 7162 <sub>ωj</sub> <sup>2</sup> ÷ g kips/ft			Fac <sub>tor</sub> = 3849 <sub>ωj</sub> <sup>2</sup> ÷ g kips/ft			Fac <sub>tor</sub> = 4413 <sub>ωj</sub> <sup>2</sup> ÷ g kips/ft		

Table 6.2  
Bending Moment Coefficients

Stack → x + h	Clifty Creek h = 707'			Modified Selby h = 605'			Kyger Creek h = 562'		
	M <sub>1</sub> □ <sub>1</sub>	M <sub>2</sub> □ <sub>2</sub>	M <sub>3</sub> □ <sub>3</sub>	M <sub>1</sub> □ <sub>1</sub>	M <sub>2</sub> □ <sub>2</sub>	M <sub>3</sub> □ <sub>3</sub>	M <sub>1</sub> □ <sub>1</sub>	M <sub>2</sub> □ <sub>2</sub>	M <sub>3</sub> □ <sub>3</sub>
1.0	0	0	0	0	0	0	0	0	0
.9	.015	-.012	-.008	.013	-.011	.007	.014	-.011	.008
.8	.058	-.038	.017	.053	-.037	.018	.058	-.039	.021
.7	.124	-.063	.014	.118	-.064	.016	.129	-.065	.019
.6	.211	-.075	-.002	.204	-.077	-.001	.219	-.078	.002
.5	.318	-.064	-.024	.310	-.068	-.024	.326	-.067	-.023
.4	.438	-.027	-.037	.430	-.032	-.040	.444	-.030	-.041
.3	.570	.033	-.031	.562	.032	-.035	.573	.036	-.039
.2	.709	.116	0	.704	.122	-.002	.711	.134	-.004
.1	.854	.214	.051	.851	.228	.050	.855	.253	.060
0	1.000	.316	.111	1.000	.342	.114	1.000	.380	.134
	Factor = 3,467,000 ω <sub>j</sub> <sup>2</sup> + ft-kips/ft			Factor = 1,560,000 ω <sub>j</sub> <sup>2</sup> + g ft-kips/ft			Factor = 1,708,000 ω <sub>j</sub> <sup>2</sup> + g ft-kips/ft		

FIG. 6.1. INSTANTANEOUS SHEAR CURVES.

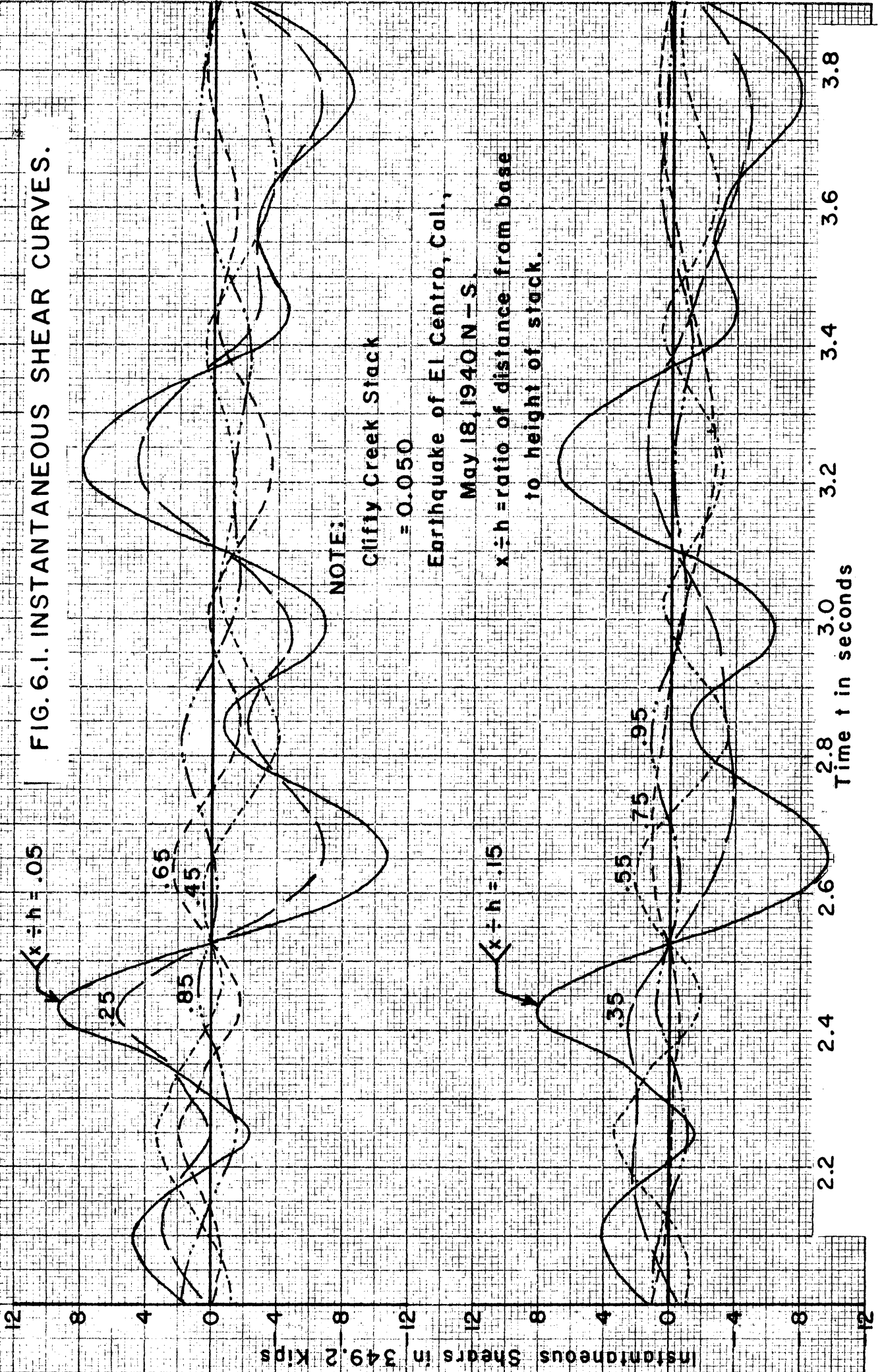
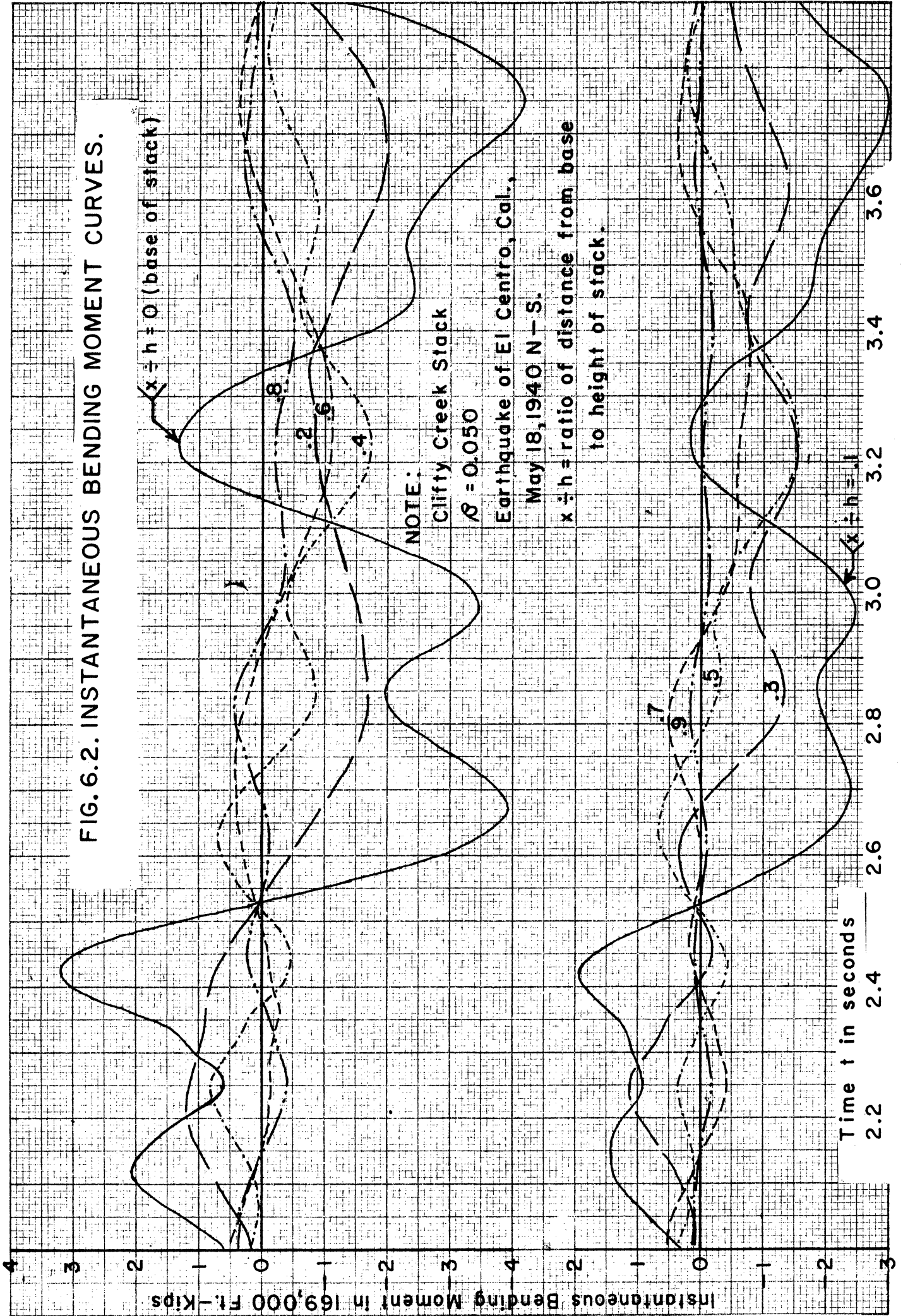


FIG. 6.2. INSTANTANEOUS BENDING MOMENT CURVES.



## CHAPTER VII

### CONCLUSIONS AND DESIGN RECOMMENDATIONS

The shears and bending moments along the height of the chimneys are computed by the use of the empirical seismic coefficient  $K_e$  for a particular locality. The seismic coefficient is multiplied by the weight of the chimney above the section under consideration to get the forces.

The maximum shears and bending moments along the height of the stack obtained in Chapter VI are also plotted.

Then the shears and bending moments derived from the previous chapter are divided by the shears and bending moments derived by the use of the seismic coefficient. The result of the division is defined as the magnification factor. These magnification factors are the basis of the recommendation for the preliminary design rules of reinforced concrete chimneys.

The results of the computations for the illustrative stack are shown in Figs. 7.1 and 7.2. Figures 7.3 and 7.4 show that the shear and bending moment magnification factor curves for damping coefficient of 7-1/2% are below the curves for 5% but the deviation is not significant enough to affect the recommended design formulas.

The most recent ACI Code (26) Title No. 49-26 reported by the ACI Committee 505 is quoted below:

#### 403 - Moments due to Earthquakes

(a) Where earthquakes are likely to occur, chimneys shall be designed to resist the forces set up by an earthquake of the maximum severity anticipated from the earthquake experience record for the region under consideration. The moments from earthquake shock,  $M_e$ , shall be computed by eq. (51) and (52).

1. Where the section under consideration is at or below 1/5 of the total chimney height measured from the base of chimney

$$M_e = Fh'' \quad (51)$$

2. Where the section under consideration is more than 1/5 of the total chimney height measured from the base of the chimney

$$M_e = Fh'' \left[ 1 + \frac{h'}{100} \right] \quad (52)$$

where

$$F = W'a/g = W'K_e,$$

W' = Weight of chimney above section under consideration, including any portion of lining supported from the chimney shell, lb.,

h'' = Distance from section under consideration to center of gravity of chimney mass above the section, in.,

h' = Distance from section under consideration to the section that is 1/5 of the total height of the chimney above base, ft.,

a = Acceleration due to the earthquake, fps per sec.,

g = Acceleration due to gravity, fps per sec.,

K<sub>e</sub> = a/g = Seismic coefficient to be determined for locality where chimney is to be constructed.

The magnification factors corresponding to  $(1 + h'/100)$  based on the ACI Code quoted above are plotted. These magnification curves are compared with the ones obtained by means of the dynamic analyses made in this study. The ACI Code is found to be insufficient as shown in Fig. 7.5, for regions where strong-motion earthquakes occur even if the value of  $K_e = 0.20$  is used. Therefore, new formulas for the magnification factors need to be derived.

An envelope is drawn for the magnification factor curves, and parabolic fitted curves are obtained and recommended for preliminary design. The fitted curves are shown in Figs. 7.3 and 7.5.

After the formulas for the magnification factor curves have been derived, it is necessary to assign values to the seismic coefficients  $K_e$  for different localities. The ideal thing to do is to make similar studies of available accelerograph records of earthquakes for the particular locality and then determine  $K_e$ . However, in the absence of accelerograph records, the engineer is referred to the map showing occurrences of earthquakes of various intensities for different localities in the U.S. put out by the American Standards Association (27).

In this study, earthquake regions are divided into three groups namely:

1. Strong-motion region, where the accelerograph records show maximum accelerations of from 0.0875 g to 0.325 g,
2. Medium-intensity region, where the accelerograph records show maximum accelerations of from 0.05 g to 0.0875 g, and
3. Light-intensity region, where the accelerograph records show maximum accelerations of less than 0.05 g.

The recommended design formulas for the shears and bending moments are:

$$V = W'K_e h'' \left[ 1.8 + 8 \left( \frac{x - .5h}{.5h} \right)^2 \right], \quad x \geq .5h, \quad (7.1)$$

$$= 1.8W'K_e h'' \quad x \leq .5h, \quad (7.1a)$$

$$M = W'K_e h'' \left[ 1 + 8 \left( \frac{x - .2h}{.8h} \right)^2 \right], \quad x \geq .2h, \quad (7.2)$$

$$= W'K_e h'' , \quad x \leq .2h, \quad (7.2a)$$

for stacks whose fundamental periods are from 2.4 to 3.0 seconds per cycle.



The recommended seismic coefficients for the different regions discussed above are:

Region (1),  $K_e = 0.20$  ,

Region (2),  $K_e = 0.06$  ,

Region (3),  $K_e = 0.03$ .

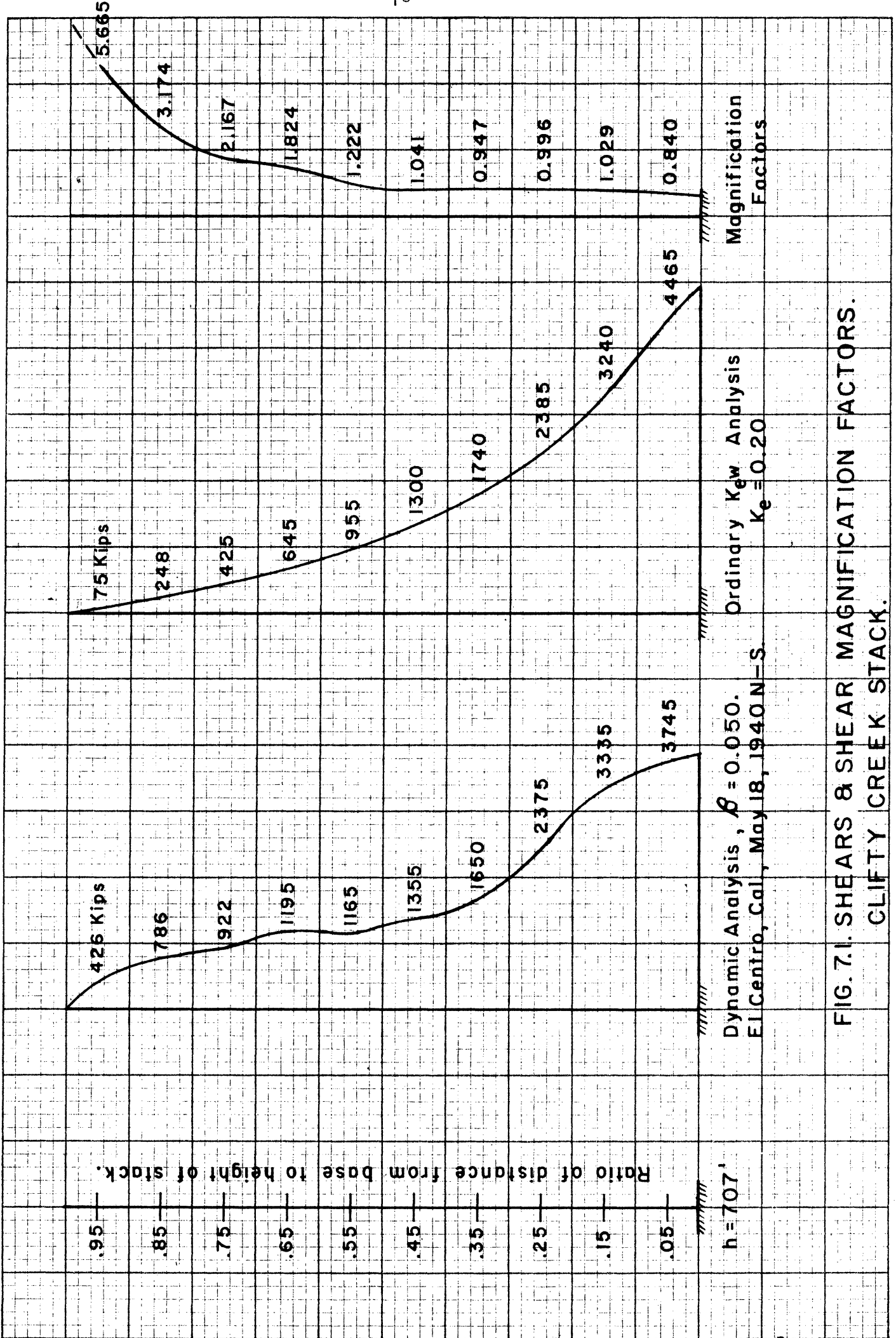


FIG. 7.1. SHEARS & SHEAR MAGNIFICATION FACTORS.  
 CLIFTY CREEK STACK.

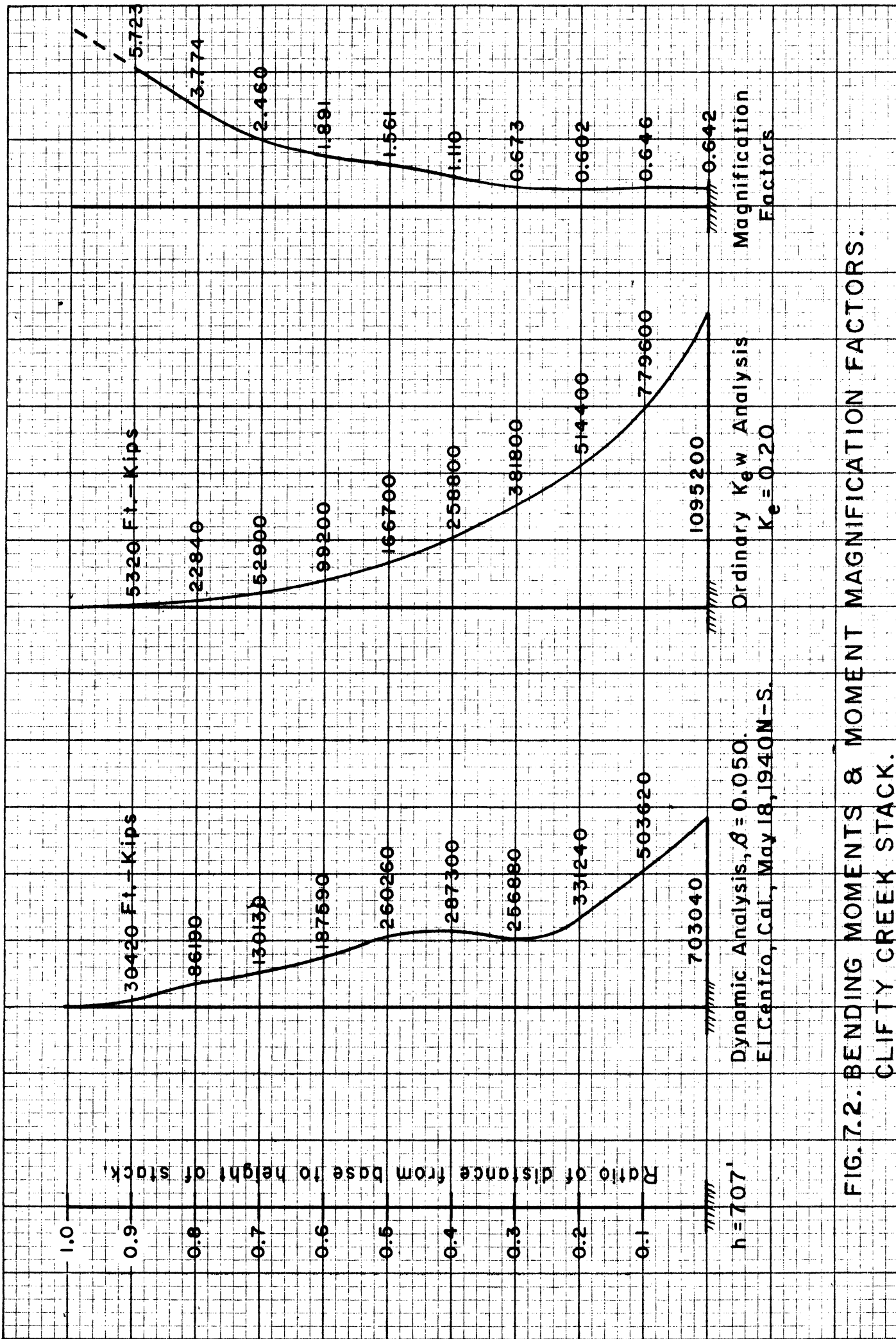


FIG. 7.2. BENDING MOMENTS & MOMENT MAGNIFICATION FACTORS.  
 CLIFTY CREEK STACK.

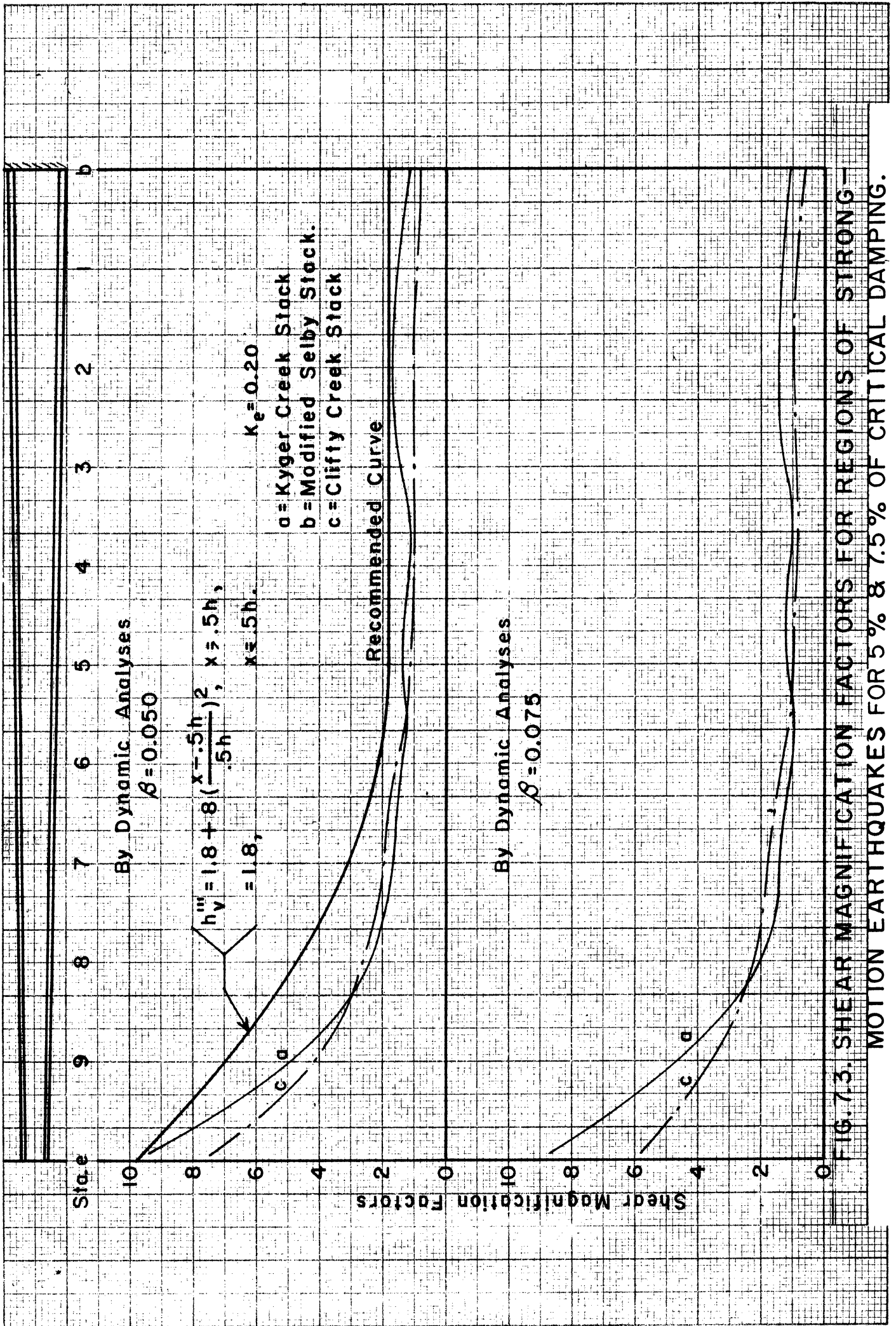


FIG. 7.3. SHEAR MAGNIFICATION FACTORS FOR REGIONS OF STRONG-MOTION EARTHQUAKES FOR 5% & 7.5% OF CRITICAL DAMPING.

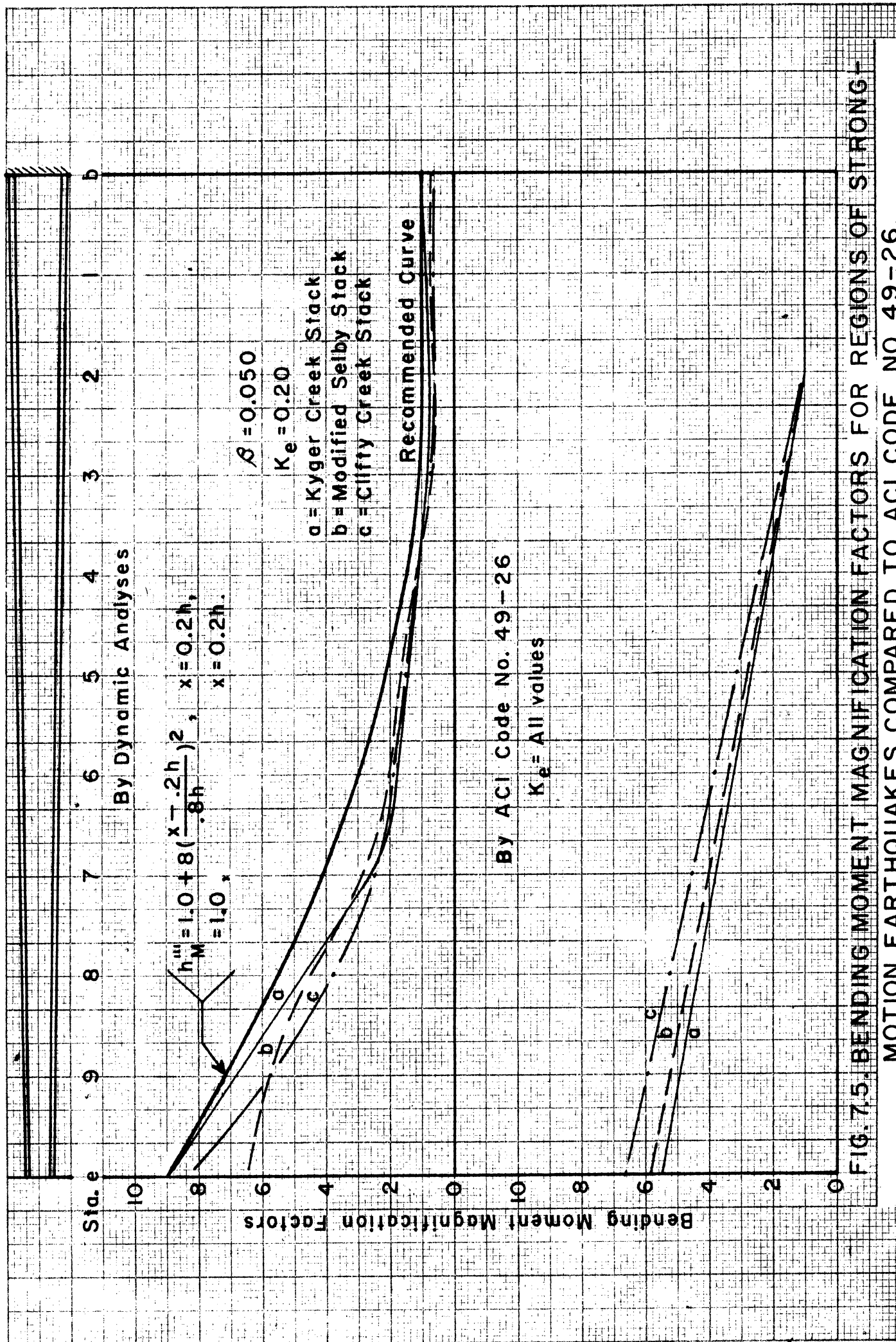


FIG. 7.5. BENDING MOMENT MAGNIFICATION FACTORS FOR REGIONS OF STRONG-

MOTION EARTHQUAKES COMPARED TO ACI CODE NO. 49-26.



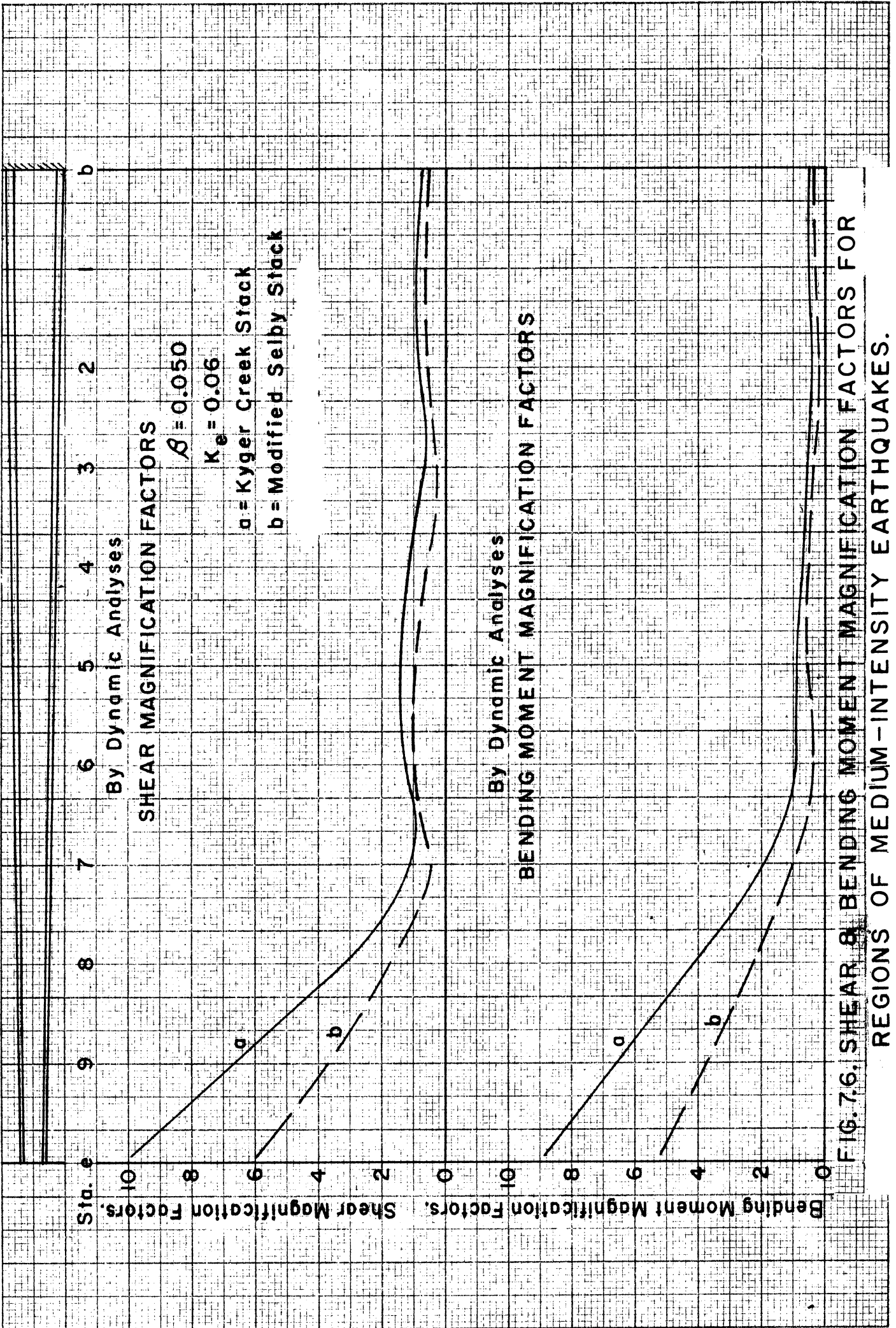


FIG. 7.6. SHEAR & BENDING MOMENT MAGNIFICATION FACTORS FOR REGIONS OF MEDIUM-INTENSITY EARTHQUAKES.

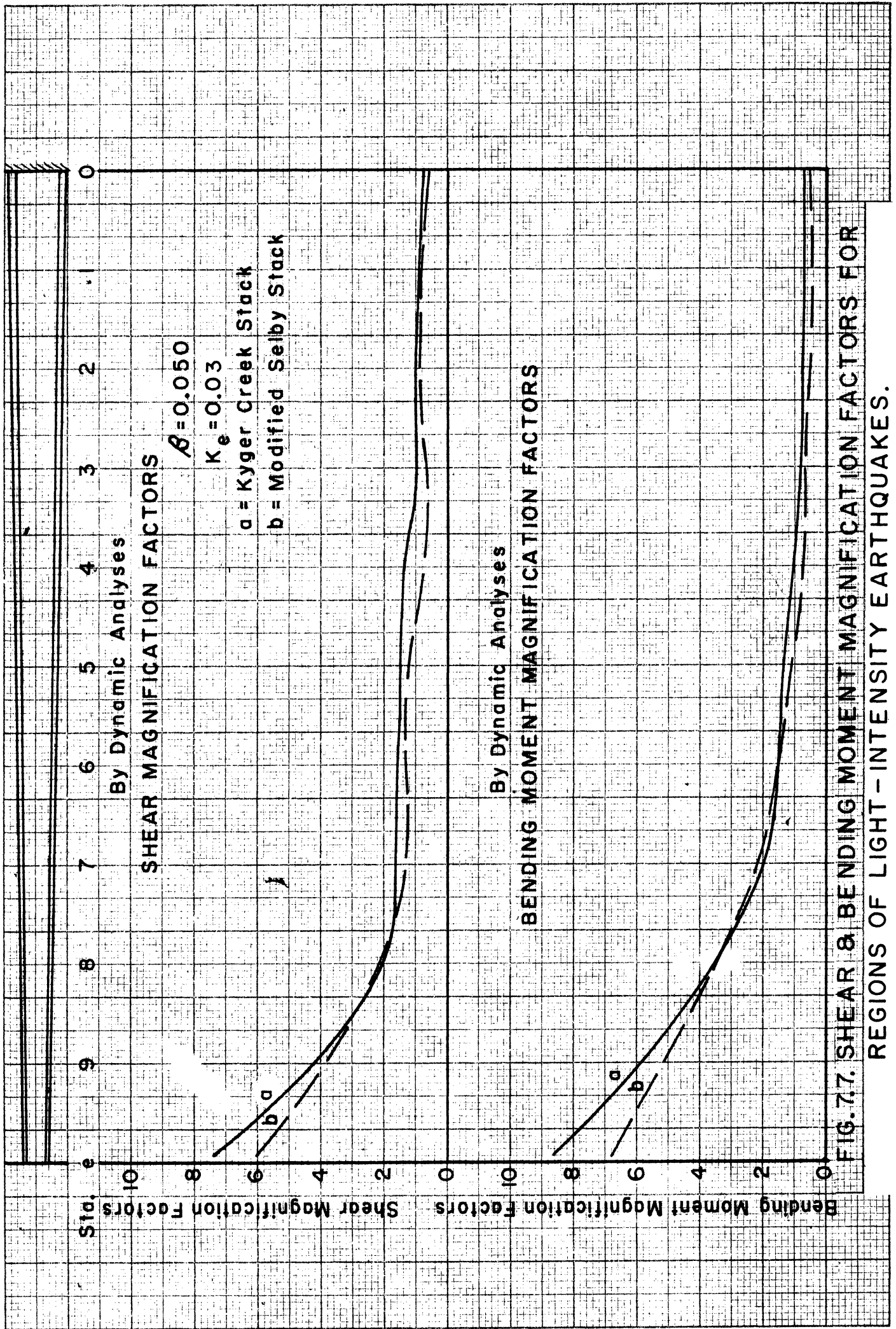


FIG. 7.7. SHEAR & BENDING MOMENT MAGNIFICATION FACTORS FOR REGIONS OF LIGHT-INTENSITY EARTHQUAKES.

APPENDIX  
Additional Data



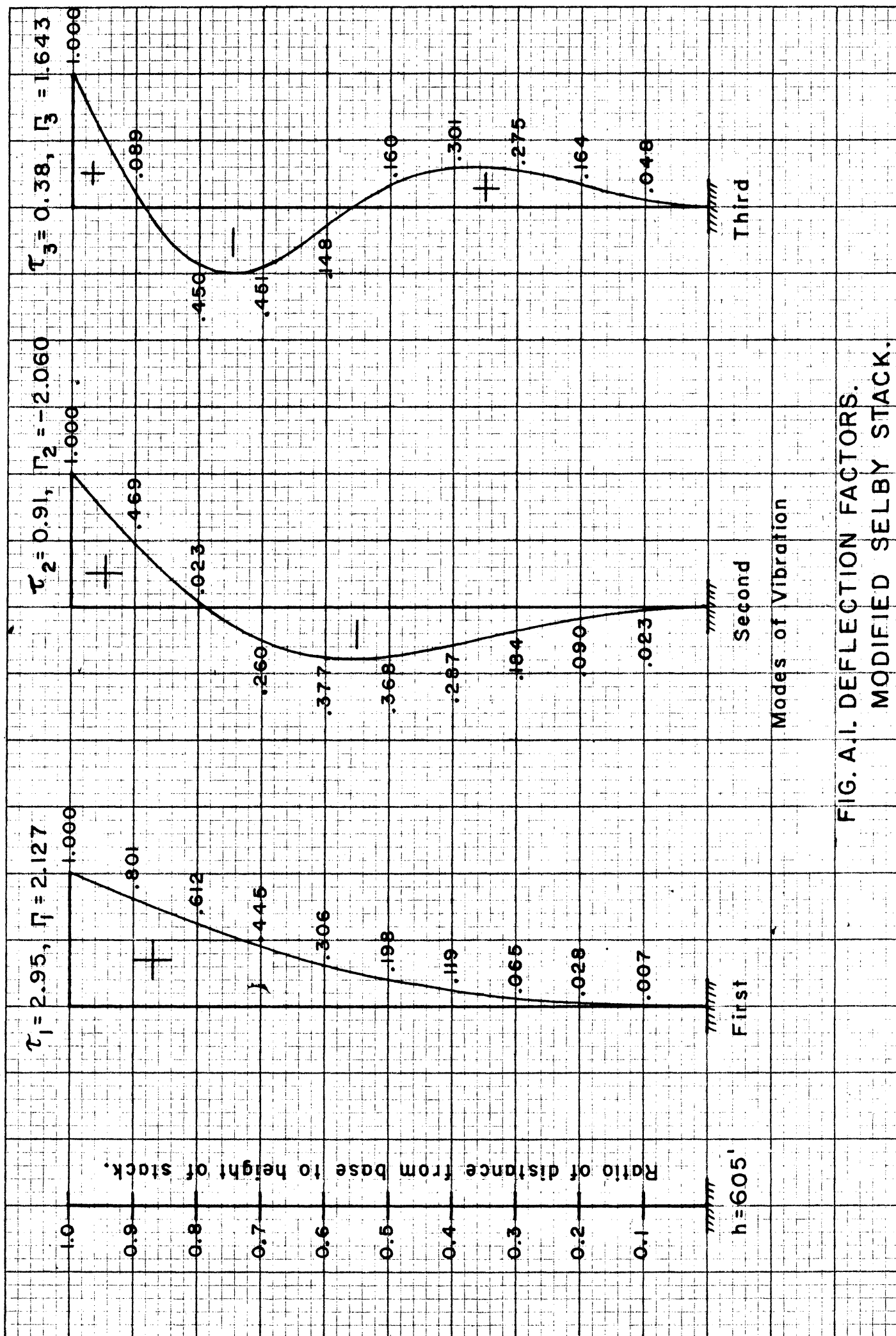


FIG. A.1. DEFLECTION FACTORS.  
MODIFIED SELBY STACK.

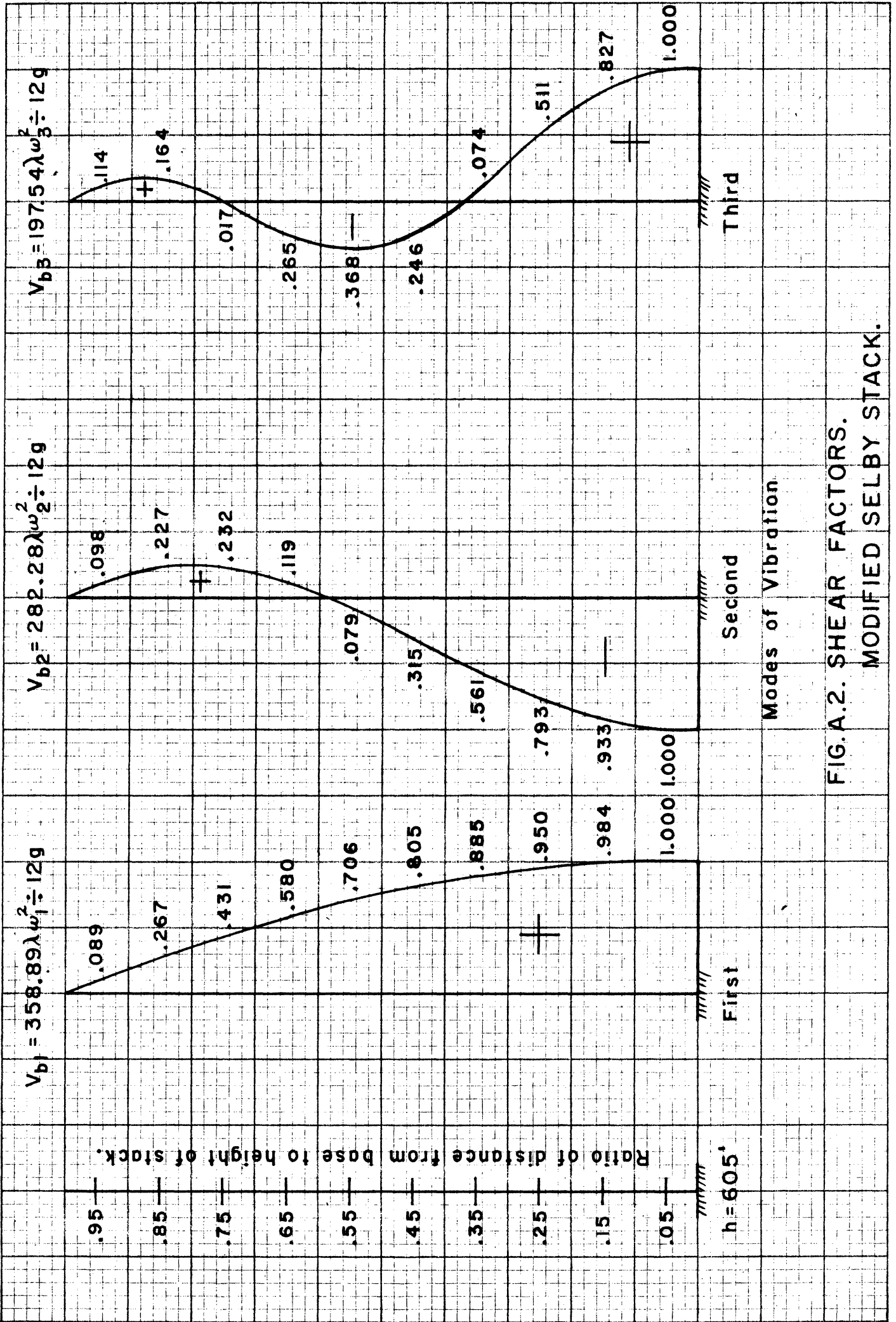


FIG.A.2. SHEAR FACTORS.  
MODIFIED SELBY STACK.

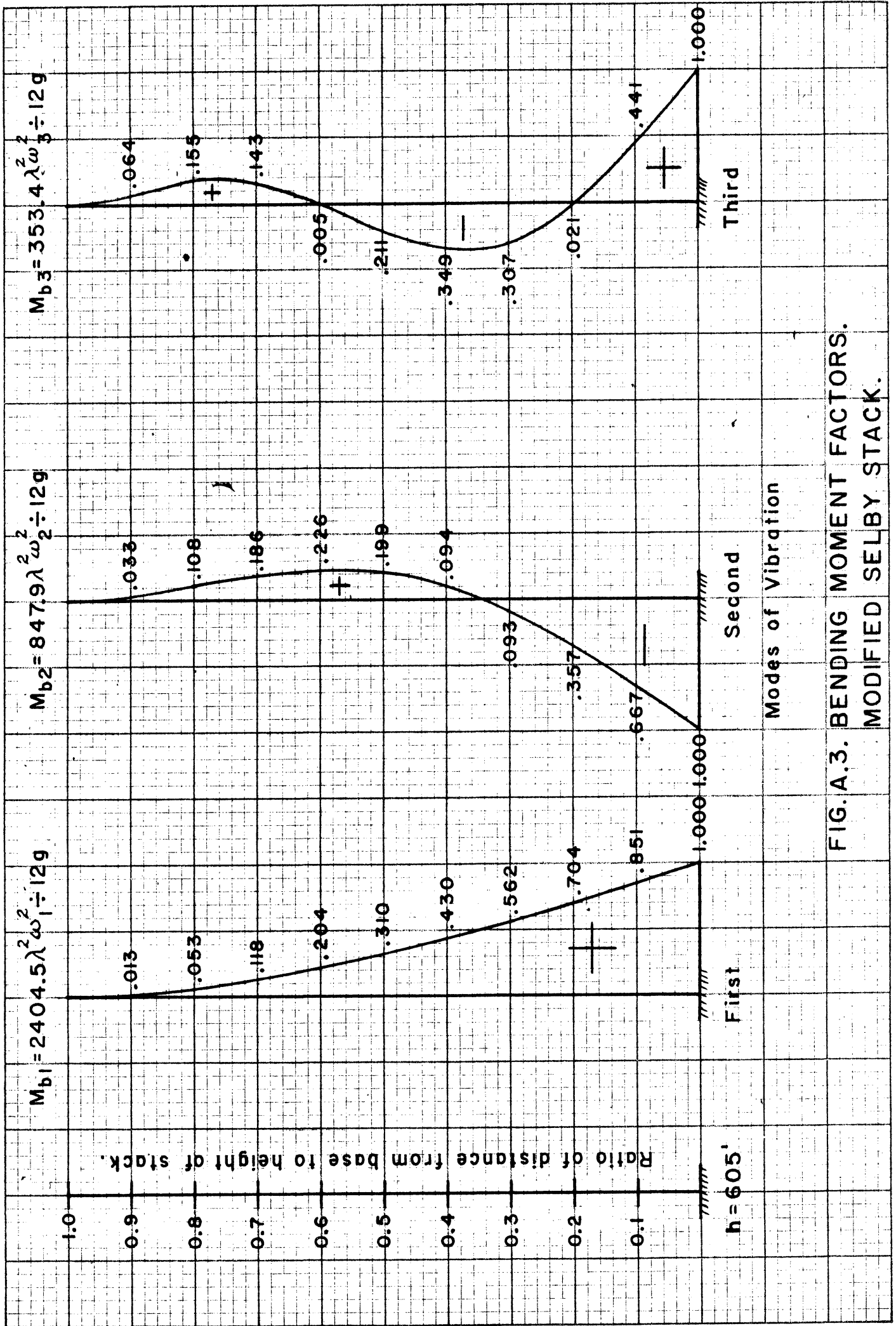


FIG. A.3. BENDING MOMENT FACTORS. MODIFIED SELBY STACK.

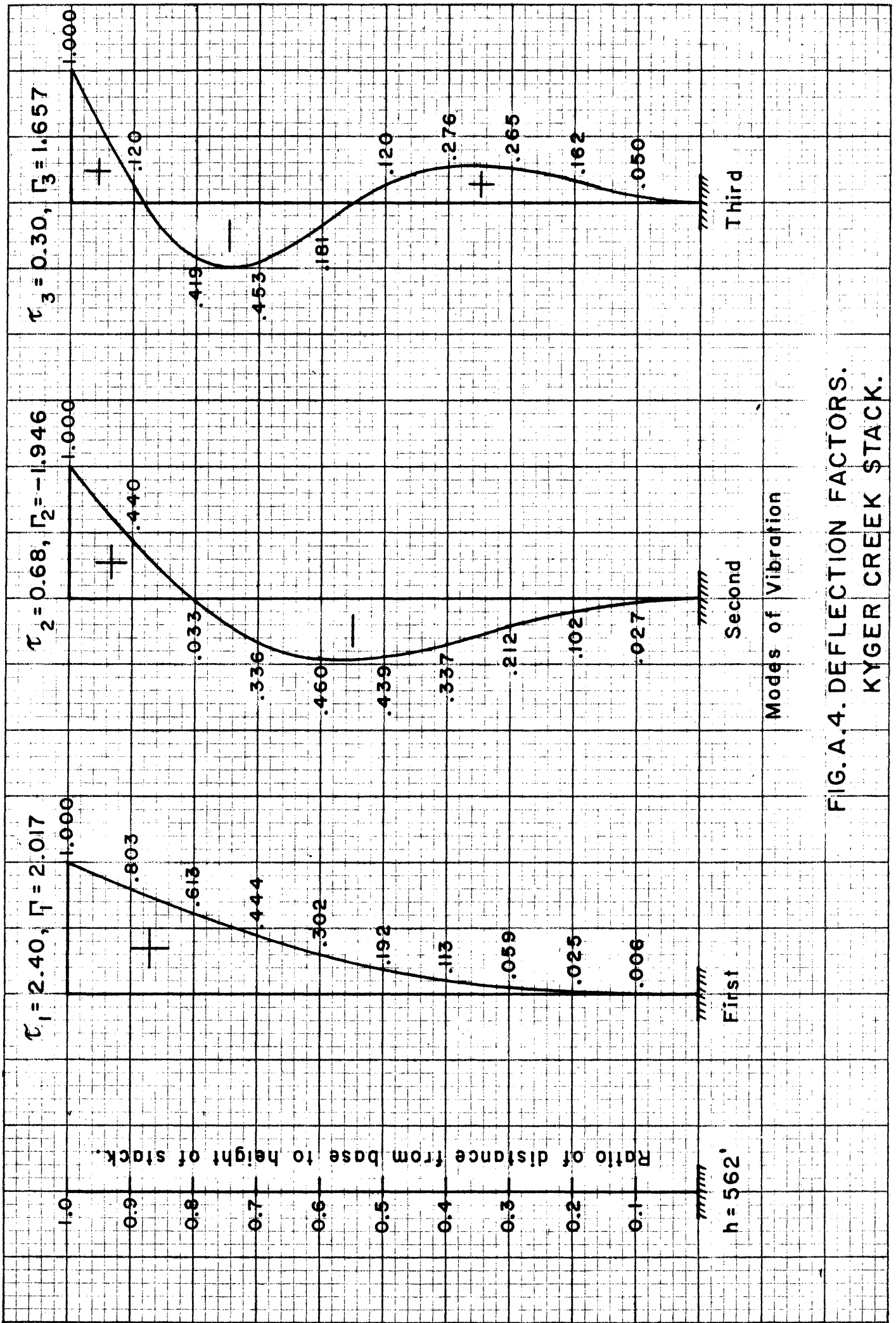


FIG. A. 4. DEFLECTION FACTORS.  
KYGER CREEK STACK.

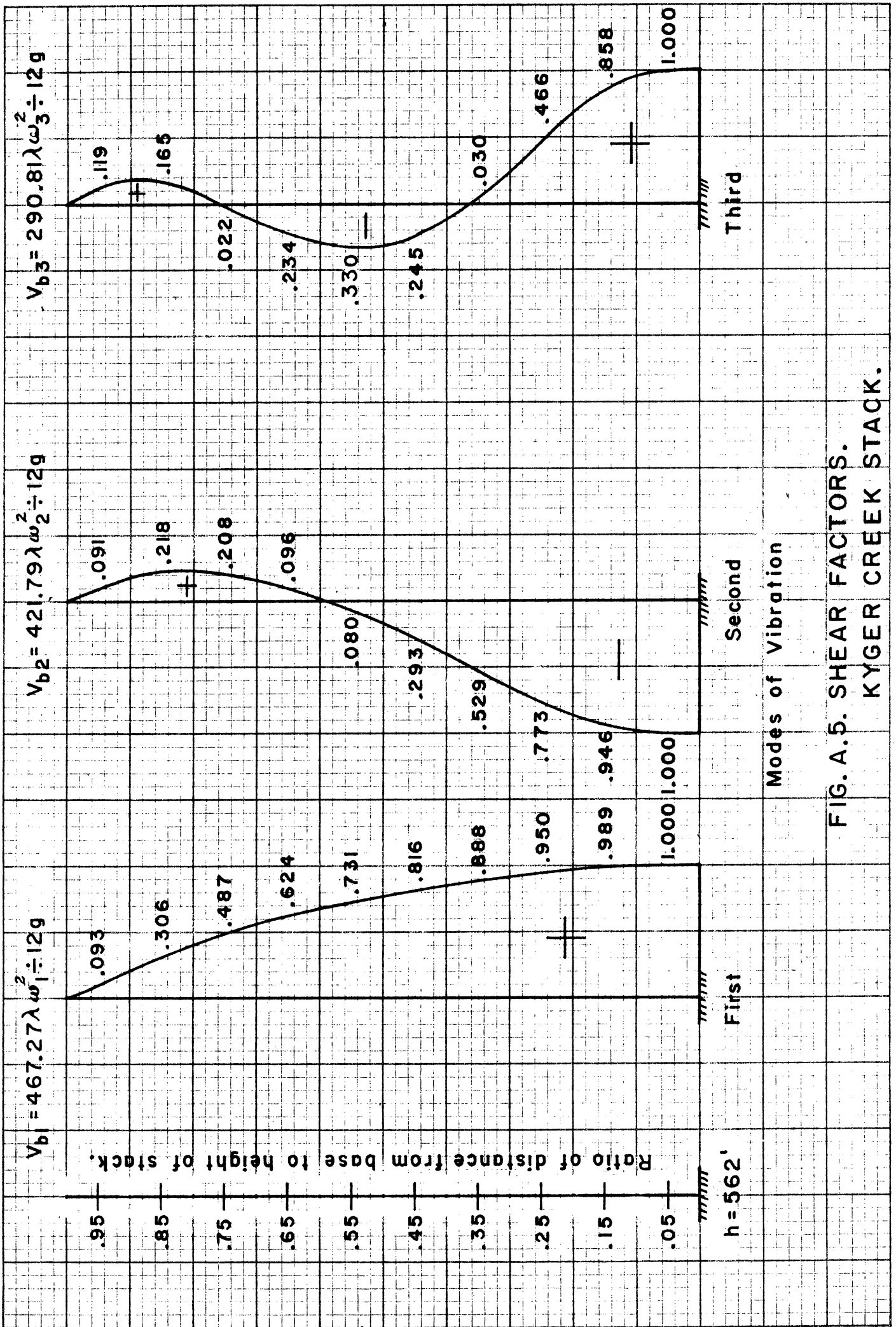


FIG. A.5. SHEAR FACTORS.  
KYGER CREEK STACK.

## BIBLIOGRAPHY

1. Alford, J. L., Housner, G. W., and Martel, R. R. "Spectrum Analyses of Strong-Motion Earthquakes," First Technical Report under Office of Naval Research, Contract N6onr-244, California Institute of Technology, Pasadena, California, August, 1951.
2. Hisada, T. "Nonlinear Vibrations of Two Story Buildings," Transactions of the Architectural Institute of Japan, March, 1955.
3. Merritt, R. G. "Effect of Foundation Compliance on the Earthquake Stresses in Typical Tall Buildings," Thesis, California Institute of Technology, Pasadena, California, 1952.
4. White, M. P. "Friction in Buildings: Its Magnitude and Its Importance in Limiting Earthquake Stresses," Bull. Seism. Soc. Amer., Vol. 31, pp. 93-99, 1941.
5. Hansen, H. M., and Chenea, P. F. "Mechanics of Vibrations," John Wiley and Sons, Inc., New York, 1952.
6. Timoshenko, S. P. "Vibration Problems in Engineering," D. Van Nostrand Co., Inc., New York, 2nd ed. pp. 331-358, 1937.
7. Churchill, R. V. "Fourier Series and Boundary Value Problems," McGraw-Hill Book Co., Inc., New York, pp. 21-32, 1941.
8. Den Hartog, J. P. "Mechanical Vibrations," McGraw-Hill Book Co., Inc., New York, 3rd ed., pp. 194-198, 1947.
9. Churchill, R. V. "Modern Operational Mathematics in Engineering," McGraw-Hill Book Co., Inc., New York, 1944.
10. Myklestad, N. O., "Vibration Analysis," McGraw-Hill Book Co., Inc. New York, 1944.
11. Timoshenko, S. P. "Vibration Problems in Engineering," D. Van Nostrand Co., Inc., New York, 2nd ed., pp. 32-37, 1937.
12. Johnston, B. G., "C.E. 231 Lecture Notes," University of Michigan Spring, 1952.
13. Newmark, N. M. "Bounds and Convergence of Relaxation and Iteration Procedures," Proceedings of the First National Congress of Applied Mechanics, Amer. Soc. of Mechanical Engineers, New York, 1951.
14. Timoshenko, S. P. "Vibration Problems in Engineering," D. Van Nostrand Co., Inc., New York, 2nd ed., pp. 337-338, 1937.
15. Jacobsen, L. S. "Natural Periods of Uniform Cantilever Beams," Proceedings Amer. Soc. of Civil Engineers, vol. 64, pp. 431-460, 1938.
16. Maugh, L. C. and Legatski, L. M. "Structural Behavior of the Reinforced Concrete Stacks of the Clifty Creek Power Plant," Engineering Research Institute, University of Michigan, Ann Arbor, Michigan, Project 2151, 1953.

17. Den Hartog, J. P. "Mechanical Vibrations," McGraw-Hill Book Co., Inc., New York, 3rd ed., p. 201, 1947.
18. Muktabhant, C. "A Study of Earthquake-Resistant Chimneys," University of Michigan, Ann Arbor, Michigan, 1953.
19. Den Hartog, J. P. "Mechanical Vibrations," McGraw-Hill Book Co., Inc., New York, 3rd ed., pp. 202-205, 1947.
20. Churchill, R. V. "Fourier Series and Boundary Value Problems," McGraw-Hill Book Co., Inc., New York, pp. 34-51, 1941.
21. Den Hartog, J. P. "Mechanical Vibrations," McGraw-Hill Book Co., Inc., New York, 3rd ed., pp. 198-201, 1947.
22. Amer. Smelting and Refining Co. "Chimney Height Sets Record," Engineering News Record, Vol. 119, p. 1040, 1937.
23. Maugh, L. C., and Legatski, L. M. "Structural Behavior of the Reinforced Concrete Stacks of the Kyger Creek Power Plant," Engineering Research Institute, University of Michigan, Ann Arbor, Michigan, Project 2182, 1953.
24. Newmark, N. M. "Methods of Analysis for Structures Subjected to Dynamic Loading," Directorate of Intelligence, U.S. Air Force, Washington, D. C., 1950.
25. Howe, C. E. and Howe, R. M. "A Tabletop Electronic Differential Analyzer," Department of Aeronautical Engineering, University of Michigan, Ann Arbor, October 1953.
26. Amer. Concrete Institute Committee 505 "Proposed Standard Specification for the Design and Construction of Reinforced Concrete Chimneys," Journal of the Amer. Concrete Institute, Vol. 24, pp. 353-400, January, 1953.
27. Amer. Standards Association, "Minimum Design Loads in Buildings and Other Structures," Amer. Standards Association, New York, 1945.

UNIVERSITY OF MICHIGAN



3 9015 03025 1881